The Identification of the Cardiac Neural Crest and its Role in the Premature Death (*p*) Mutation in *Ambystoma mexicanum*

by Naazish S. Bashir

Thesis submitted to the
School of Graduate Studies and Research
University of Ottawa
in partial fulfillment of the requirements for the M. Sc. degree in the
Ottawa-Carleton Institute of Biology

Thèse soumise à
l'École des études supérieures et de la recherche
Université d'Ottawa
en vue de l'obtention de la maîtrise ès sciences à
L'Institut de biologie d'Ottawa-Carleton

Naazish S. Bashir
Université d'Ottawa
Novembre 1996

ISBN 0-612-19928-2

Canada

UNIVERSITÉ D'OTTAWA
UNIVERSITY OF OTTAWA

Acknowledgements

First, I would like to thank Dr. John B. Armstrong for his guidance, support and undying patience throughout the last several years, (thanks for giving me a chance). I hope someday his enthusiasm and drive would rub off on me.

I would like to thank Bea Valentine and Andrew Vaillant for their invaluable assistance with the microscopy.

I would also like to thank Rob Langille, and the members of my committee for their technical advice.

Thanks also go to Bill Fletcher and to Christof Nolte for their axolotl expertise--a rare and valuable commodity.

I would like to thank Zareen Bashir for her help in putting this thesis together. I must thank my family for "putting up with me", and "putting me up" through all this.

Last, but not least, I would like to mention the axolotls, because without their tolerance and cooperation, this work would not exist. I would also like to thank them for showing me that amphibians can have a sense of humour too.

Abstract

The cardiac neural crest is a subpopulation of neural crest cells necessary for normal development of the cardiovascular system. The cardiac neural crest has been mapped to a defined region of the cranial neural crest in the developing chick and mouse embryo, and has been shown to primarily contribute to the development of the outflow septation of the heart. However, little is known as to the location of the cardiac neural crest and its contribution to cardiovascular system in the developing amphibian embryo. I have attempted to identify and define the boundaries of the cardiac neural crest in the neurula stage wild type axolotl *(Ambystoma mexicanum)* embryo by labelling the cardiac neural crest cells with the fluorescent lineage label, DiI. Cardiac neural crest cells were found to be located posterior to the hindbrain region of the neural folds, and above the first two somites, before migrating ventrally to provide ectomesenchymal support in the anterior outflow portion of the heart. My results indicate that the role and location of the cardiac neural crest in the axolotl are similar to the role and location of the cardiac crest in other vertebrates.

While attempting to isolate the cardiac neural crest, I also labelled other regions of the cranial neural fold in the stage 20 axolotl embryo. I constructed a fate map of the cranial neural folds in the late neurula stage embryo. Anterior neural fold cells contributed to the anterior structures of the brain and visceral skeleton, while more caudally located neural fold cells formed more posterior structures. My fate map corresponded to those previously constructed at earlier stages in neurulation.

I have also examined the development of the cardiac neural crest in axolotl embryos exhibiting the premature death (*p*) mutation. Homozygous (*p/p*) embryos develop up to stage 37 after which the superficial tissue begins to disintegrate, secondary gill filaments fail to form, a plug of undifferentiated cells replaces the endocardium in the anterior regions of the heart and circulation is never established. It has been suggested that the mutation affects a subpopulation of neural crest cells and possibly cardiac neural cells. I examined cardiac neural crest development in *(p/p)* mutants with DiI-labelling. Any deleterious effects of the premature death mutation were not detectable in cardiac neural crest. However, the migration and specification of the cranial neural crest involved in gill formation was noticeably hindered, thus substantiating that certain neural crest cells in the mutant fail to respond to inductive signals.

Résumé

La crête neurale cardiaque est une sous-population des cellules de la crête neurale nécessaire au développement normal du système cardio-vasculaire. La crête neurale cardiaque a été localisée dans une region définie de la crête neurale céphalique dans les embryons de poulet et de souris, et il a été aussi démontré qu'elle contribue au développement des divisions artérielles du coeur. Toutefois, l'on sait peu à propos de l'emplacement de la crête neurale cardiaque et de sa contribution au système cardio-vasculaire chez les embryons d'amphibiens. Nous avons tenté d'identifier et de définir les limites de la crête neurale cardiaque à un stade tardif de neurulation chez l'embryon du l'urodèle, *Ambystoma mexicanum* , en marquant ses cellules constituantes avec l'étiquette fluorescente de lignage "DiI". Nous avons observé que les cellules de la crête neurale cardiaque se retrouvent derrière la région postérieure du cerveau dans les bourrelets médullaires, et au-dessus des deux premiers somites. La crête cardiaque migre ventralement pour fournir un support ectomésenchymateux dans la portion antérieure de la circulation cardiaque. Nos résultats indiquent que le rôle et l'emplacement de la crête neurale cardiaque chez les amphibiens sont semblables à ce l'on a décrit chez les autres vertébrés.

Alors que nous tentions d'identifier la crête neurale cardiaque, nous avons également marqué d'autres régions des bourrelets médullaires céphaliques au stade 20 du développement d'*A. mexicanum*. Nous avons élaboré un "plan de destination" des bourrelets médullaires céphaliques à un stade tardif de la neurulation. Nous avons observé que les cellules antérieures des bourrelets médullaires antérieurs contribuent aux structures antérieures du cerveau et du squelette crânien, alors que les cellules des bourrelets médullaires situés plus caudalement forment des structures postérieures. Notre "plan de destination" correspond aux plans preparés antérieurement à partir d'embryons plus jeunes.

Nous avons aussi étudié le développement de la crête neurale cardiaque chez les embryons d'axolotls homozygotes pour la mutation de la mort prématurée (*p*, premature death, mutation) . Les embryons homozygotes (*p/p*) se développent jusqu'au stade 37, à partir duquel le tissu superficiel commence à se désintégrer, les filaments des branchies n'arrivent pas à se former, une masse de cellules non-différenciées remplace l'endocarde dans les regions antérieures du coeur et la circulation n'est jamais etablie. Il a été suggéré que la mutation affecte une sous-population de cellules de la crête neurale et possiblement les cellules neurales cardiaques. Nous avons suivi le développement de la crête neurale

cardiaque avec le "DiI". Nous n'avons noté aucun effet pernicieux de la mutation sur la crête neurale cardiaque. Cependant, la migration et la spécification de la crête neurale céphalique impliquée dans la formation des branchies ont été notablement inhibées. Ainsi, nos résultats supportent l'hypothèse que certaines cellules de la crête neurale chez les embryons mutants ne peuvent pas répondre aux signaux inducteurs.

Table of Contents

Table Of Contents (cont'd.)

List of Tables and Figures

Chapter I

List of Tables and Figures (cont'd.)

Chapter I

Introduction

This project consists of the examination of the cardiac neural crest, a subpopulation of cranial neural crest cells involved in heart development. We have focused on determining the exact location of cardiac neural crest in the amphibian *Ambystoma mexicanum* and have accomplished this via a lineage labelling technique, specifically by using the fluorescent vital dye, DiI. We have also further investigated the premature death mutation (*p/p*), a naturally occurring recessive mutation affecting *A. mexicanum* embryos. Embryos affected by the premature death (*p/p*) mutation arrest in development at an early stage and slowly begin to disintegrate. So far it has been established that the mutation affects chondrogenic neural crest cells, a subpopulation of cranial neural crest cells. We have examined whether the cardiac neural crest is also one of the several targets of the mutation's pleiotropic effects. The following pages describe the neural crest (specifically, the cardiac neural crest), lineage labelling and fate mapping with DiI, and the development of the Mexican axolotl. These elements, elaborated on separately, are intrinsically linked in this project.

1.1 The Neural Crest

In vertebrates, the neural tube differentiates into the central nervous system (the brain and spinal cord). The neural crest, an entity unique to vertebrate embryos, is a transient structure that develops at the time of closure of the neural tube and the fusion of the epidermis at the dorsal midline (reviewed in Le Douarin, 1982; Hall and Horstadius, 1988). The neural crest cells detach themselves from the neuroepithelium and migrate laterally and ventrally between the epidermis and the spinal cord (see Fig. 1A) to form neurons and glia of the peripheral nervous system, and various non-neural derivatives (reviewed below, and in Bronner-Fraser, 1993) (see Fig. 1B).

The neural crest extends along the entire craniocaudal axis, but neural crest cell migration occurs first rostrally. Migration is supported by various components of the extracellular matrix along these pathways: fibronectin, laminin, tenascin, collagen and proteoglycans (Newgreen and Thiery, 1980; Krotoski et al., 1986; Duband et al., 1987; Perris et al., 1991a; 1991b; Tan et al., 1991). Whether these components play an active role in determining migration pathways is controversial and is outside the scope of this chapter.

The neural crest is divided into two regions based on the developmental capabilities of each region (Le Douarin 1982; Noden, 1984; Hall and Horstadius 1988). In the chick embryo, the neural crest extending from the mid-diencephalon to the level of the fifth somite is referred to as the cranial neural crest and the rest of the neural crest extending from somite six to the caudal limit of the neural tube is referred to as trunk neural crest (reviewed in Kirby, 1991).

The trunk neural crest cells migrating along the dorsolateral pathway under the ectoderm form pigment cells. Those migrating along the ventral pathway through the rostral half of each sclerotome form the dorsal root ganglia, sympathetic ganglia and adrenomedullary cells (reviewed in Bronner-Fraser, 1993). Cell types derived from the

trunk neural crest include neurons, chromaffin cells, non-neuronal supporting cells, including Schwann cells and satellite cells, and melanocytes.

The cranial neural crest cells migrate ventrally in segmental sheets below the ectoderm (reviewed in Graveson, 1993). They contribute to the parasympathetic ganglia, the proximal ganglia of the cranial nerves V, VII, IX, and X, the enteric nervous system, [including all the cell types derived from trunk neural crest (reviewed in Kirby, 1991)], and a variety of non-neural derivatives. These include:

- the cartilages and connective tissues of the head, pigment cells, the meninges, and the dentine of the teeth (Hall and Horstadius, 1988)
- the mesenchymal components of the glands arising from the pharyngeal and buccal epithelium, such as the pituitary and salivary glands (Le Douarin, 1982)
- the connective tissue of the thymus, the thyroid and the parathyroids (Le Lièvre and Le Douarin, 1975)
- the connective tissue of the tongue, eye, and ventrolateral part of the neck (Le Lièvre and Le Douarin, 1975; Johnston et al., 1979; Le Douarin, 1982).

Figure 1. A) Pathways of avian trunk neural crest migration. These are: 1) a dorsolateral pathway between the ectoderm and somite to give rise to pigment cells; 2) a ventral pathway in the intersomitic space, to give rise to portions of the sympathetic ganglia; 3) a ventral pathway through the anterior half of the somite to form the sensory and sympathetic ganglia. EC=ectoderm (pulled back); DM=dermamyotome; SC=sclerotome; NT=neural tube; N=notochord; (adapted from Le Douarin et al., 1984; and Bronner-Fraser, 1993). B) Neural crest derivatives. Diagram showing that neural crest cells arising from different axial levels follow different pathways of migration and give rise to divergent cell types (redrawn from Bronner-Fraser, 1993).

PATHWAYS OF NEURAL CREST MIGRATION

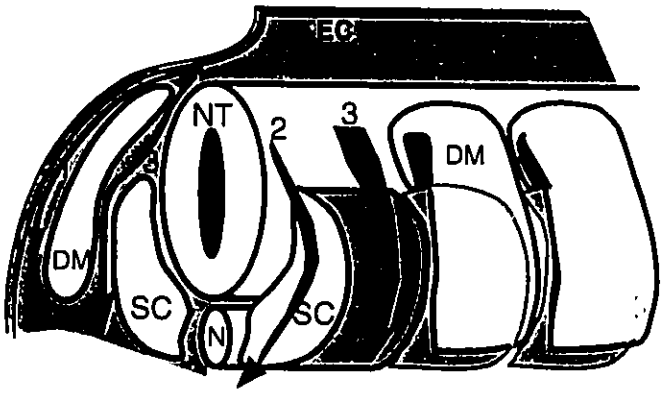

A

NEURAL CREST DERIVATIVES

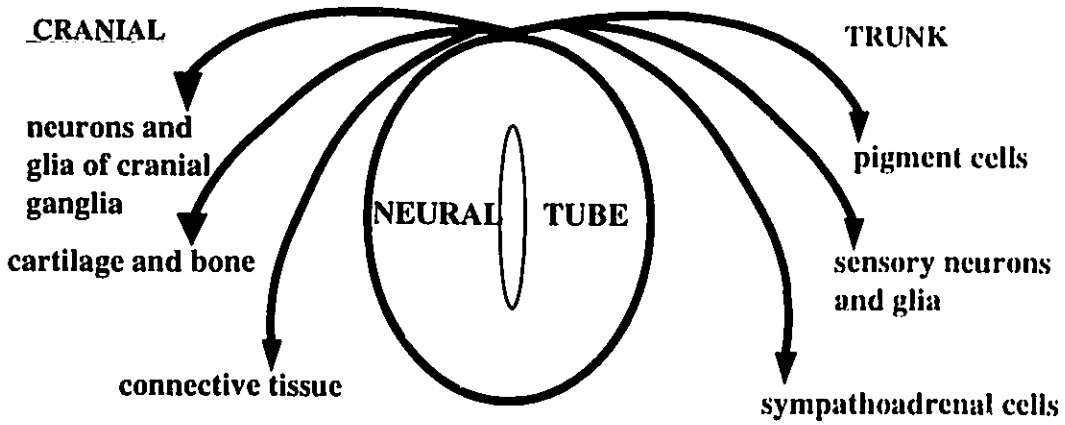

B

1.2 The Cardiac Neural Crest

The cardiac or vagal neural crest, a subdivision of the cranial neural crest, contributes to parts of the cardiovascular system (Kuratani and Kirby, 1992; for reviews see Kirby and Bockman, 1984; Kirby and Waldo, 1990; Kirby, 1991). Though most studies of cardiac neural crest have been in avian embryos (Le Lièvre and Le Douarin, 1975; Kirby et al., 1983; Stewart et al., 1986; Phillips et al., 1987; Rosenquist et al., 1990; Takamura et al., 1990), some work has also been done in the rat (Fukiishi and Morriss-Kay, 1992) and in the frog, *Xenopus laevis* (Sadaghiani and Thiébaud, 1987).

The cardiac neural crest is located at the boundary between cranial and trunk crest, just posterior to the hindbrain neural crest cells. In the chick, the cardiac neural crest is defined as the region between the otic placode and somite 3 (see Fig. 2A) (Kirby, 1991). The cardiac neural crest migrates from the neural fold into pharyngeal arches 3, 4, and 6 (Miyagawa et al., 1989). In the pharyngeal arches, the cells derived from the neural crest provide support for the endothelium of the aortic arch arteries (Bockman et al., 1989). Some cells migrate from the pharyngeal arches into the outflow tract where they form the aorticopulmonary septum and populate the truncal folds (see Fig. 2B) (Bockman et al., 1989). Others contribute to the *tunica media* of the great arteries, to the connective tissue of the thyroid, thymus and parathyroids, and to the calcitonin-producing cells of thyroid glands (Kirby, 1991). The largest population of neural crest cells in the outflow tract is derived from the region of the neural fold that will populate pharyngeal arch 4 (Phillips et al., 1987).

In the rat, Fukiishi and Morriss-Kay (1992), observed that labelled cells between occipital somites 1 and 2, or 3 and 4, migrated within and dorsal to the third and fourth pharyngeal arches respectively, and into the outflow tract of the heart (see Fig. 3).

Figure 2. A) Diagrammatic representation of the avian neural crest highlighting the region of the cardiac neural crest. The division between the trunk and cranial neural crest is at somite 5. The cardiac area is located between the midotic placode and somite 3. This area of neural crest migrates into the pharyngeal arches 3, 4, and 6 (adapted from Kirby and Waldo, 1990).

B) Diagram illustrating the cranial neural crest migratory pathway through the pharyngeal region in the embryonic chick. Some of the neural crest cells in pharyngeal arches 3, 4, and 6 continue their migration from the pharyngeal region into the outflow tract of the developing heart where they participate in the formation of the aorticopulmonary and truncal septa (adapted from Kirby and Waldo, 1990).

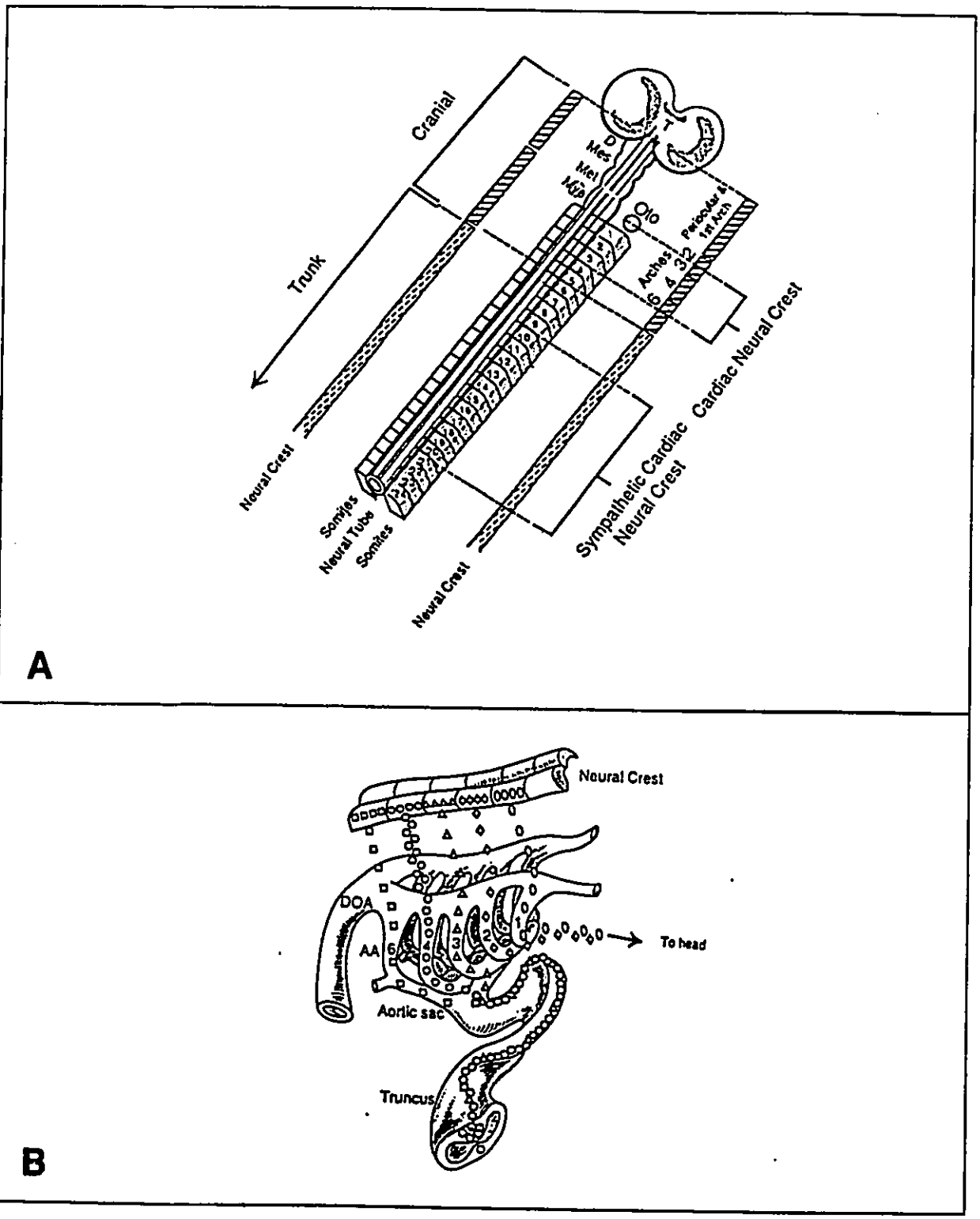
Cranial
Trunk
Neural Crest
Somites
Neural Tube
Somites
Neural Crest
Sympathetic Cardiac Neural Crest
Cardiac Neural Crest
Mes
Mel
Met
Otic
Pericardial 1st Arch
Arches
6 4 3 2
A
Neural Crest
DOA
AA
6
3
2
1
To head
Aortic sac
Truncus
B

Figure 3. Cranial neural crest migration pathways in the embryonic mouse. Cells labelled between occipital somites 1 and 2 or 3 and 4 migrate within and dorsal to the third and fourth pharyngeal arches and into the outflow tract of the heart. The colours and numbers represent the different axial levels of the neural crest and their migratory pathways. Region "6" (orange) indicates the area of cardiac neural crest in the developing mouse embryo (adapted from Fukiishi and Morriss-Kay, 1992).

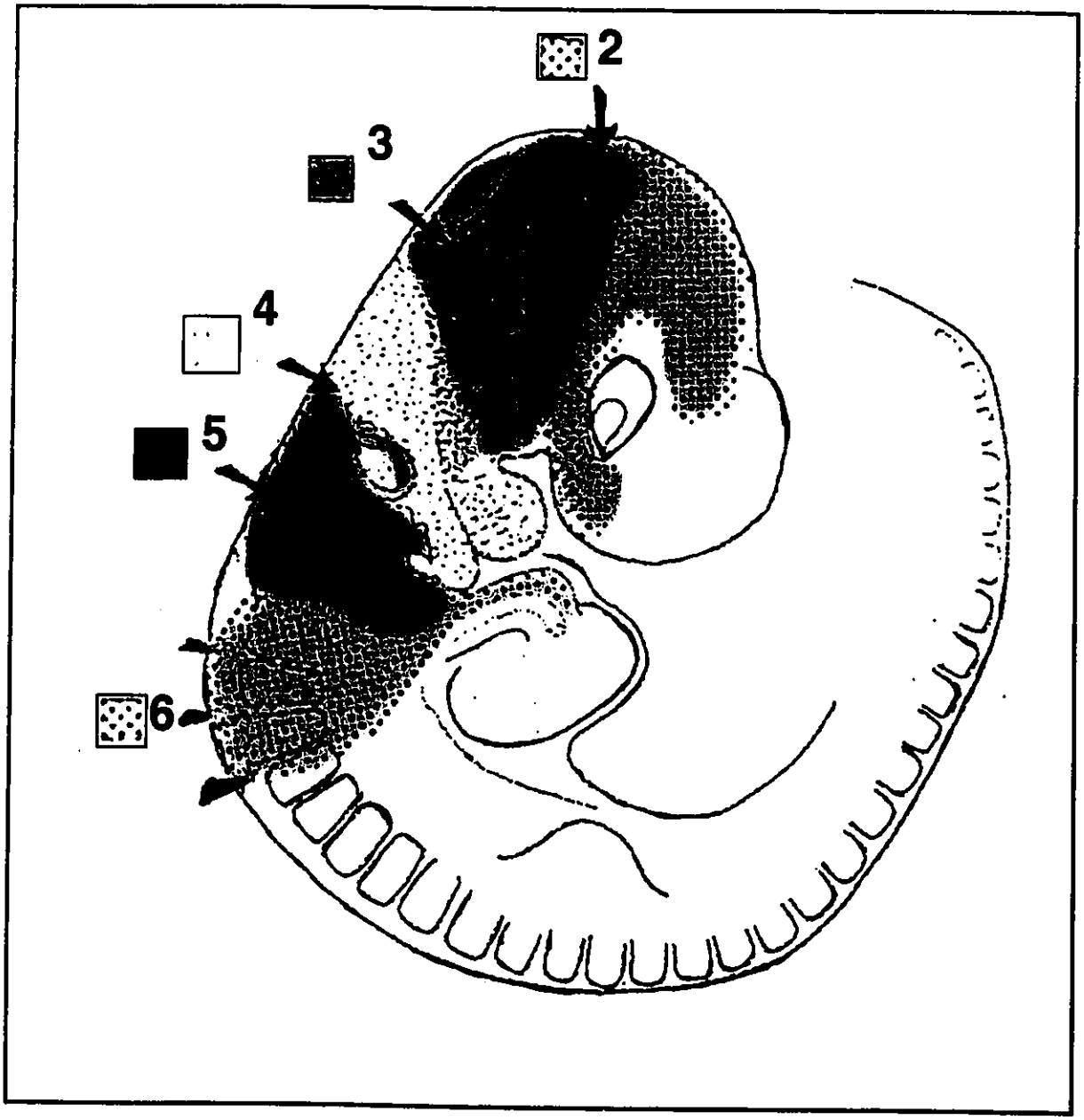
2
3
4
5
6

While specific boundaries for the cardiac neural crest have been established in chick and rats, the location of cardiac neural crest has not been as well defined in amphibians. Sadaghiani and Thiébaud (1987) observed that, in *Xenopus* embryos, the branchial crest segment (the neural crest cells from the posterior part of the rhombencephalon) contributes to the branchial arches, and its cells were later seen in the loose connective tissue under the pharyngeal epithelium and in the mesenchyme of the gills. They also noted that some of these cells penetrate into the wall of the *truncus arteriosis*. The vagal crest cells, which originally denoted crest cells over the first and second somites, differentiated into Schwann cells, neuroblasts and had also penetrated into the mesentery of the digestive system (Sadaghiani and Thiébaud, 1987). However, they did not mention whether vagal crest cells, which are located posterior to the branchial crest segment, made any contribution to the developing cardiovascular system.

Other studies have focussed largely on the pathways of trunk crest, and have not concentrated on the establishment of a specific cardiac neural crest (Krotoski et al., 1988; Collazo et al., 1993). Our study, in the axolotl, is the first to define a specific boundary for the cardiac neural crest in amphibians.

Most of the information on the role of the neural crest in cardiovascular development has been obtained from lineage labelling (see next section), and neural crest ablation (Kirby et al., 1983; Stewart et al., 1986; Kuratani et al., 1992). Cardiac neural crest ablation has resulted in malformations such as nonseptation of the outflow tract (Kirby and Waldo, 1990). These cardiovascular abnormalities, observed in the chick, are comparable to those found in patients with DiGeorge Syndrome and Down Syndrome (Kirby and Waldo, 1990; Kirby, 1991). This suggests that the neural crest cells may be implicated in congenital heart defects. The possibility of such a connection was the rationale for our investigation of the possible involvement of the neural crest in the

abnormal cardiovascular development in the axolotl *premature death (p)* mutant (see next chapter).

1.3 Lineage Labelling of Neural Crest Cells

Due to the dynamic nature of neural crest cell migration and differentiation, an appropriate cell marker must be used to monitor the cells during development. The marker or label must not be deleterious to the cells, nor alter their differentiation or migration. The label must not fade or be diluted over short periods of time. The marker must be specific to the labelled cells and should not be able to diffuse between marked and neighbouring unmarked cells. Finally, it should be easily visualized. Several types of neural crest markers have managed to fill most, if not all these criteria. Some examples of lineage labels include the use of chimeras, immunocytochemistry with specific antibodies, fluorescent vital dyes, radioactive labels and intrinsic genetic markers (reviewed in Ruiz i Altaba, 1994).

Early methods of tracing neural crest cell migration involved the labelling of cells with ^{3}H-thymidine, in which cells synthesizing DNA would be labelled (Weston, 1963; Chibon, 1964; reviewed in Le Douarin, 1982; Hall and Horstadius, 1988; Bronner-Fraser, 1993). However, the label was diluted by each new round of DNA synthesis and so could not be followed for long periods of time.

Later, intrinsic genetic markers were used to distinguish between labelled and unlabelled cells. This type of labelling usually involves the transplantation of cells with a unique and easily perceivable genetic marker into a genetically different host. Considerable data concerning the migration of avian neural crest has been accumulated employing this technique. (Generally, quail cells are grafted into chick hosts.) The quail-chick marker system exploits the differences between quail and chick nuclei. The quail nucleolus is concentrated with a mass of heterochromatin and the nuclei can be distinguished quite

easily under light microscopy from chick nuclei (Le Douarin, 1982). The mesenchymal derivatives of the avian neural crest were first determined using this marker system (Le Lièvre and Le Douarin, 1975; Le Douarin, 1982; Phillips et al., 1987).

A similar interspecific chimera can be created in frogs. *Xenopus borealis* nuclei exhibit a punctate pattern of fluorescence when stained with quinacrine and can be distinguished from the uniformly staining *X. laevis* nuclei when grafted into *X. laevis* hosts (Thiébaud, 1983; Sadaghiani and Thiébaud, 1987).

The use of interspecific chimeras for the study of neural crest migration is, however, somewhat limiting since it restricts the species in which experiments can be performed. Also, one must be wary of making generalizations concerning all vertebrates from the results of experiments conducted in such isolated systems.

In other amphibians, particularly in axolotls, intraspecific (as opposed to interspecific) genetic markers have been developed. One example is the use of triploid-diploid chimeras. Triploid cells contain three nucleoli while diploid cells contain two. Triploid axolotls can be generated by exposing newly fertilized eggs to heat, cold or hydrostatic pressure (reviewed in Armstrong and Muneoka, 1989). After staining with a nucleolus-specific stain, the triploid and diploid cells can be distinguished in histological sections or whole mount preparations.

Another common genetic marker used for following cells is pigmentation. In axolotls, darkly pigmented wild-type cells have been transplanted to lightly pigmented albino hosts. The migration pattern of the transplanted cells can easily be traced by observing the paths taken by the dark cells (Graveson, 1995).

More recently, recombinant vectors have enabled the introduction of easily-assayable histochemical markers into cells that previously did not endogenously contain these markers. The most widely used lineage label of this type is the transfection of cells with a vector containing the exogenous *Escherichia coli lac Z* gene. ß-galactosidase

activity can then be detected histochemically and viewed easily under light microscopy. The *lac Z* gene can be injected into a fertilized egg and, if incorporated into the genome, will be inherited by all the progeny of the injected cell. The cells containing the *lac Z* gene can be distinguished from cells that do not contain the marker. The *lac Z* genetic marker has been successfully used in lineage labelling experiments in rodents (Sanes et al., 1986; Turner and Cepko, 1987), and also in the axolotl (Whiteley, 1990). The biggest advantage to this type of marker is that it is intrinsic to the cell and cannot diffuse into neighbouring cells. However, this approach also has one significant limitation, namely the variable expression of the foreign gene. If the expression of the marker transgene is transient or variable, detection of the labelled cells may be difficult.

Specific antigens have also been used to follow neural crest migration. The monoclonal antibody HNK-1, first generated to human natural killer cells (Abo and Balch, 1982), recognizes a carbohydrate epitope that also occurs on neural crest cells and their derivatives in birds, mammals, and fish (Vincent et al., 1983; Bronner-Fraser, 1986; Sadaghiani and Vielkind, 1990) and differentiating neurons of many vertebrates including fish, amphibians, birds and mammals (Bronner-Fraser, 1986; Holley and Yu, 1987; Schwarting et al., 1987; Norlander, 1989; Metcalfe, 1990). NC-1 is similar to HNK-1 in its immunoreactivity (Tucker et al., 1984). Although labelling with these antibodies has been used to target neural crest cells, there are some inconsistencies. The antibodies do not recognize all neural crest cells or all their derivatives (Kruse et al., 1984; Teillet et al., 1987), nor are they completely specific to neural crest cells. This is particularly true when dealing with cardiac neural crest. For example, it has been shown that in the avian embryonic heart, structures that showed HNK-1 immunoreactivity were not always of neural crest origin, and that the outflow tract cushions were HNK-1 positive prior to the neural crest cells entering that area (Luider et al., 1993). The other major problem with HNK-1 antibody labelling is that most non-neuronal neural crest derivatives lose their reactivity with HNK-1 antibody as migration progresses. This has been seen in *Xenopus*

(Norlander, 1993), chicks (Vincent and Thiery, 1984), and fish (Sadaghiani and Vielkind, 1990).

One of the most common methods of lineage labelling has been vital staining. These types of labelling techniques overcome the often cumbersome transplantation and grafting operations as they can be done *in situ* in live embryos. Several types of vital dyes or exogenous cell markers have been used to study neural crest migration. Early techniques of staining neural crest cells involved the labelling of the neural crest cells with the vital dyes Nile Blue sulphate and Neutral Red (Detweiler, 1937; Detweiler and Kehoe, 1939; Horstadius and Sellman, 1946). The major drawback of these two vital dyes is fading.

Two other labels are wheat germ agglutinin-gold conjugate and horseradish peroxidase. The wheat germ agglutinin-gold conjugate has been successfully used to label and follow presumptive cephalic neural crest in the rat and mouse (Tan and Morriss-Kay, 1986; Smits van Prooije et al., 1986; Chan and Tam, 1988). Horseradish peroxidase has been especially successful when used as a heritable intracellular label to mark and follow amphibian blastomere derivatives in the central nervous system (Jacobson and Hirose, 1978, 1981; Smith and Slack, 1983).

1.4 Use of the Vital Dye, DiI, as a Cell Marker in the Axolotl

Recently, the advent of fluorescent vital dyes has allowed more detailed exploration of neural crest migration. The fluorescent nature of these dyes allows us to exploit epifluorescent and confocal laser scanning microscopy when examining specimens. Morphogenetic movements of labelled cells can be further scrutinized, adding to data collected from light and electron microscopy. Several types of fluorescent dyes are available as cell tracers. The three most common types of dyes are the lysinated fluorescent dextrans (such as lysinated-rhodamine dextran and lysinated-fluorescein dextran), the

carboxyfluorescein tracers (such as carboxyfluorescein diacetate succinimidyl ester and carboxydicholorofluorescein diacetate succinimidyl ester), and the carbocyanine dyes such as DiI (1,1-dioctadecyl-3,3,3',3'-tetramethylindocarbocyanine perchlorate) and DiO (3,3'-dioctadecyloxacarbocyanine perchlorate).

Lysinated fluorescent dextrans can be injected into single cells and the labelled progeny can be followed for up to 10 cell divisions (Ruiz i Altaba et al., 1994). Lysinated fluorescein dextran has been used as lineage tracers in the labelling of single blastomeres in amphibians (Gimlich and Cooke, 1983) and in tracing neural crest migration in zebrafish (Schilling and Kimmel, 1994; Raible and Eisen, 1994). The dextrans can however be quite viscous, making the injection of small cells difficult (Armstrong, personal communication).

Carboxyfluorescein tracers have been used to study epithelial-mesenchymal transformations during palatal fusion in mouse embryos (Griffith and Hay, 1992). Carboxydichlorofluorescein diacetate succinimidyl ester (CCFSE) diffuses across the cell membrane, where intracellular esterases cleave off the acetates to release the fluorophore as a water soluble compound that cannot diffuse out of the labelled cells. This stable cytoplasmic marker can easily withstand formaldehyde fixation and paraffin embedding (Griffith and Hay, 1992).

By far the most common vital dyes used currently for the labelling of neural crest cells and neuronal derivatives are the fluorescent, lipophillic dyes DiI (1,1-dioctadecyl-3,3,3',3'-tetramethylindocarbocyanine perchlorate) and DiO (3,3'-dioctadecyloxacarbocyanine perchlorate). The carbocyanine DiI is a brightly fluorescent dye with an excitation maximum of 550 nm and an emission maximum of 565 nm, similar to that of rhodamine, while DiO has an excitation maximum of 484 nm and an emission maximum of 501 nm. DiI has been used more often since it yields more satisfactory staining results in living cells than DiO (Honig and Hume, 1986). DiI can also be photoconverted with diaminobenzidine to an insoluble, electron-dense product for visualization at the ultrastructural level

(Gansmuller et al., 1992; Lubke, 1993; Ruiz i Altaba et al., 1994). Once injected onto, or into the cell, the long-alkyl chain carbocyanine dye diffuses laterally within the plasma membrane, superficially embedding itself in the lipid membrane (see Fig. 4). The dye is not toxic to cells. Transfer of the dye between intact membranes is negligible, and it will last, without marked fading, for at least two to three weeks in living tissue and for several months in fixed tissue (Ruiz i Altaba et al., 1994). The dye does not alter cell surface properties and, as a result, does not alter the migrational pattern of cells (Pomeranz et al., 1991) making it an ideal label for following the migration of neural crest cells and their derivatives.

DiI labelling has been exceptionally useful in the retrograde labelling of neuronal cells in culture (Honig and Hume,1986). Other cell types labelled with DiI in culture include erythrocytes (Unthank et al., 1993), hepatocytes (Soriano et al., 1992), endothelial and smooth muscle cells (Ragnarson et al., 1992). DiI has been used extensively for neuronal tracing experiments in a variety of vertebrates with either live or fixed tissue. Some of these experiments include the tracing of axons in the brains of salmon (Holmqvist et al., 1992), zebrafish (Kaethner and Stuermer, 1992), *Xenopus* (Fraser and O'Rourke, 1990), axolotl (Krug et al., 1993), hamster (Pires-Neto and Lent, 1993), mouse (Gransmuller et al., 1992), cat (Elberger, 1993) and man (Meyer and Gonzalez, 1993; Wadhwa et al., 1993).

DiI has been proven to be a very successful lineage label in neural crest migration studies in several embryonic systems. Trunk neural crest migration has been studied in zebrafish (Raible and Eisen, 1994), *Xenopus* (Collazo et al., 1993), chick (Serbedzija et al., 1989; 1991; Pomeranz, 1991) and mouse (Serbedzija et al., 1991). Cranial neural crest migration has been investigated in the chick (Kuratani and Kirby, 1992; Scherson et al., 1993) and mouse (Serbedzija et al., 1992; Trainor and Tam, 1995). Our study is the first to use DiI as a label for cranial neural crest migration in amphibians.

Figure 4. Diagram illustrating the DiI molecule superficially embedded in the phospholipid bilayer of the plasma membrane once it is injected. The dye diffuses laterally within the plasma membrane, thus labelling it. (Molecule is not drawn to scale.)

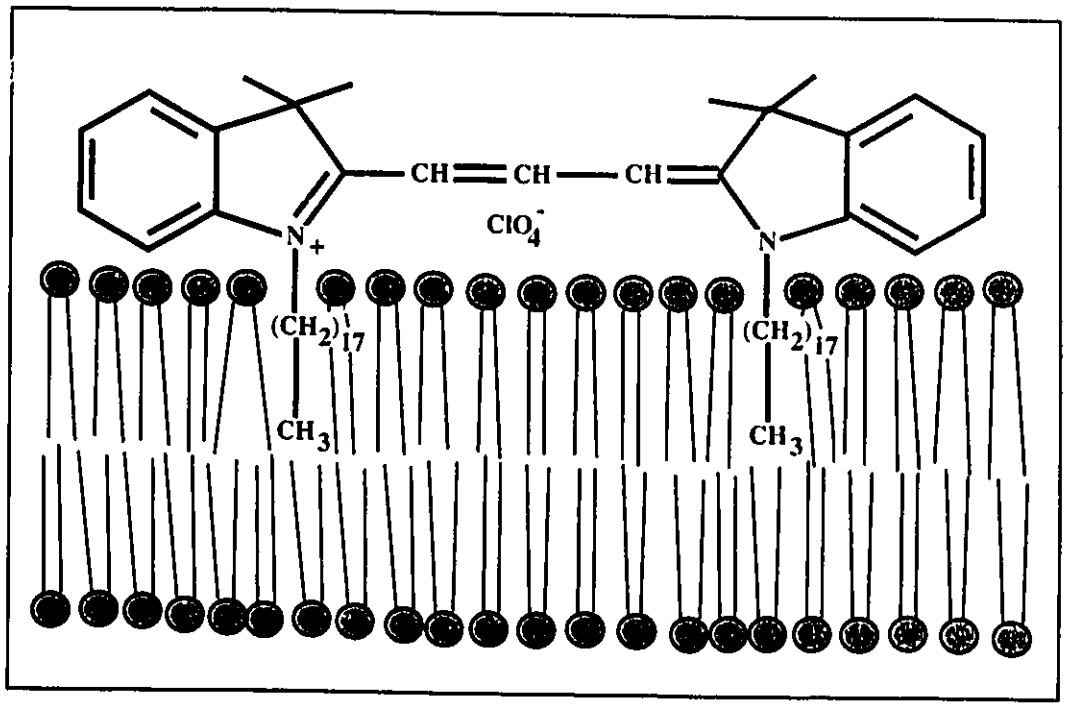
CH
CH
CH
ClO_4^-
N+
N
$(CH_2)_{17}$
CH_3
$(CH_2)_{17}$
CH_3

Cardiac neural crest has been labelled and followed with DiI in the chick embryo (Kuratani and Kirby, 1992; Kirby et al., 1993). DiI has shown to be an invaluable technique for fate mapping studies even prior to neural crest migration in certain vertebrate embryos. The fate map of the primitive streak of the early mouse embryo and of Hensen's node in the chick embryo were constructed using DiI labelling (Selleck and Stern, 1991; J.L. Smith et al., 1994). The fates of presumptive small mesenchymal cells have been determined from labelling studies of blastula stage sea urchins (Ruffins and Ettensohn, 1993). DiI has also been used to label the blastopore lip in the early *Xenopus* gastrula (Gont et al., 1993).

Due to the wide-spread and successful use of DiI in recent fate mapping experiments, we decided to use DiI as the marker of choice for tracing the fate of the cardiac neural crest in neurula stage *A. mexicanum* embryos. When we began this project, the only published work on DiI in the axolotl involved the labelling of nerves in fixed adult tissue (Krug et al., 1993; Nagai, 1993). Krug et al. (1993) examined afferent and efferent connections of the thalamic eminence in the brain of the adult axolotl, while Nagai (1993) studied the IX nerve and the innervation of taste buds in the lingual epithelium. In 1995, Barlow and Northcutt published a study in which they labelled the presumptive cephalic endoderm of early axolotl gastrulae with DiI and found that it contributed to the development of the taste buds.

1.5 Gross Morphological Development of the Amphibian Heart

In order to analyze the relationship between cardiac neural crest and other cardiac primordia we must first try to understand the sequence of events in early heart development. The morphogenetic movements of mesodermal heart primordium in *Ambystoma* have been described by Copenhaver (1926) , Wilens (1955) and Lemanski (1971). These early studies focussed mainly on the morphology of heart development. More recent studies have been concerned more with initial heart induction by the pharyngeal endoderm (Jacobsen, 1960; 1961; Jacobsen and Duncan, 1968; Sater and Jacobsen, 1989; Smith and Armstrong, 1990).

The following brief synopsis of heart development is based primarily on the work of Lemanski (1973). During gastrulation, the right and left mesoderm halves become located laterally on each side of the blastopore lip, and remain paired in late neurula and early tailbud stages. Following neurulation, the two mesoderm sheets thicken and converge toward the ventral midline of the embryo. In early tailbud stages, the leading edges give rise to a small number of loosely-organized pre-endocardial cells. These cells accumulate as a longitudinal strand which eventually hollows out to form the thin-walled tube of the endocardium. The tube then bifurcates at both ends and becomes continuous with the linings of adjoining blood vessels.

During endocardial development, thickened borders of the right and left mesoderm sheets fuse to form a "trough" of prospective myocardium, which continues to grow and surround the endocardium. The location of the heart field mesoderm in a stage 20 *A. mexicanum* embryo can be seen in Figure 5. Growth occurs in a dorso-ventral direction. Heart beat and completion of the heart tube occur at approximately stage 34-35 (see Table 1 in Appendix II, for staging). The tubular heart is straight at first, and later develops convoluted chambers: 1) the sinus venosus; 2) the atrium; 3) the ventricle; 4) the conus arteriosis (see Fig. 6). At stage 39, the conus arteriosis is continuous with the ventral

aortae anteriorly and extends posteriorly to join the ventricle at a sharp angle. The ventricle is elongated at this stage, and is positioned almost laterally with respect to the longitudinal axis of the embryo. The atrium is oriented longitudinally and the sinus venosus is continuous with the vitelline veins and located anterior to the liver. After stage 41, the heart acquires its adult form. The atrium and sinus venosus enlarge but retain their thin walls while the ventricle also increases in size and acquires a thicker-walled appearance.

The contribution of neural crest in *Ambystoma* heart development has not been previously examined. However, since the heart is primarily of mesodermal origin, it is important to understand the morphogenetic movements of the heart field mesoderm during heart development, prior to possible neural crest involvement. Since it has been shown that neural crest is involved in cardiovascular development in other vertebrates, we hypothesize that the neural crest of *Ambystoma* embryos is also involved in heart development, but plays a part in the later stages of cardiovascular development, during arterial outflow tract development.

Figure 5. Diagram showing the location of the heart-forming mesoderm in the stage 20 axolotl embryo. The diagram shows the right side of a stage 20 embryo with the epidermal ectoderm removed. The orange-coloured region defines the location of the heart-forming mesoderm (H) at the anterior edge of the mesodermal mantle. Me=mesoderm; M=mandibular mesoderm; EN=underlying endoderm; NF=neural fold; S=somites; A=anterior of embryo; P=posterior of embryo; D=dorsal side of embryo; V=ventral side of embryo; (redrawn from Smith and Armstrong, 1993).

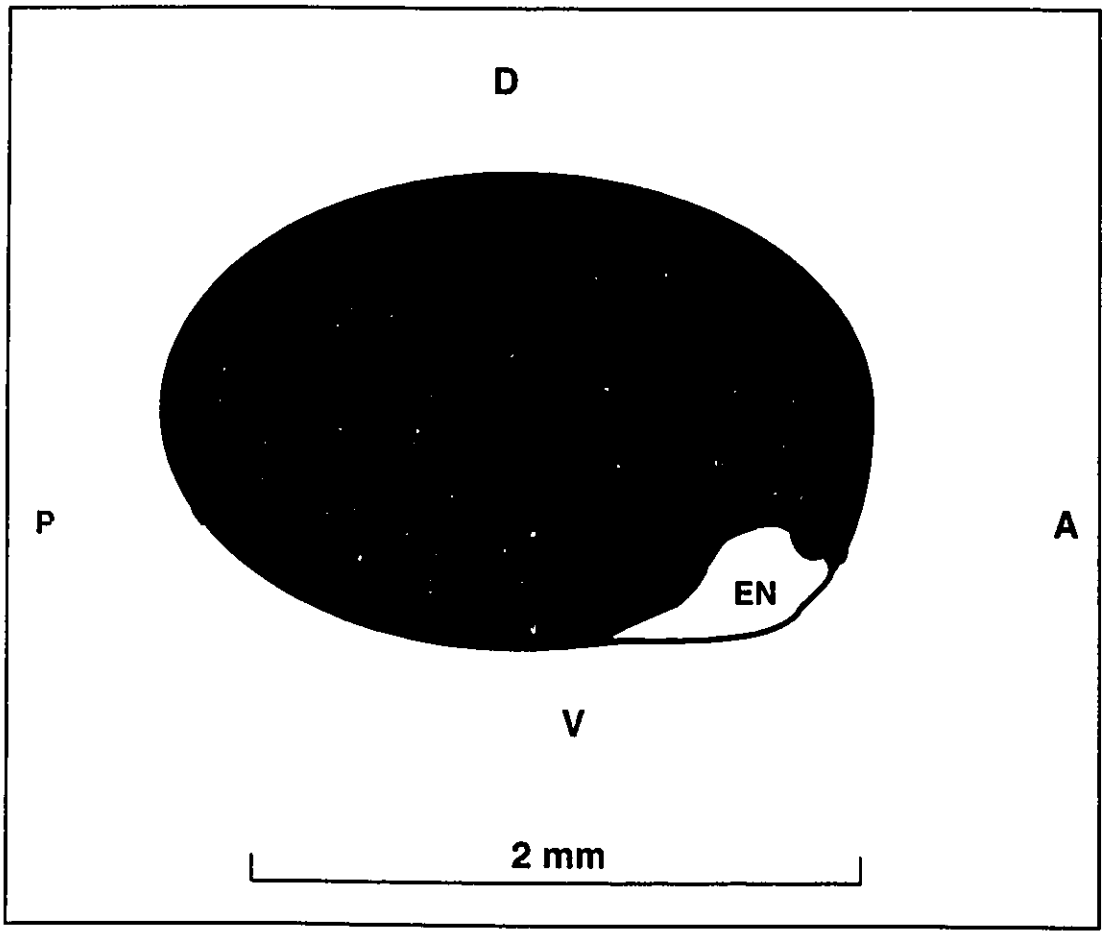
D
P
A
EN
V
2 mm

Figure 6. Frontal view of a stage 40 *A. mexicanum* heart. The drawing shows the convoluted nature of the developing heart and its subdivisions. B=bulbus; C=conus; V=ventricle; A=atrium; S=sinus venosus; magnification = 80x.

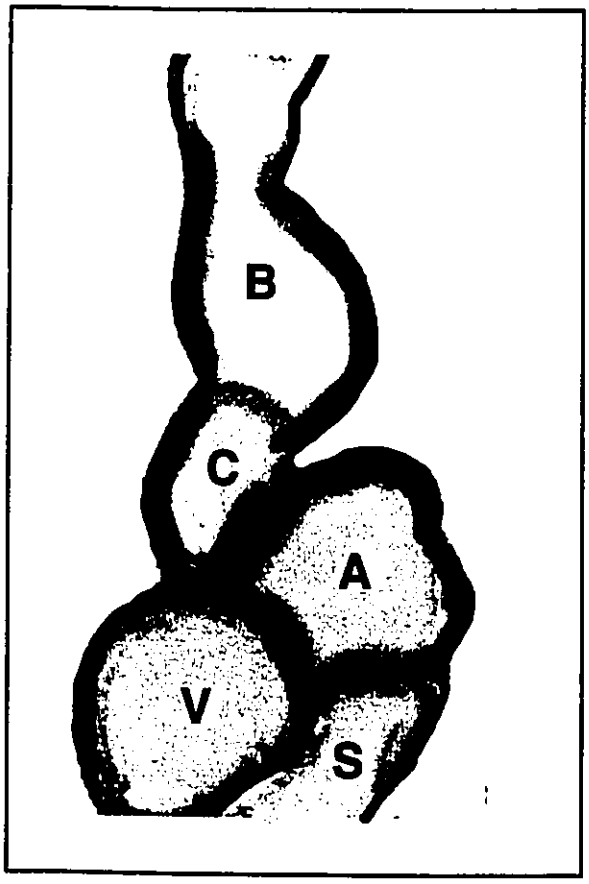
B
C
A
V
S

1.6 The Mexican Axolotl

Ambystoma mexicanum, a native of Lake Xochimilco near Mexico City, is a neotenous urodele which has been used extensively in developmental biology studies. This salamander possesses many qualities which make it useful for vertebrate developmental experiments. Adults can be allowed to mate and eggs can be collected throughout the year. Each successful spawning yields 300-600 eggs (Armstrong et al., 1989). The eggs are approximately 2 mm in diameter when laid and can easily be surgically removed from their protective, transparent, jelly coat. The large size of the embryo and the ability to withstand surgical manipulation without severe disruption in development has made these organisms very popular for transplantation and extirpation experiments.

Axolotls have been raised in laboratories for over a hundred years. As a result, much has already been documented about their development and physiology. A detailed staging table has been constructed to monitor embryological development (Bordzilovskaya et al., 1979). Several genetic mutations have also been characterized which may aid in elucidating the patterns involved in normal development (Armstrong, 1985).

We have chosen to use the axolotl for our study of the neural crest for several reasons. First of all, axolotl embryos were easily obtained from the University of Ottawa Axolotl Colony. Secondly, the large size of the embryos and of the neural folds themselves allowed easy access to the underlying neural crest. Thirdly, cranial and trunk neural crest migration has been well documented in amphibians (Hall and Horstadius, 1988), but cardiac neural crest has yet to be well defined to a particular region of the neural folds. Fourthly, we were interested in examining the role of cardiac neural crest in the premature death mutation (*p*), a recessive mutation particular to the axolotl affecting a subpopulation of neural crest cells.

1.7 Previous Fate Maps of the Urodele Cranial Neural Crest

Over the past few decades, several researchers have successfully created fate maps of the cranial neural crest in neurula stage urodele embryos. They have examined several species and looked at various stages of neurulation, focussing primarily on early and mid-neurula stages.

One of the earliest fate maps created for the neural crest in the head was by Landacre (1921) in *Plethodon glutinosis (Ambystoma jeffersoniam)*. He observed the embryos through several stages of neurulation and neural crest migration. Landacre noted that most of the dorsal portion of the migrating neural crest sheet gives rise to the general cutaneous and general visceral portions of cranial ganglia V, VII, IX, and X, while the rest of this portion of neural crest forms mesenchyme. The ventral portion of the neural crest sheet migrates downwards into the head region and into the mandibular and branchial bars and later differentiates into loose ectodermal mesenchyme and dense cartilage primordia. The resulting visceral cartilages from the neural crest include the anterior portion of the trabeculae, Meckel's cartilage, the palatoquadrate bar, and all the branchial cartilages except the second basibranchial. The fate map constructed by Landacre for the *Plethodon* head is shown in Figure 7A.

A few years later, Stone corroborated Landacre's results with extirpation studies in *Ambystoma punctatum* (1922, 1926) and in the anuran, *Rana palustris* (1929). Stone confirmed that the cranial neural crest contributed to the formation of Meckel's cartilage, the palatoquadrate, the anterior portions of the trabeculae and the hyobranchial skeleton, except for the second basibranchium. Stone also managed to map out which regions of the cranial crest contributed to which areas of the visceral skeleton (see Fig. 7B). Similar studies on trunk neural crest migration in *Ambystoma* were performed by Raven (1931) and Detweiler (1934, 1937).

In 1946, Horstadius and Sellman meticulously marked 8 different sections along the anterior neural ridge at open neural plate stages (ie. stage 16 in *A. mexicanum* embryos) to determine which section of the neural fold contributed to which cartilaginous element of the visceral skeleton. Using vital staining techniques, they found that certain areas of the neural fold specified particular members of the chondrocranium (see Fig. 8). They also found that there was some crossover across the midline between cells on opposite folds. Their results were reminiscent of those from Stone and Landacre but were more specific and mapped out the fate of crest cells earlier in neurulation (mid-neurula stage).

More recently, Chibon (1966) defined specific axial levels of the stage 17 *Pleurodeles waltlii* neural fold, and determined the fate of each axial level with respect to elements of the visceral skeleton (see Fig. 9 for outline of axial levels). He found that the area defined by 0°-30° produced no skeletal elements. The area between 30°-50° formed the anterior portion of the trabeculae. The area defined by 50°-70° formed the posterior portions of the trabeculae, the basal plate and the palatoquadrates. The area marked as 70°-100° specified Meckel's cartilage and the hyoid arches. 100°-120° formed the first basibranchial, the hypobranchials and the anterior branchial arches, while the areas designated as 120°-150° formed the posterior branchial arches. Chibon's results were very similar to those of Horstadius and Sellman for urodele mid-neurula stages.

We have constructed a similar fate map for the cranial neural crest in late neurula stage (stage 19-20) *A. mexicanum* embryos. We have used specific landmarks on the embryo only distinguishable at this late stage to demarcate specific areas of the neural fold. These landmarks include the varying thickness and bulbous quality of the neural fold at the forebrain, fore-midbrain and mid-hindbrain regions, and the appearance and extent of emerging somites. We have mapped out the contribution of different sections of the anterior neural fold to the visceral skeleton at the stage when the neural folds are about to fuse at the dorsal midline. Our fate map is the first, to our knowledge, to use easily identifiable landmarks on the *A. mexicanum* embryo as reference points for injection of a

fluorescent vital dye. It is also the first fate map of the anterior neural folds and cranial neural crest at the late neurula stage in *A. mexicanum*.

Figure 7. A) Diagram showing the early migration of the anterior neural crest sheet (blue) over the mesoderm (beige) in a 3 mm long *Plethodon* larva. Op=optical vesicle; M=mandibular bar; X, IX, VII, V, refer to cranial nerves; N=notochord; Ne=neural canal (adapted from Landacre, 1921). B) Diagram showing the extent of the cranial neural crest (purple) and its derivatives in the stage 26-27 *Ambystoma punctatum* embryo. Bre=branchial ectomesenchyme; Au=auditory vesicle; He=hyoid ectomesenchyme; Me=mandibular ectomesenchyme; Op=optical vesicle (redrawn from Stone, 1926).

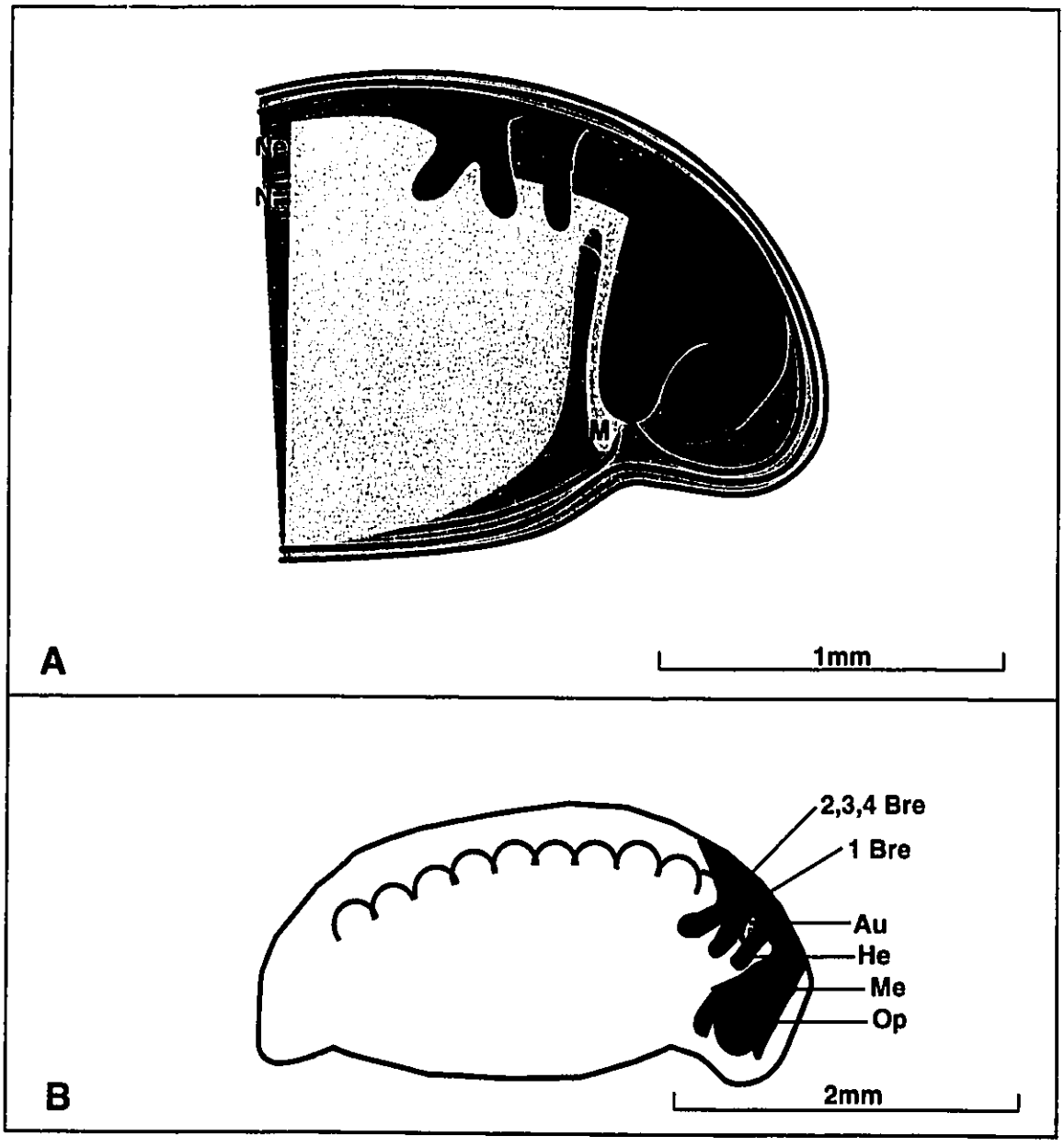
A
1mm
B
2,3,4 Bre
1 Bre
Au
He
Me
Op
2mm

Figure 8. Horstadius and Sellman's fate map. A) Diagram of open neural-plate stage (stage 16) *Ambystoma mexicanum* embryo with the head neural ridge divided into eight zones. Shown are the right side positions of the presumptive anterior trabeculae (AT), mandibular arch (Ma), hyoid arch (Ha), and gill arches (Ga 1, 2, 3, 4), in relation to zones 1-8. A=anterior; P=posterior. B) Diagram of the stained (shown as stippling) ectomesenchyme migrating under the epidermis along the endomesodermal mandibular, hyoid, 1, 2, and 3 + 4 gill arches. (From Horstadius and Sellman, 1946.)

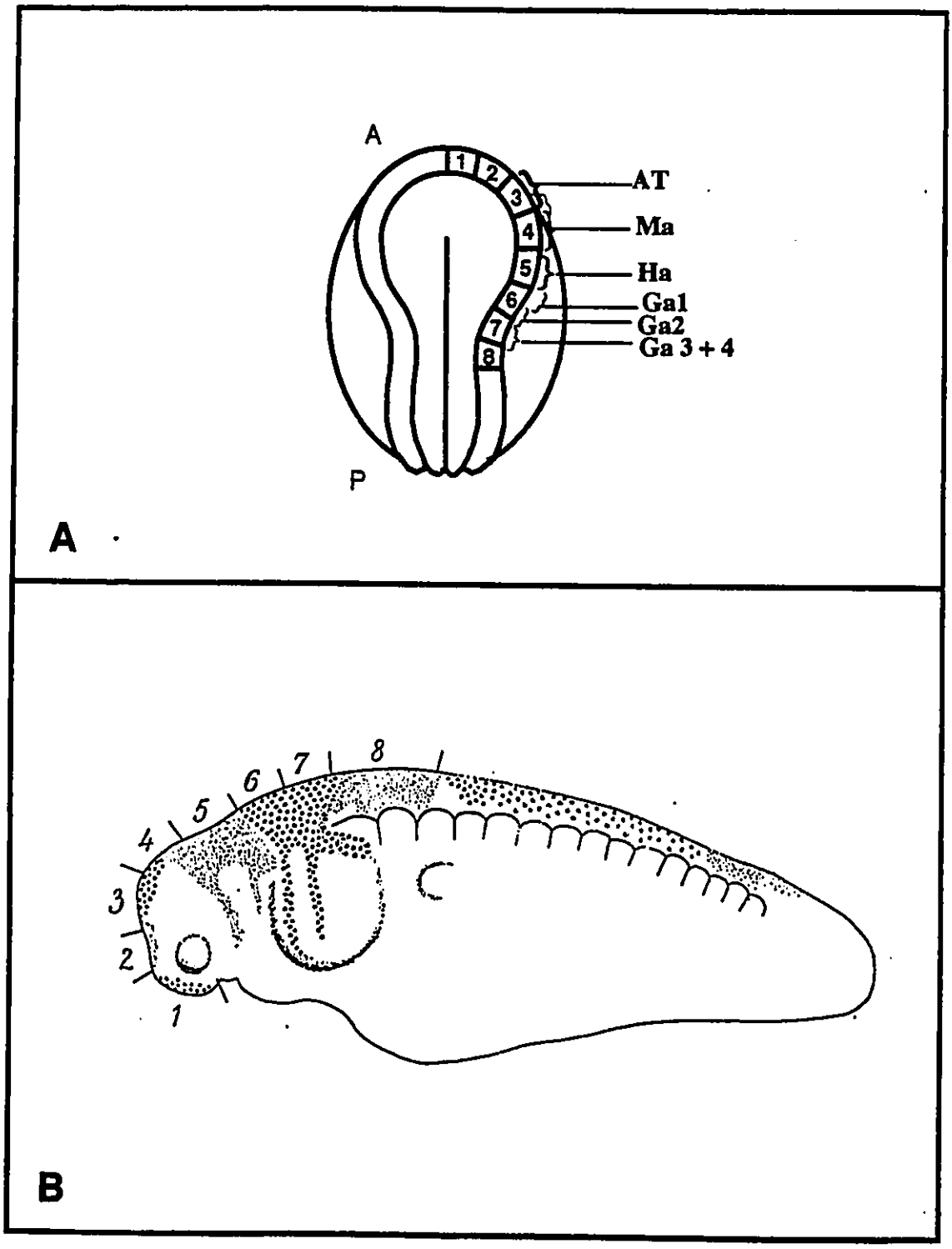
A
1
2
3
4
5
6
7
8
AT
Ma
Ha
Ga1
Ga2
Ga 3 + 4
P
A
1
2
3
4
5
6
7
8
B

Figure 9. Dorsal view of a stage 17 *Ambystoma* embryo indicating the axial levels defined by Chibon (1966). The derivatives of the neural fold between the areas defined as 30 degrees and 150 degrees from the dorsal midline were mapped. Chibon used angle measurements to designate areas of the neural fold (redrawn from Chibon, 1966). A=anterior of embryo; P=posterior of embryo.

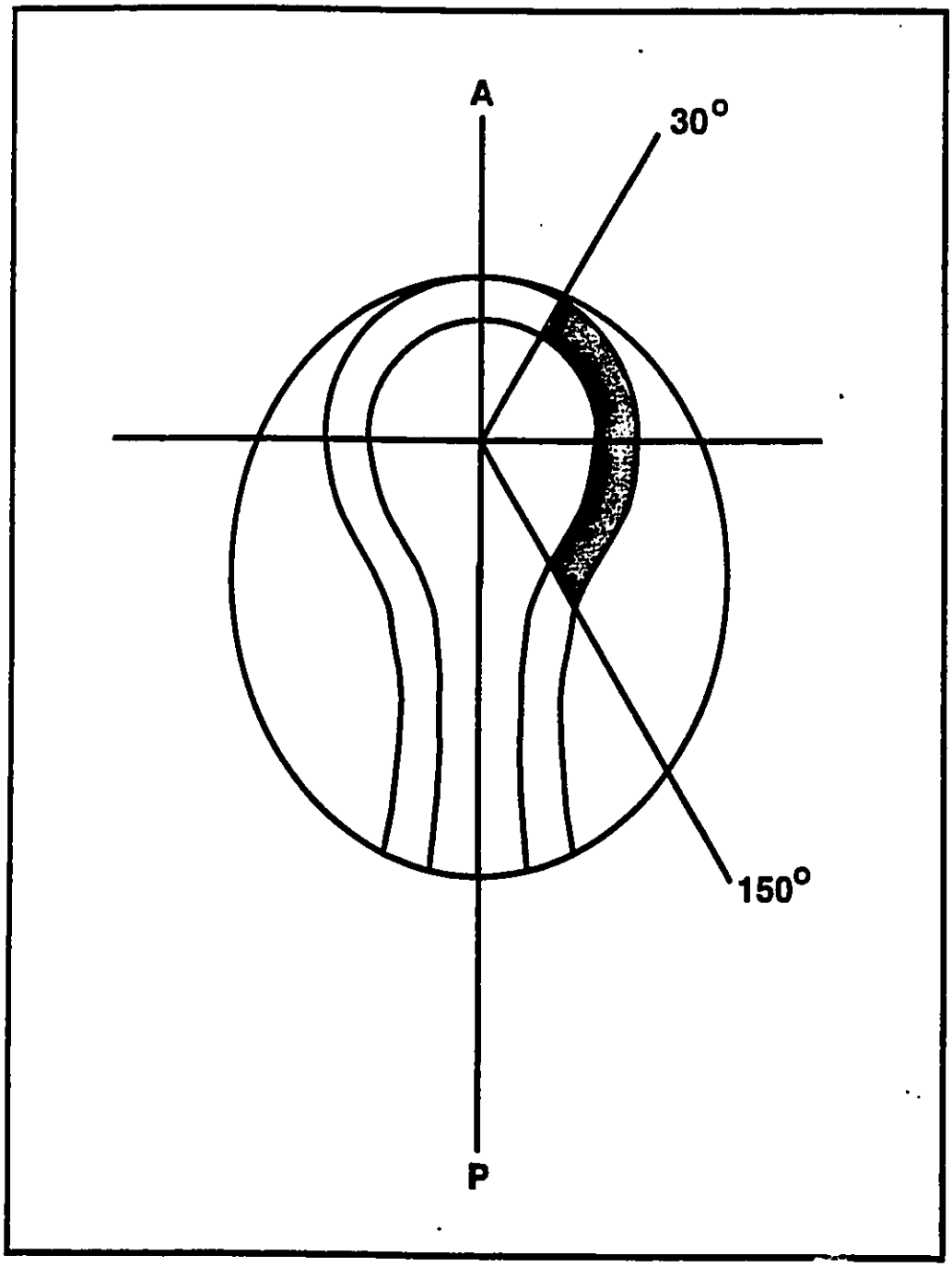
A
30°
150°
P

1.8 The Fate Map of the Cranial and Cardiac Neural Crest in the Axolotl

The purpose of this project is to define the boundaries for the cardiac neural crest in the axolotl. The cardiac neural crest plays a significant role in the development of the cardiovascular system in other vertebrates. Defects in the cardiac neural crest can lead to several congenital heart abnormalities in avians and mammals. It is for this reason that we thought it would be advantageous to investigate the cardiac neural crest in amphibians. Just as we have seen in birds and mammals, determining the role of the cardiac neural crest in amphibians may aid in elucidating the mechanisms involved in abnormal amphibian development. Keeping this thought in mind, we decided to investigate the possible connection between the cardiac neural crest and the manifestation of the premature death (*p*) mutation in the axolotl (in chapter II of this thesis).

While determining the boundaries of the cardiac neural crest, we also mapped out the fate of the cranial neural crest in the stage 20 axolotl embryo. We have found that the cardiac neural crest is located at the region defined above the first two somites in the late neurula stage embryo. The amphibian cardiac crest follows a ventral migratory pathway towards the rostral end of the endocardial cavity and goes on to form the ectomesenchymal support of the truncus arteriosis and the aortic arches. The neural crest located anterior to the cardiac crest forms the components of the cranial skeleton and the brain. The neural crest posterior to the cardiac crest does not contribute to the visceral skeletal components but forms pigment cells. Determining the fate of cranial and cardiac neural crest in the axolotl can allow us to examine further the mechanisms involved in neural crest development in amphibians and in vertebrates in general.

Materials and Methods

2.1 Embryos

Wild-type *A. mexicanum* embryos were obtained from spawnings performed at the University of Ottawa axolotl colony. The embryos were kept in small bowls containing modified 25% Holtfreter's solution (see Table 1 in Appendix I) at 18-20 °C. Developmental stages were determined using the staging table and diagrams prepared by Bordzilovskaya et al. (1989; also see Table 1 in Appendix II) for *A. mexicanum*. Stage 19-20, late neurula stage embryos (neural folds are in contact throughout but have not yet fused in the anterior region of the embryo) were used in the microinjection labelling procedure. Prior to microinjection, the jelly coat and vitelline membrane were removed from each embryo with a watchmaker's forceps. Stage 19-20 embryos were passed through one rinse in filter-sterilized 100% Steinberg's solution (see Table 2 in Appendix I) with 0.1 % gentamicin prior to being transferred to an operating dish containing filter-sterilized 100% Steinberg's solution with gentamicin. Operating dishes consisted of glass petri dishes containing a Permoplast-Paraplast mixture which was moulded to keep the embryos in place during operations (Frost et al., 1989).

2.2 Microinjection of DiI

A 0.3% stock solution of the vital dye, 1,1-dioctadecyl 3,3,3',3' tetramethylindocarbocyanine perchlorate (DiI, Molecular Probes Inc.) was made up in 30% dimethylformamide. This stock solution was further diluted in a 0.3 M sucrose solution for a final concentration of 0.03% DiI.

Borosilicate micropipets (Drummond Inc.) were pulled on a Vertical Pipette Puller Model 700C (David Kopf Instruments) to give a tip diameter of 10μm. The pipets were

attached to a microinjection apparatus similar to that described by Stephens et al. (1981). A schematic diagram of the set-up is shown in Figure 10. DiI injections were made by inserting a micropipet into the neural fold and expelling a small amount of the pink dye solution. Approximately 50-100 nl of the dye solution was injected per embryo. A Zeiss dissecting microscope was used to observe the injection.

The neural folds of each embryo were divided into five different adjacent zones from the anterior to posterior end as shown in Figure 11. Each embryo was labelled in one unilateral zone of the neural fold. Both right and left sides of the neural folds were labelled in separate embryos. Visual inspection of the embryo confirmed that the bright pink dye was confined to the area labelled. After the injection, the embryos were allowed to heal in the operating dish for approximately one hour. The injected embryos were transferred to 24-well dishes (Falcon) containing 100% Steinberg's solution with gentamicin overnight, and then transferred to 24-well dishes containing 25% Holtfreter's solution with 0.1 mg/ml penicillin and 0.1mg/ml streptomycin the next morning. The embryos were allowed to develop for approximately two weeks, until they reached stage 44-45, by which time the heart has completely developed and is beating and the visceral cartilage has completely formed. During development, the embryos were kept at 18 °C in the dark.

Figure 10. Diagram showing the experimental set-up of the microinjection apparatus. The rubber tubing is approximately 2 cm in diameter and flexible. The injection of the dye onto the embryo is done by holding the tubing and the needle with one hand and releasing the dye using the air pressure incurred when the finger hole is covered with a finger from the experimenter's other hand, all while observing the injection process through the dissecting microscope. A 3-tiered valve controls either air pushing through the needle or the vacuum sucking up the dye solution into the needle. The embryo is immobilized in the operating dish prior to injection.

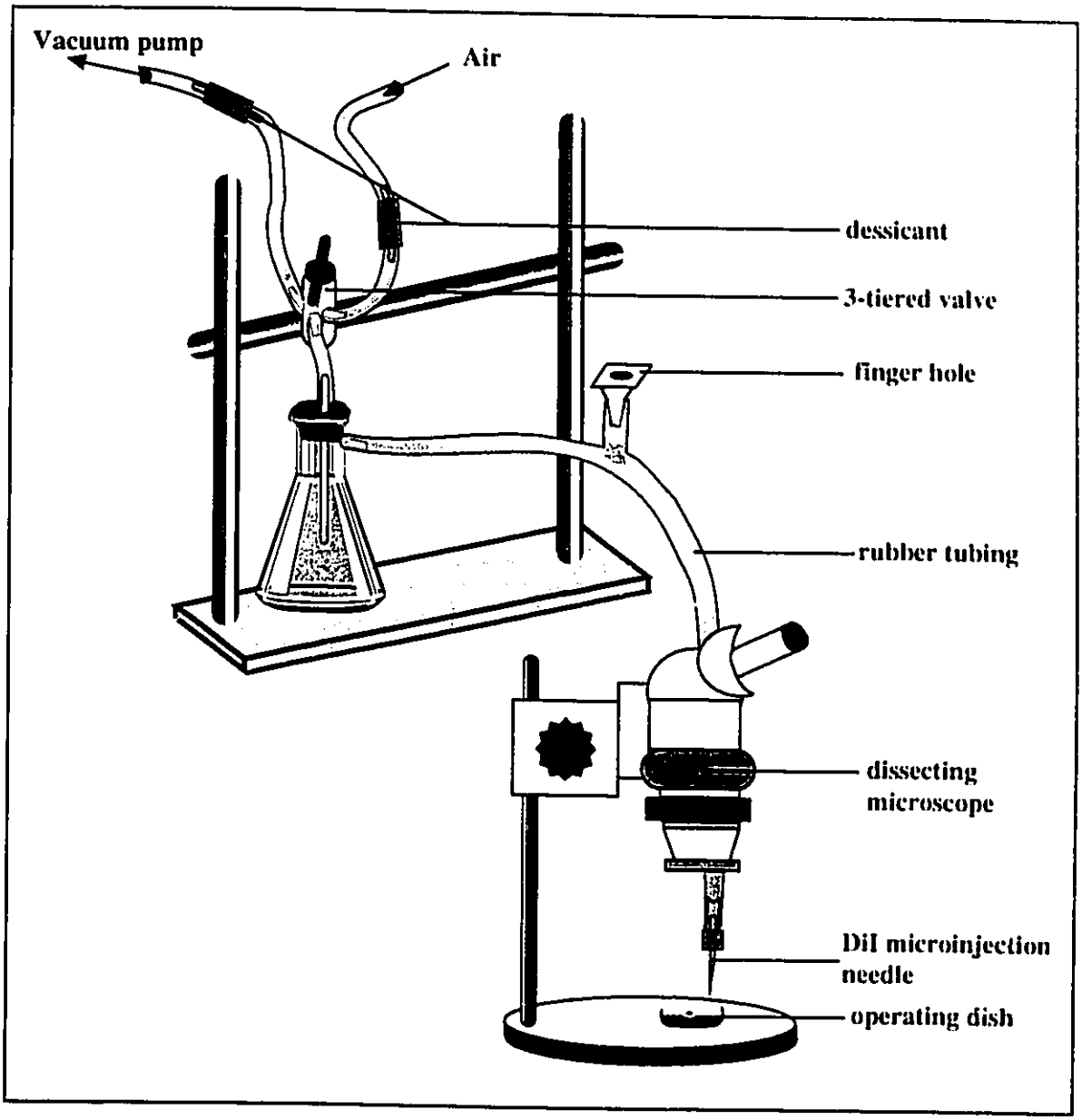
Vacuum pump
Air
dessicant
3-tiered valve
finger hole
rubber tubing
dissecting
microscope
DiI microinjection
needle
operating dish

Figure 11. Lateral view of the right side of a stage 20 axolotl embryo indicating the zones demarcated along the neural fold. Each region was defined using visible landmarks (such as indentations along the neural fold and the appearance of somites) in the embryo as reference points for the different sections. Zone "1" comprises the most anterior part of the neural fold, or the presumptive anterior forebrain region. Zone "2" refers to the fore-midbrain region of the fold. Zone "3" defines the more dorsally located mid-hindbrain region. Zone "4" indicates the extremely dorsal area marked by the first two visible somites. Sections "a" and "b" are each one somite in length. Zone "5" refers to the more posterior, straight, dorsal part of the fold which is also two somites in length. Each section was labelled individually in order to determine its particular derivatives. This diagram shows only the right neural fold. However, some embryos were unilaterally labelled in a similar fashion along the left neural fold.

Lateral View of Stage 20 Axolotl Embryo Outlining the Zones in the Neural Fold

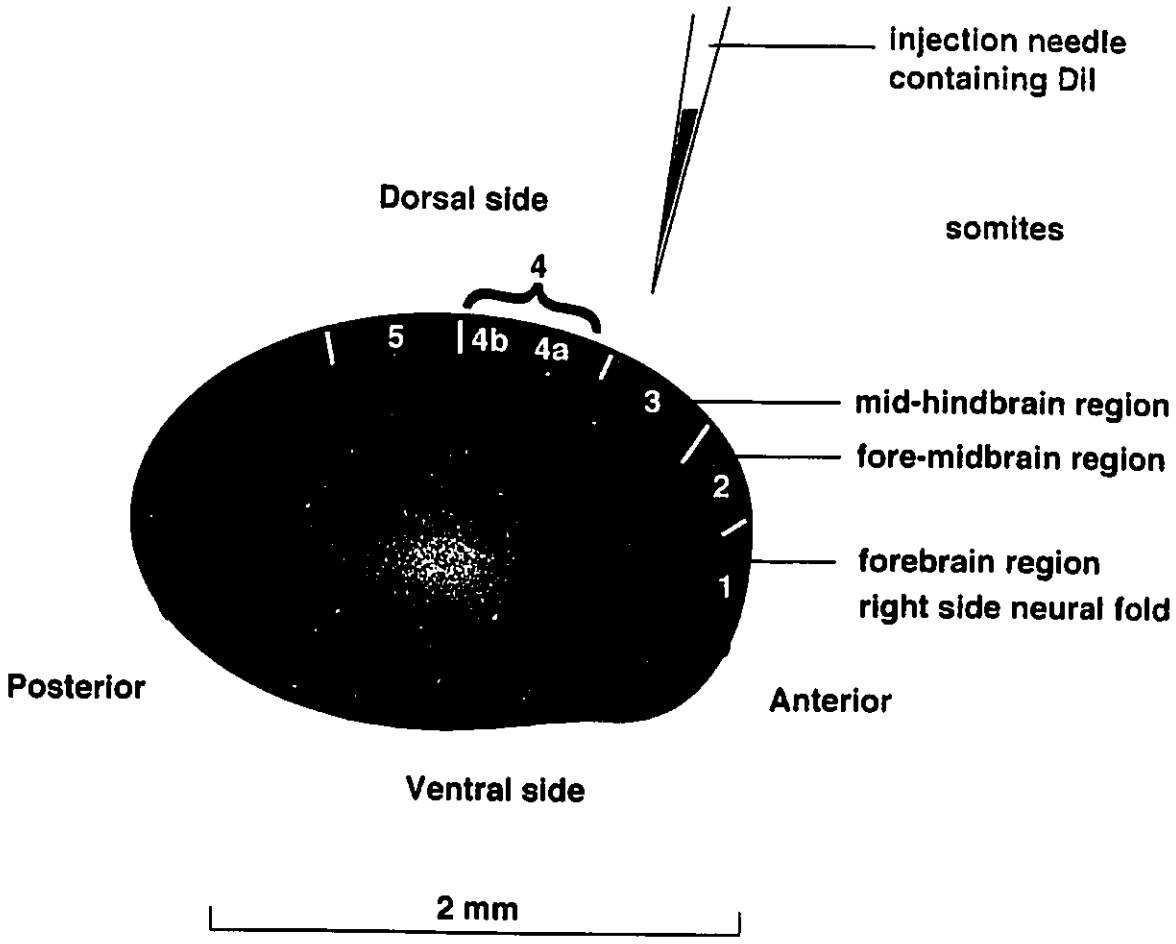

2.3 Cryostat sections and microscopy

After reaching stage 44, the control and labelled embryos were anaesthetized in 0.02% tricaine methansulfonate (MS-222, Sigma Chemical Co.), and then fixed in 4% paraformaldehyde/0.25% glutaraldehyde in PBS (phosphate buffered saline) for at least 12 hours. Embryos were rinsed three times in 1mg/ml sodium borohydride in PBS, then rinsed three times in PBS, and soaked in a 15% sucrose solution for 12 hours at 4 °C. They were embedded in a 15% sucrose/7.5% gelatin (Sigma, bloom 300) solution for 2 hours at 37°C and then rapidly frozen in liquid nitrogen. Embryos were sectioned at a thickness of 14-20 μm on an Ames cryostat. Sections were mounted on slides with Geltol (Lipshaw Immunon) and covered with glass coverslips for viewing under epifluorescence on a Zeiss Axiophot microscope and a confocal laser scanning microscope. Photographs of the sections were taken using Ilford XP2 ASA 400 film and Black's colour ASA 400. Photographs were manipulated (ie. montages and labels were created) with the Adobe Photoshop 3.0 software.

Results

3.1 DiI Labelling of the Neural Fold

Wild-type axolotl embryos were microinjected with the DiI solution upon reaching stage 19-20. The right or left neural fold was injected with the DiI solution in one of five zones defined in Figure 11[1]. The injection was made to specifically target the neural crest cells in the neural fold. Each embryo was injected with approximately 50-100 nl of the dye solution. The injection needle was inserted under the surface of the converging neural folds and the viscous liquid dye was expelled with air pressure. The dye then diffused into immediately surrounding cells. The area injected was restricted to one of the regions along the neural fold outlined in Figure 11. The bright pink dye was easily visible under the dissecting microscope. After the injection process, the embryos were allowed to heal for one hour.

To ensure that only a specific region was initially labelled, and that the dye had not diffused into neighbouring areas of the neural fold, several stage 20 embryos were fixed after the one hour healing period following the injection. The embryos were then embedded, cryosectioned and observed under the epifluorescent microscope to see the extent of the labelled area. These embryos were used as standards for the labelling procedure. The dye remained confined to the "zone" (along the anterior-posterior axis) that it was intentionally injected into, and had not diffused into a more anterior or posterior region on the fold (see Fig.12). For example, if zone 2 was labelled along the neural fold, the dye did not creep into zone 1 or zone 3.

In observing sections taken from stage 19-20 embryos, we also saw that the dye was confined to the converging neural folds and presumptive neural tube, thus primarily targeting premigratory neural crest cells. As seen in Figure 13, the region that contains the

[1] Throughout the rest of the chapter, zones "1", "2", "3", "4" and "5" refer to the regions along the neural fold of the stage 19-20 axolotl embryo defined in Figure 11 (in the Materials and Methods section).

majority of the label is the neural fold. The ability to target neural crest cells of a specified area, made the DiI labelling technique a useful method for fate mapping experiments.

Figure 12. (A) Transverse section through the anterior neural folds of a stage 19 axolotl embryo. A juxtaposition of the fluorescent image over the phase-contrast image of the same section is shown to indicate the boundaries of the dye after the injection. This embryo was injected along the left neural fold (shown on right) in zone "2" (the presumptive fore-midbrain region, see Fig. 11). The dye was targeted to the presumptive fore-midbrain region and is confined to that area. The arrows indicate the indentations in the neural fold which were used as landmarks to define the boundaries between the fore-midbrain region and the mid-hindbrain region (small arrow), and between the forebrain and fore-midbrain region (large arrow). Note that there are some cells which also got labelled on the contralateral side of the neural fold. rh=presumptive right anterior hindbrain; rm=presumptive mid and forebrain; rf=right forebrain; lh, lm, lf, indicate the same regions but on the left neural fold. Bar, 100μm. (B) Diagram of the lateral view (shown on left) and dorsal view (shown on right) of a stage 19 axolotl embryo indicating the plane of section (shown on lateral view) of the embryo in (A). a=anterior; p=posterior; d=dorsal; v=ventral.

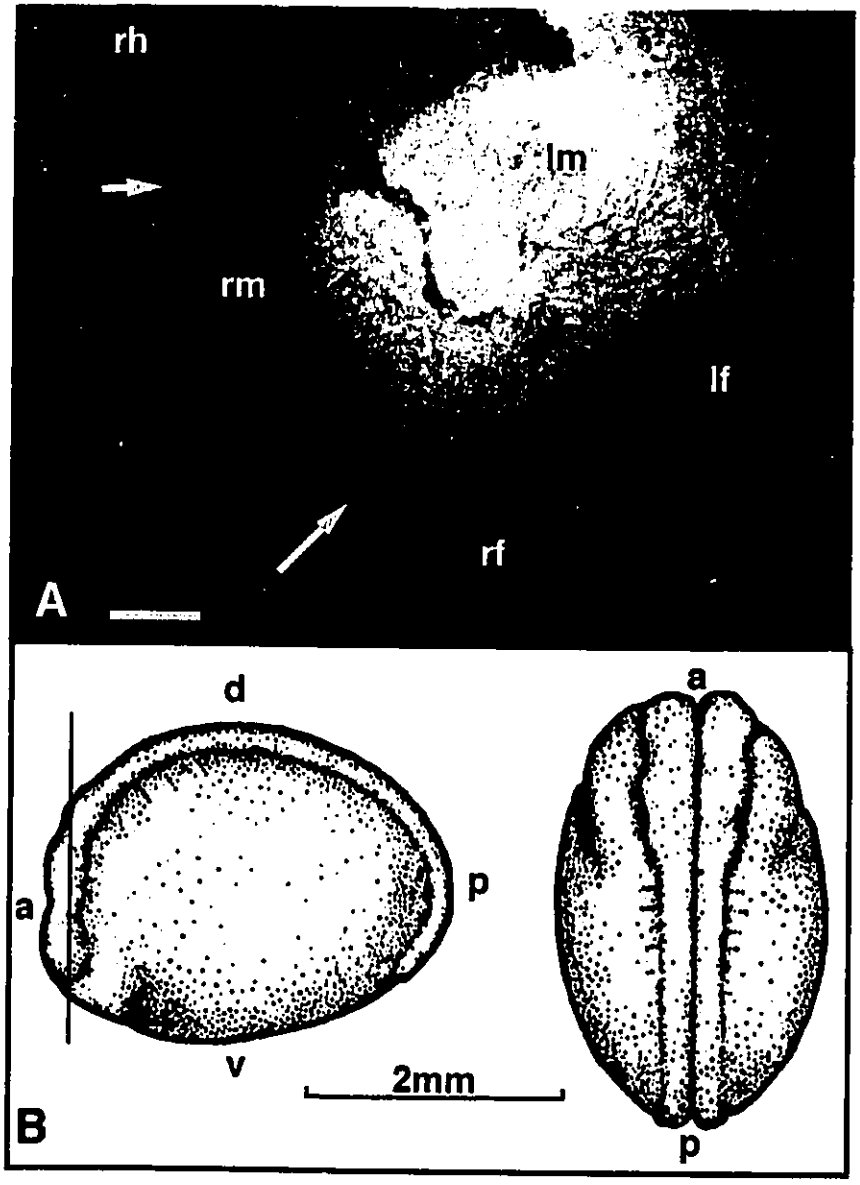
rh
lm
rm
lf
rf
A
d
a
p
v
2mm
a
p
B

Figure 13. (A), (B) Cross section through zone "4" (refer to Fig. 11) of the neural fold. Fluorescent image (A) indicates the areas in the neural fold and the neural tube (nt) labelled with DiI. This stage 19 embryo was injected in the right neural fold (rnf) in zone 4, targeting the neural crest cells (nc) of this area. (B) Phase contrast image of the same section as in (A). Bar, (A, B) , 100 μm. (C) Lateral view diagram of the right side of a stage 19 axolotl embryo indicating the plane of section in (A) and (B); a=anterior; p=posterior; d=dorsal; v=ventral.

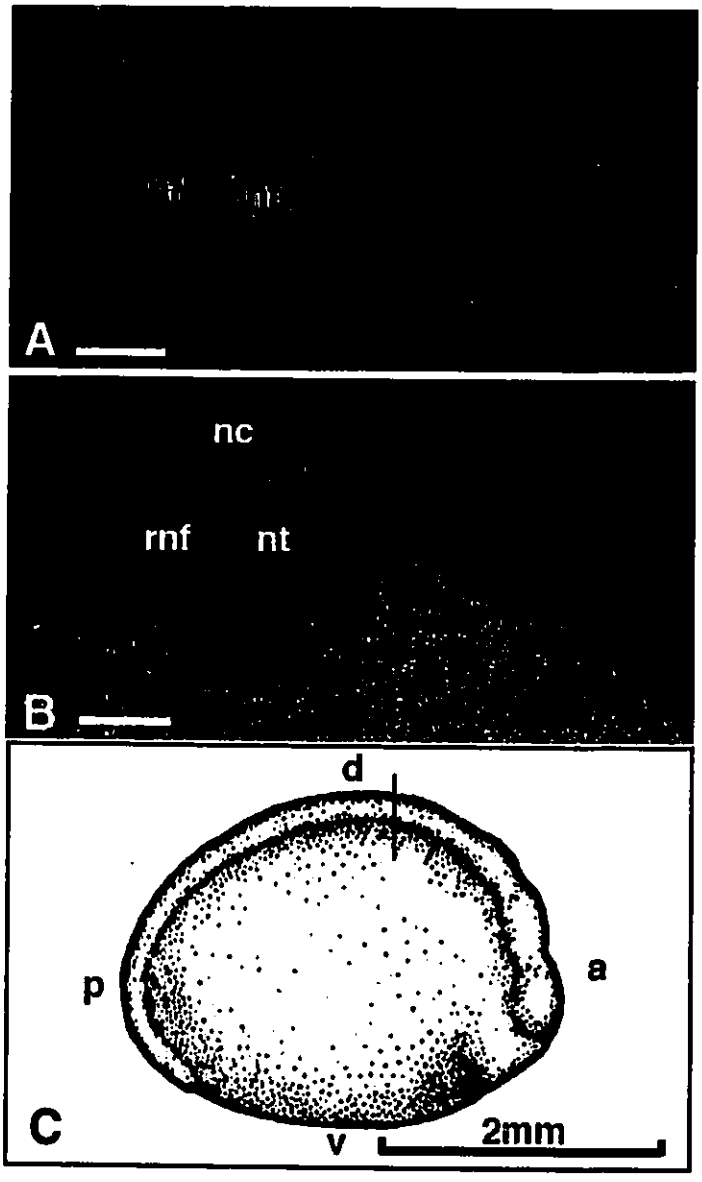
A
nc
rnf
nt
B
d
p
a
C
v
2mm

3.2 Labelling Pattern of the DiI

After the DiI microinjection, the embryos that had not been fixed at stage 20, were allowed to develop until they reached stage 44-45 (approximately 400 hours old). Upon reaching stages 44-45, at which time the cartilaginous visceral skeleton had completely formed, heart development had reached its juvenile stage, and secondary gill filaments were prominent, the embryos were anaesthetized and fixed. Following fixation, the embryos were embedded in a sucrose/gelatin solution and cryosectioned. Sections were observed under epifluorescence with either a confocal laser scanning microscope or a Zeiss Axiophot.

The DiI labelling of the neural crest derivatives was very bright and very distinct. The red fluorescent label appeared around the perimeter of the cells corresponding to labelling of the cell membrane. The label did not uniformly stain the cell membrane and the intensity of the label varied from cell to cell (see Fig. 14). We observed that not all the cells of a particular area were labelled, confirming that the dye does not diffuse between neighbouring labelled and unlabelled cells. Once DiI labels a cell, it remains in that cell and its progeny, thus making it a stable lineage label. The fluorescent label was stable for at least two weeks in living axolotl tissue, without fading.

Figure 14. The staining pattern of DiI-labelled cells of neural crest origin. (A) Phase contrast image of chondrocytic cells in the Meckel's cartilage. (B) Confocal laser scanning photomicrograph of the same chondrocytic cells as in (A) (arrows refer to two typical DiI-labelled cells). The arrows in (A) and (B) denote the same cells. Note the fluorescence around the perimeter of the labelled cells. (C) A confocal image of chondrocytic cells is shown. Note that the intensity of the DiI label varies among cells of the same region and within the individual cell. (D) Confocal image of the anterior outflow portion of the axolotl heart (h) and cells of the posterior left branchial arches. Arrow indicates one intensely labelled branchial arch cell. (E) Confocal image at higher magnification of the cell in (D). Note the labelling pattern of the cell membrane. No label is visible inside the cell. Also note that not all cells of a particular region are labelled. Scale bars for (A, B, C, and D), 100 μm; scale bar for (E), 50 μm.

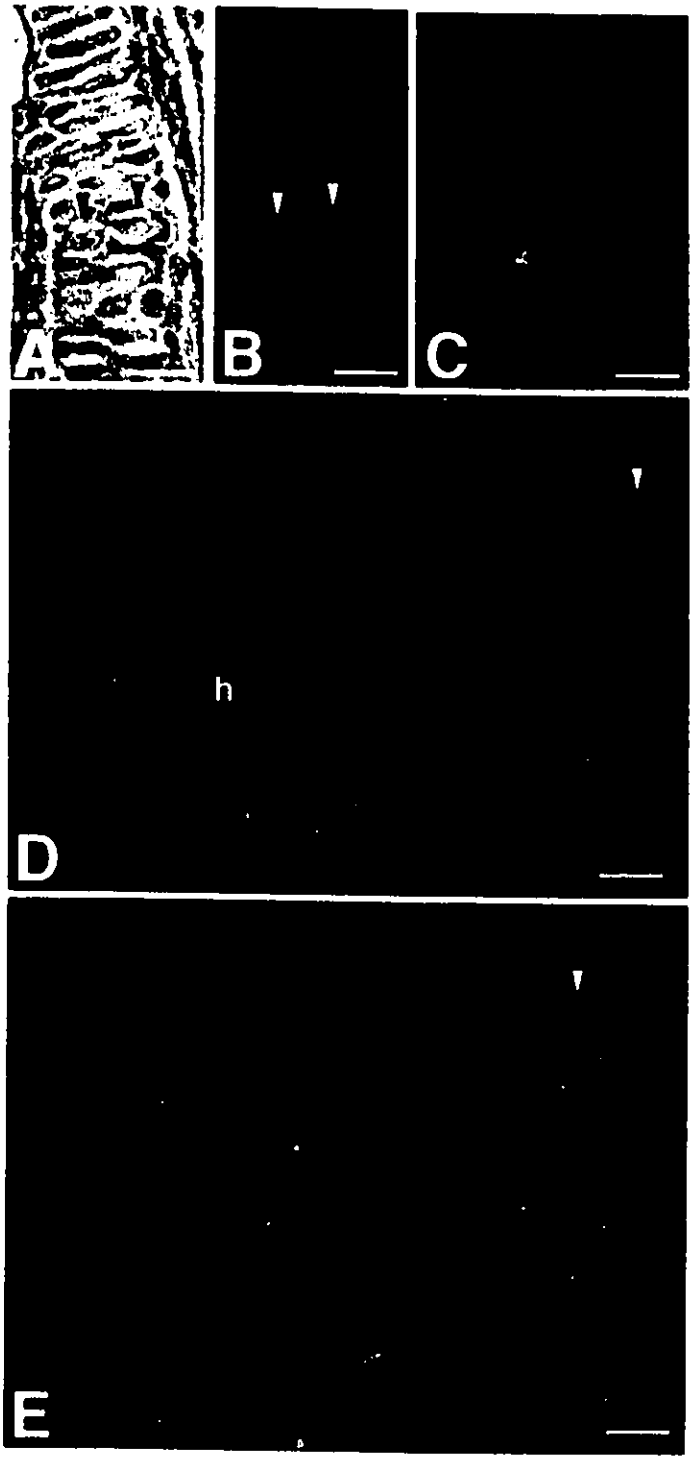
A
B
C
h
D
E

3.3 Controls

No significant abnormal development was observed in injected embryos. To ensure that the DiI was not deleterious to the development of the embryos, and that the fluorescence observed was from the vital dye, we compared the development of DiI-injected embryos to that of controls. The control embryos were injected with 30% dimethylformamide (DMF) in 0.3M sucrose (the dye solution without the DiI). The development of uninjected embryos was also observed from the same spawnings. Neither the DiI, nor the DMF injection caused any developmental problems in the embryos (see Table 1).

Sections of embryos injected with only the DiI solvent (dimethylformamide and sucrose) were observed to ensure that any significant fluorescence observed was from the DiI and not due to background fluorescence. Each control embryo was injected in a different zone (refer to Fig. 11) along the anterior neural folds. Irrespective of the zone that was injected, all embryos (at stage 45) showed some background fluorescence in the liver and the gut, but none elsewhere (see Fig. 15). The heart region did not show any type of autofluorescence (see Fig. 15H). These observations assured us that any type of fluorescence that we did see in the DiI labelled embryos, other than in the gut or the liver, was not an artifact. If any embryo did show labelling in the gut or in the liver, it was not significantly distinguishable from the background fluorescence and thus was disregarded.

Table 1. The Development and Survival of Embryos Following Microinjection.

	Total # of embryos	# of embryos with normal development (%)	# of embryos with abnormal development or that aborted (%)
Embryos injected with DiI solution (DiI + DMF + sucrose)	54	47 (87.0%)	7 (13.0%)*
Embryos injected with DMF solution (DMF + sucrose)	18	17 (94.4%)	1 (5.6%)*
Uninjected embryos	6	6 (100%)	0 (0%)*

Table 1. The development of embryos was followed after injection with the DiI solution to see whether the DiI caused any observable abnormalities in development. Control embryos consisted of those injected with only the DiI solvent [dimethylformamide (DMF) + sucrose]. No significant difference in development or survival was observed between these two classes or between uninjected embryos. These observations indicate that the DiI solution and the injection procedure did not affect embryonic development.

* Not significantly different using the Chi-square test ($p_{0.5}$).

Figure 15. Frontal sections of stage 45 "control" embryos injected with only dimethylformamide and sucrose (DiI solvent). These embryos were observed to test the degree of autofluorescence in the axolotl embryo. (A) Phase contrast image of the liver (l) in a stage 45 embryo. (B) Fluorescent image of the same section as in (A). Note the dim autofluorescence in some hepatocytes.
(C) Phase contrast image of the the posterior cartilages of the visceral skeleton. (D) Fluorescent image of the same section as in (C). Note the lack of fluorescence in any of the cartilaginous elements. For (C and D): (mc). Meckel's cartilage; (ba), branchial arch; (hb), hypobranchial. (E) Phase contrast image of the lumen of the gut (g). (F) Fluorescent image of the same section as in (E). Note the autofluorescence in the enteric region. (G) Phase contrast image of the anterior portion (truncus arteriosis) of the heart (h).
(H) Fluorescent image of the same section as in (G). Scale bars for (A-H), 100 μm. For all panels the anterior of the embryo is at the top of the plate.

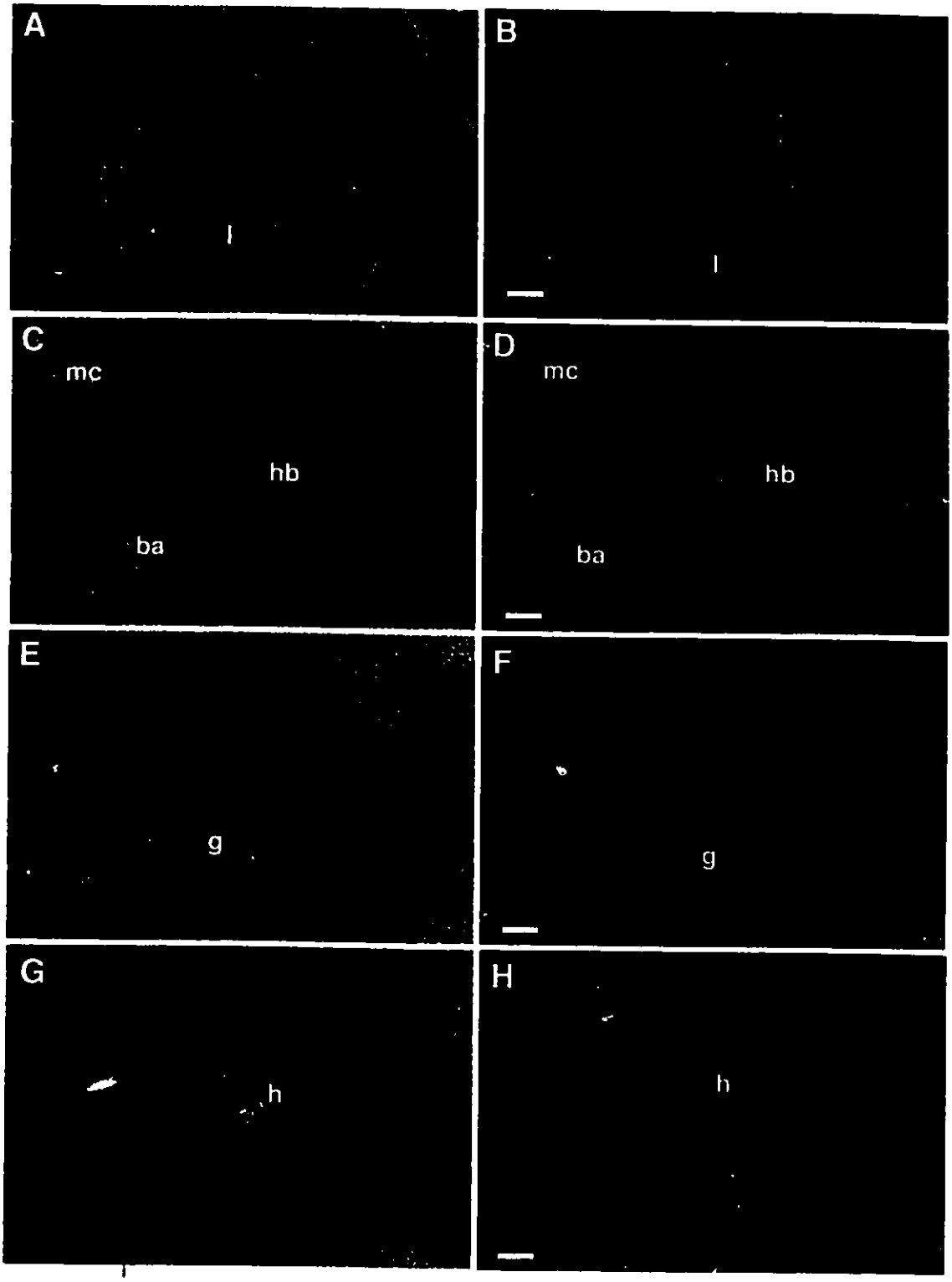
A
l
B
l
C
mc
hb
ba
D
mc
hb
ba
E
g
F
g
G
h
H
h

3.4 General Results after Labelling the Five Neural Fold Zones

Typical lineage labelling experiments were performed in which DiI was injected into one of five zones (defined in Fig. 11) along the amphibian neural fold in the hopes of determining the derivatives of the cranial neural crest and neural tube. Stage 20 embryos were injected and stage 44-45 larvae were observed for fluorescently labelled cells. The derivatives and progeny of the originally labelled neural cells exhibited a bright red fluorescence around the cell membrane. The following three tables (Tables 2, 3, and 4) give an account of our general results. The tables outline the numbers of embryos that were labelled in each zone and the number of times fluorescently labelled cells were detected in a particular element. Each cartilaginous element, brain region, or other organ was scored positive if five or more distinct cells in that element were fluorescently labelled in that area.

Using the Chi-squared statistic, we found that finding labelled cells in a particular region is dependent on the zone of the neural fold that was originally stained. In other words, neural crest and neural tube derivatives have a specific fate depending on their origin along the antero-posterior location along the neural tube. The following tables give a quantitative account of our results. In the tables, each zone comprises of embryos that were labelled on either the right or left neural fold. We found that both sides of the neural fold produced the same derivatives, so the data was pooled. Table 2 indicates the neural crest derivatives of the cranial skeleton. Table 3 outlines the contribution of different zones of the neural fold to different sections of the brain, and Table 4 shows the non-cartilaginous and non-neuronal derivatives of the neural crest. A detailed description of the outcome of labelling the different neural fold zones is given in the sections following the tables. Our original goal of identifying the cardiac neural crest was achieved. We found that it was located at the posterior end of the cranial neural fold--in zone "4".

Table 2. The Frequency of Fluorescent Labelling in Cranial Skeletal Elements after Injection of Different Neural Fold Zones.

		Number (%) of embryos exhibiting labelling in the various cranial skeletal elements										
Zone initially labelled	Number of Embryos Examined per Zone	Meckel's cartilage		Basibranchials and Hypobranchials	Trabeculae (cornu,anterior)	Palatoquadrates	Hyoid Arch (ceratohyal and hypohyal)	Branchial arches				
		anterior	posterior					1	2	3	4	
1	6	0 (0%)	0 (0%)	0 (0%)	0 (0%)	0 (0%)	0 (0%)	0 (0%)	0 (0%)	0 (0%)	0 (0%)	*
2	10	10 (100%)	8 (80%)	2 (20%)	10 (100%)	10 (100%)	9 (90%)	1 (10%)	0 (0%)	0 (0%)	0 (0%)	*
3	8	3 (37.5%)	7 (87.5%)	6 (75%)	4 (50%)	2 (25%)	6 (75%)	8 (100%)	8 (100%)	8 (100%)	2 (25%)	*
4	15	0 (0%)	0 (0%)	1 (6.7%)	0 (0%)	0 (0%)	0 (0%)	1 (6.7%)	8 (53%)	15 (100%)	15 (100%)	*
5	8	0 (0%)	0 (0%)	0 (0%)	0 (0%)	0 (0%)	0 (0%)	0 (0%)	0 (0%)	0 (0%)	0 (0%)	*

Table 2. The number of times fluorescence was detected in a specific cranial skeletal element per zone at stage 45 is shown. The percentage of embryos per zone exhibiting fluorescence in a particular element is also indicated. A positive score was given to each element containing more than five individually labelled cells. Zone 1 cells did not contribute to any cartilaginous element. Zone 2 cells were found in the Meckel's cartilage, the trabeculae, the hyoid arch and the palatoquadrates. Zone 3 neural crest cells were found in almost every element of the cranial skeleton. Zone 4 cells contributed to the branchial arches while zone 5 cells did not form any cartilaginous element.
*The elements containing the labelled cells were significantly dependent on the zone that was originally labelled ($P_{0.5}$).

Table 3. The Frequency of Fluorescent Labelling in the Brain after Injection of Different Neural Fold Zones.

Zone initially labelled	Number of Embryos Examined per Zone	Number of embryos (%) showing labelling in the brain regions					
		Prosencephalon		Mesencephalon	Rhombencephalon	Spinal cord	
		anterior	posterior				
1	6	6 (100%)	2 (33.3%)	0 (0%)	0 (0%)	0 (0%)	*
2	10	1 (10.0%)	10 (100%)	3 (30.0%)	0 (0%)	0 (0%)	*
3	8	0 (0%)	4 (50.0%)	8 (100%)	0 (0%)	0 (0%)	*
4	15	0 (0%)	0 (0%)	0 (0%)	15 (100%)	0 (0%)	*
5	8	0 (0%)	0 (0%)	0 (0%)	0 (0%)	8 (100%)	*

Table 3. The number of times fluorescence was detected in a particular region of the brain per zone at stage 45. The percentage of embryos exhibiting fluorescently labelled cells in a particular brain region per zone is also indicated. Zone 1 cells contributed to the anterior prosencephalon. Zone 2 neural cells contributed largely to the posterior prosencephalon. Zone 3 cells to the mesencephalon and zone 4 to the rhombencephalon. Zone 5 derivatives were only found in the spinal cord. Each time fluorescence was detected in a particular region, a positive score was counted.
* The region of the brain that labelling appears in is significantly dependent on the zone that was labelled ($P_{0.5}$).

Table 4. The Freqency of Fluorescent Labelling in a Particular Organ or Cell Type after Injection of Different Neural Fold Zones.

Zone initially labelled	Number of Embryos Examined per Zone	Number (%) of embryos showing labelling in the heart		Number (%) of embryos showing labelling in other cell types			
		Anterior (truncus and conus)	Posterior (ventricle and atrium)	Liver and Gut	Mesenchyme	Pigment cells	
1	6	0 (0%)	0 (0%)	3 (50%)	4 (66.7%)	1 (16.7%)	*
2	10	0 (0%)	0 (0%)	7 (70%)	10 (100%)	7 (70%)	*
3	8	1 (12.5%)	0 (0%)	6 (75%)	8 (100%)	4 (50%)	*
4	15	13 (87%)	0 (0%)	15 (100%)	15 (100%)	8 (53.3%)	*
5	8	0 (0%)	0 (0%)	7 (87.5%)	6 (75%)	7 (87.5%)	*

Table 4. The number of times fluorescence was detected in a particular organ or cell type per zone. The percentage of embryos exhibiting fluorescently labelled cells in a particular organ or cell type (at stage 45) is also shown. Zone 4 cells contribute to the anterior heart. All the cells also formed mesenchyme and pigment cells.
* The organ or cell type that contained labelled cells was significantly dependent on the zone that was originally labelled ($P_{0.5}$).

3.5 The Fate of Cells From Zone "1" of the Anterior Neural Fold

DiI injected embryos were sectioned upon reaching stage 44-45. Embryos that had initially been labelled at stage 20, in the most rostral right or left neural fold (zone 1) displayed fluorescently-labelled cells in the anterior forebrain region at stage 45. The original neural fold cells of zone 1 developed into the neuronal network of the anterior prosencephalon (see Fig. 16).

No labelled cells were found in any other region of the embryo. Cells from zone 1 did not contribute to any cartilaginous structure of the cranial skeleton or to any other organ rudiment. Zone 1 cells did not have any chondrocytic derivatives. This can be seen by the lack of labelling in the trabeculae (see Fig. 16). These results indicate that the anterior neural fold cells from zone 1 are restricted to form only neuronal derivatives in the prosencephalic region. This suggests that these neural fold cells have a limited fate and do not migrate a great distance from their point of origin.

Three embryos were labelled in zone 1 of the left neural fold, and three embryos were labelled in zone 1 of the right neural fold. The cells on one side of the neural fold largely remained on that side. For example, cells labelled on the left neural fold in zone 1 (at stage 20) later comprised cells of the left half of the prosencephalon, while cells labelled on the right neural fold were located in the right half of the prosencephalon (see Fig. 16). This indicated that there was little crossover between cells from the anterior-most contralateral folds. Our results show that, in general, cells from zone 1 form the neuronal cells of the anterior forebrain.

Figure 16. The fate of zone "1" cells. (A) Phase contrast image of a frontal section through the anterior prosencephalon (pro) of a stage 45 embryo. This embryo was initially labelled in zone "1" along the left neural fold; (at), anterior trabeculae. (B) Fluorescent image of the same section as in (A). The label is found in the left half (shown on right, since ventral view) of the anterior prosencephalon (pro). No label was found in any other area. Bar (A and B), 100 μm. (C) Diagram of stage 45 axolotl embryo showing the plane of section in (A) and (B). Arrow indicates the head region depicted in (A) and (B). In (A) and (B) the anterior of the embryo is at the top of the plate.

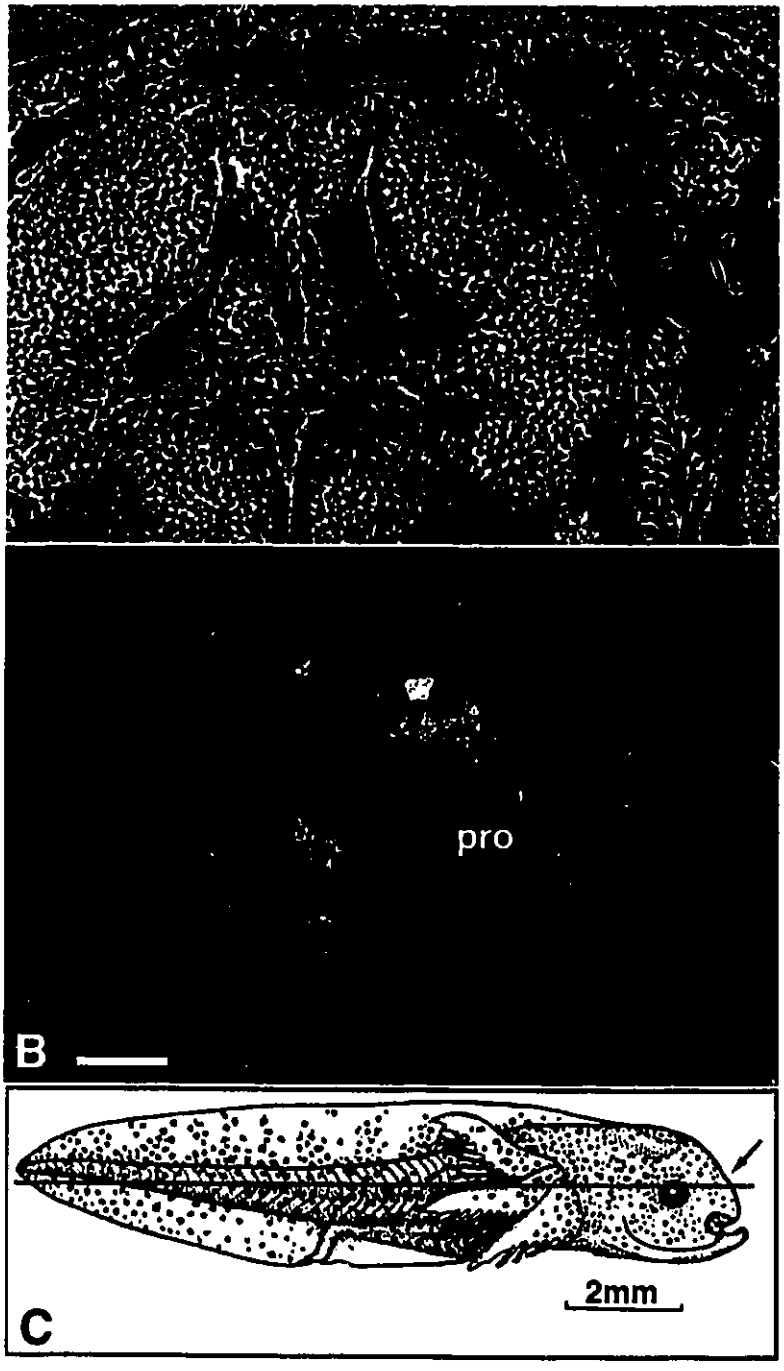
pro
B
2mm
C

3.6 The Fate of Cells from Zone "2"

The cranial neural crest cells that were labelled in zone 2, on either the right-side neural fold or the left side neural fold, contributed in a large part to the visceral skeleton of the head. These cells also made up most of the posterior forebrain region in the stage 45 larva.

The cartilaginous element of the visceral skeleton that contained the most cells from zone 2 was the Meckel's cartilage. Neural crest cells which were labelled in zone 2 migrated ventrally to form chondrocytic cells of the anterior Meckel's cartilage (see Fig. 17). Cells labelled on the right side of the fold contributed mainly to the right half of the Meckel's cartilage, while those cells labelled along the left-side neural fold contributed to the left half (see Fig. 17). However, cells from the right-side neural fold also made a minor contribution to the left half of the Meckel's cartilage and vice-versa.

Zone 2 cells also contributed to the ceratohyal cartilage, and to elements of the neurocranium (see Fig. 18). In Figure 18, we have shown that the neural crest cells end up as chondrocytes of the cornu and anterior trabeculae, but do not contribute to the posterior elements of the neurocranium such as the posterior trabeculae or the basal plate. Both the left and the right halves of the neurocranium showed signs of labelling even if only one side of the neural fold was initially dyed. This indicates that there was substantial crossover between cells of parallel folds. The other cartilaginous elements of the visceral skeleton that zone 2 cells contributed to were the palatoquadrates (see Fig. 19).

Non-cartilaginous elements of the head were also derived from zone 2 neural crest cells. There was bright labelling in the craniofacial mesenchyme, the pigment cells of the head and in cranial ganglia (see Fig. 19).

With respect to the brain region, zone 2 neural crest derivatives were highly concentrated at the forebrain-midbrain border. Labelled cells were scattered throughout the prosencephalic region but were concentrated more dorsally and posteriorly, in the telencephalon (see Fig. 20). As we have shown previously, zone 1 cells also form the

neuronal network of the prosencephalon. Our results show that the forebrain region is made up of a combination of cells from both zone 1 and zone 2. Zone 1 cells have a more anterior neuronal fate, while zone 2 cells are generally located in a more caudal position.

Surprisingly, the mesencephalon (midbrain) contained very few cells from zone 2. This suggests that in the stage 20 embryo, the region along the neural fold demarcated as zone 2 (refer to Fig. 11), does not totally consist of presumptive midbrain cells, but contains cells which remain in the posterior region of the prosencephalon. From our results (also see Table 3), we have shown that cells from zone 2 contribute to many areas of the anterior brain. Labelled neuronal cells were largely concentrated around the forebrain-midbrain junction, but some cells were also scattered more anteriorly in the prosencephalon and posteriorly in the mesencephalon. These results suggest that the fate of zone 2 cells is not severely restricted to a highly specialized location of the brain.

In Figure 20, we noticed that both sides of the brain contained labelled cells. This observation suggests that cells from one side of the fold can also contribute to elements on the contralateral side. However, it may be possible that at the time of the labelling procedure, some of the dye could have labelled the contralateral side of the fold of the same zone (as seen in Fig. 12).

The neuronal derivatives of zone 2 cells are not only confined to the brain. Very bright labelling of neural cells was also seen in the optic nerve (see Fig. 20) and in certain cranial ganglia (see Fig. 19). In summary, we have shown that zone 2 cells contribute to the majority of the cranial skeletal elements anterior to the branchial arches and to the posterior forebrain.

Figure 17. Zone "2" cells in the Meckel's cartilage. (A) Confocal laser scanning image of a frontal section of the right half (ventral view shown) of the Meckel's cartilage in a stage 45 axolotl embryo. This embryo was labelled along the right neural fold in zone "2". Note the presence of the red fluorescent label in the chondrocytic cells of the Meckel's cartilage (mc). Most of the labelled cells were found in the right half of the cartilage, rather than the left. (B) Phase contrast image of the same section as seen in (A); (mc), Meckel's cartilage. Scale bars (A and B), 100 μm. (C) Diagram of the head of a stage 45 axolotl embryo indicating the location of the plane of section shown in (A) and (B). In (A) and (B), the anterior end of the embryo is at the top of the plate.

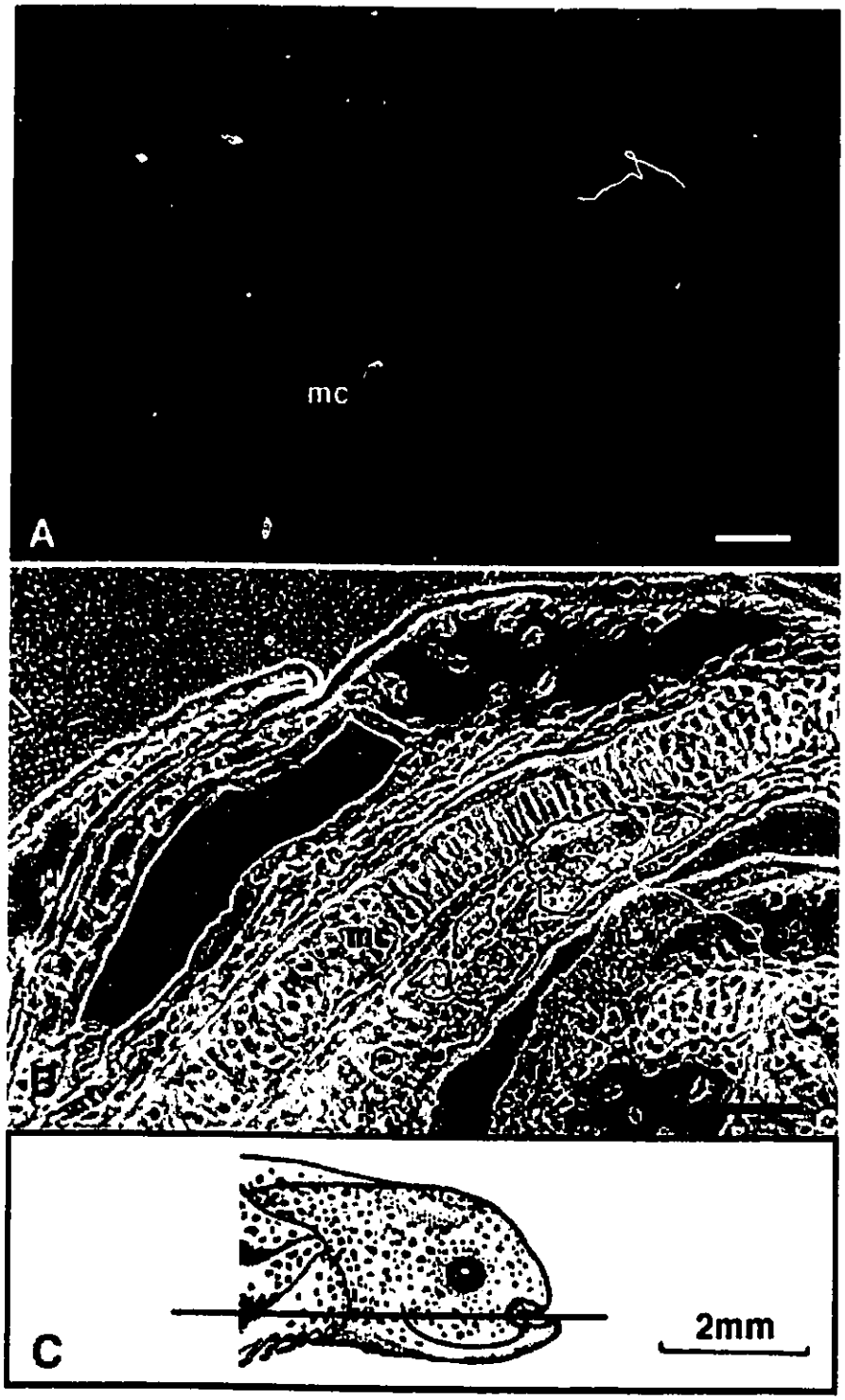
mc
A
B
C
2mm

Figure 18. Labelled cranial neural crest cells from zone "2" in the neurocranium and the hyoid arch. (A) Frontal section of the head of a stage 45 axolotl embryo (phase contrast image; ventral view). This embryo was initially labelled along the right neural fold in zone "2". For (A) and (B): (at), anterior trabeculae; (ct), cornu trabeculae; (bp), basal plate; (cl), ceratohyal; (ol), olfactory vesicle; (e), eye; (p), posterior trabeculae. (B) Fluorescent image of the same section as in (A). Labelled cells (indicated by arrows) are seen in the anterior trabeculae (at), and the cornu trabeculae (ct), but not in the basal plate (bp). Labelled cells are also seen in the left (shown on right) ceratohyal cartilage (cl) of the hyoid arch. Other labelled cells represent craniofacial mesenchyme, concentrated around the olfactory vesicles (ol), and eye (e). Scale bars (for A and B), 200 μm. (C) Diagram of a stage 44-45 axolotl head, indicating the plane of section for (A) and (B).

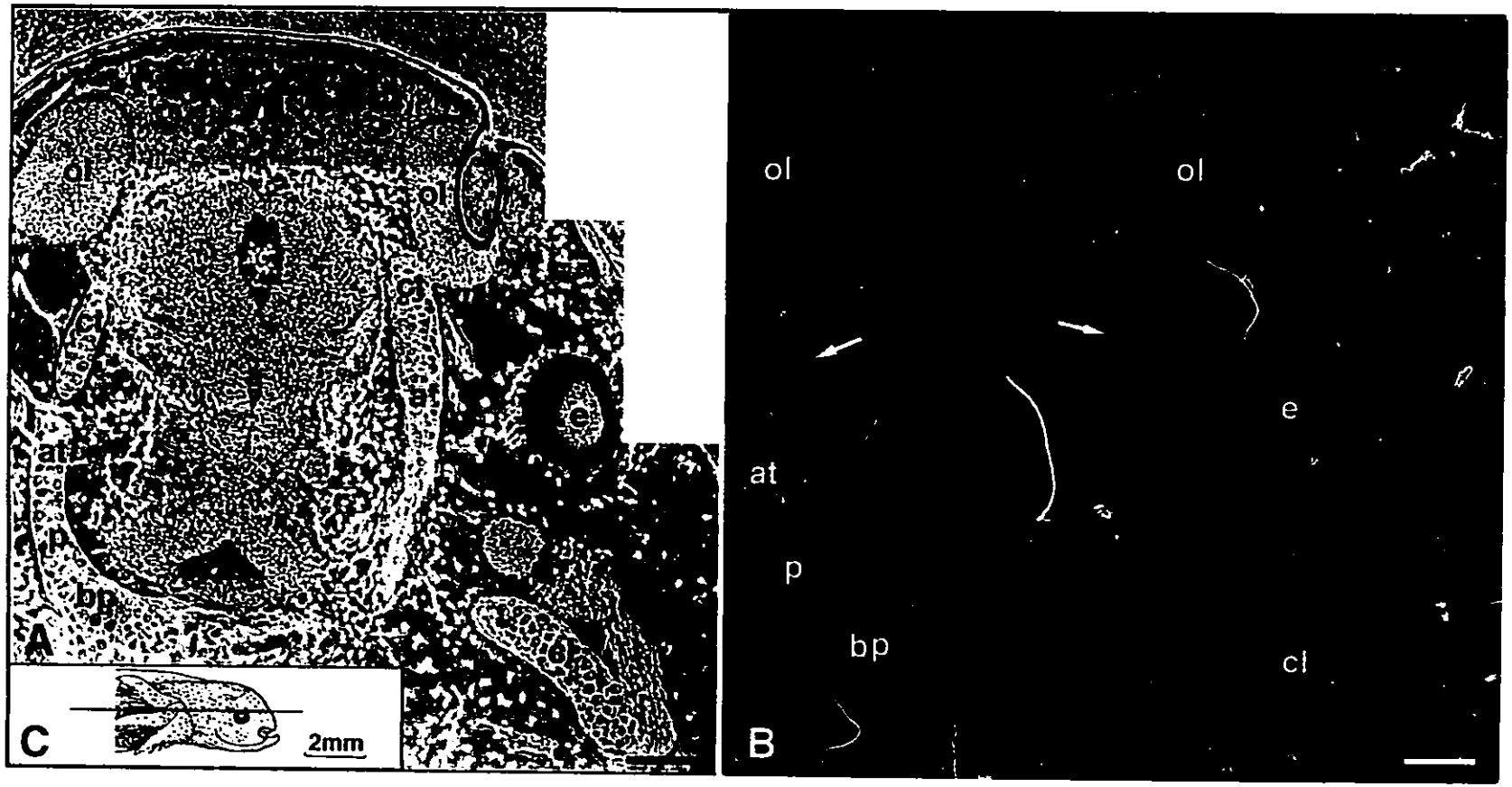
ol
ol
e
at
p
bp
A
C
2mm
ol
ol
e
at
p
bp
cl
B

Figure 19. Labelled cells from zone "2" contribute to the development of the palatoquadrates, cranial pigment cells, and cranial ganglia. (A) Frontal section through the right side of the head of a stage 45 axolotl larva. Phase contrast image (ventral view) indicating the location of the palatoquadrate (pq), mesenchyme (m), tissue surrounding the optic cup (o), cranial ganglia (cn), and pigment cells (arrows). (B) Fluorescent image of the same section as in (A). Labelled neural crest cells originally from zone 2 form the chondrocytes of the palatoquadrate (pq), the mesenchyme (m) and neuronal tissue surrounding the optic cup (o), and certain cranial ganglia (cn). Zone 2 cells also contribute to the pigment cells of the head (arrow). This embryo was originally labelled in zone "2" along the right neural fold. Scale bars (A and B), 100 µm. (C) Schematic drawing of the head of a stage 44-45 axolotl indicating the location of the plane of section in (A) and (B). In (A) and (B), the anterior end of the embryo is at the top of the plate.

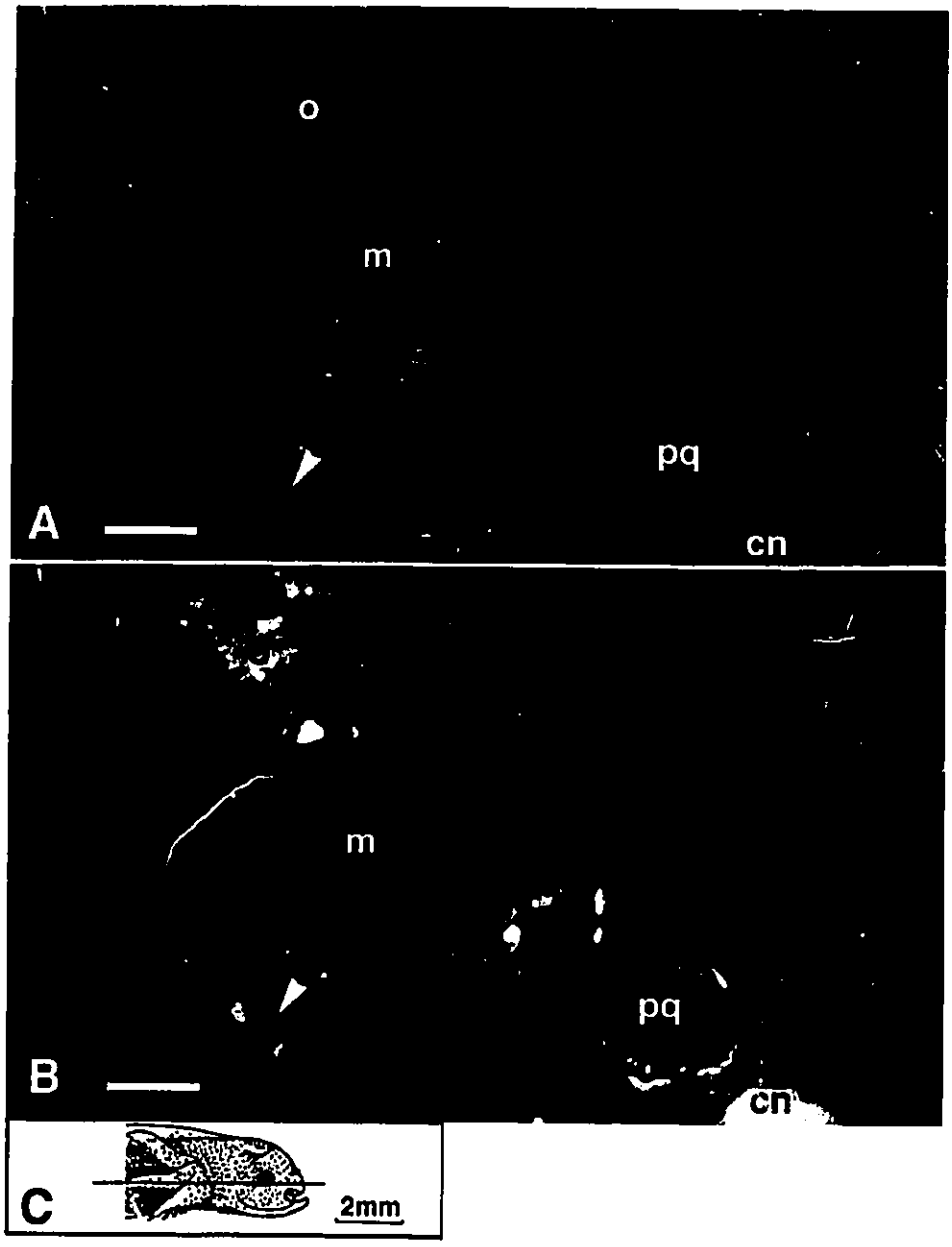
o
m
pq
A
cn
m
pq
B
cn
C
2mm

Figure 20. The contribution of zone "2" neural fold cells to the posterior forebrain. (A) Frontal section through the brain region of a stage 45 axolotl (phase contrast image shown; ventral view). This section indicates the location of the prosencephalon (pro), the forebrain-midbrain junction, referred to as the telencephalon (tel), the optic nerve (op), and the anterior trabeculae (at).
(B) Fluorescent image of the same section as in (A). Labelled cells are seen throughout the prosencephalic region (pro) but are highly concentrated at the posterior end of the forebrain or the telencephalon (tel). The cells are highly concentrated at this region which marks the boundary between the forebrain and the midbrain. There is substantial label in both hemispheres of the brain, even though this particular embryo was labelled along the left neural fold in zone 2. There is also significant labelling of the optic nerve (op) and of the anterior trabeculae (at). Scale bars (A and B), 100 μm. (C) Schematic drawing of the head of a stage 44 axolotl embryo indicating the plane of section for (A) and (B). The arrow indicates the location along the body-axis of the section shown in (A) and (B). In (A) and (B) the anterior end of the embryo is at the top of the plate.

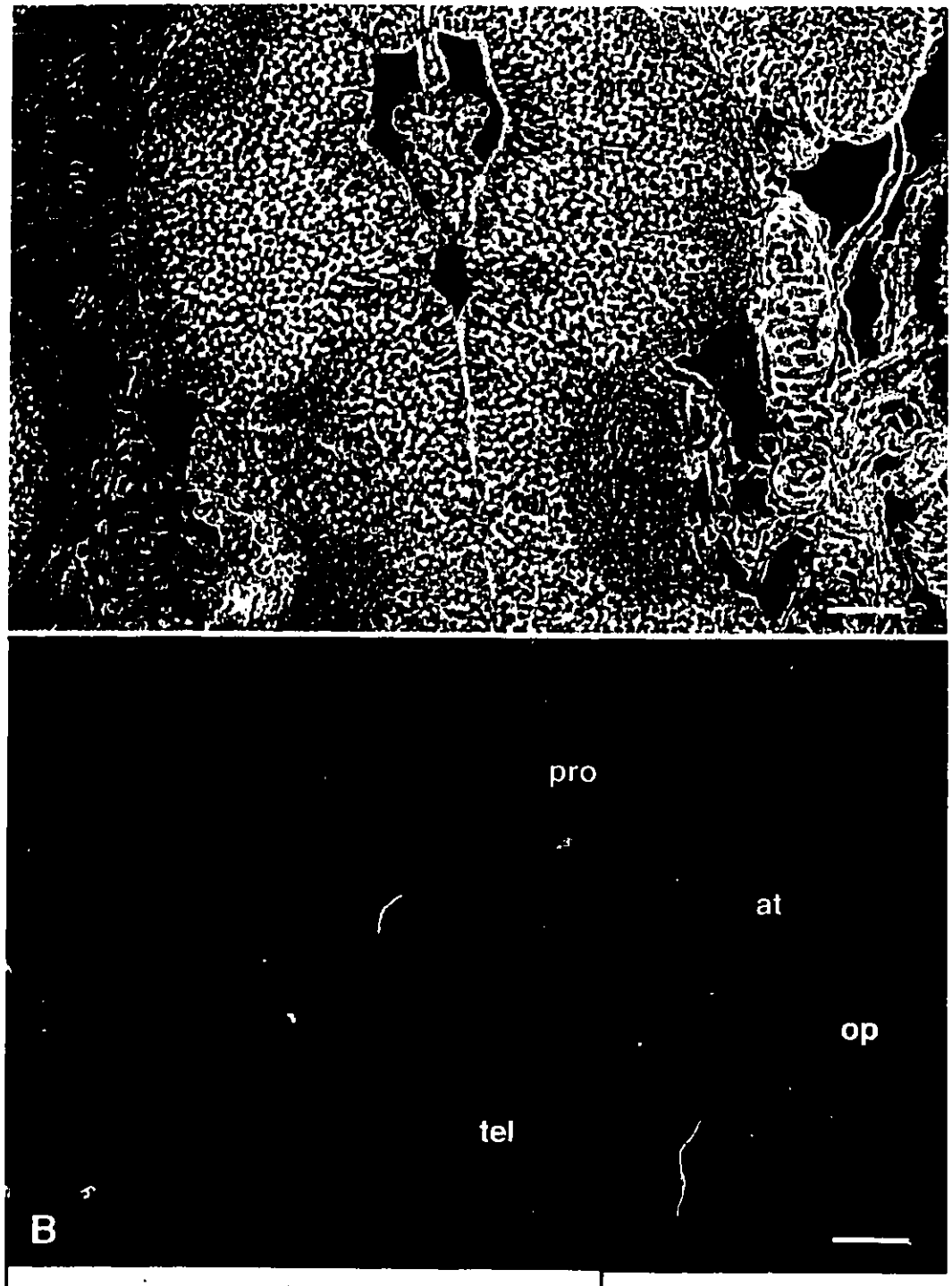
pro
at
op
tel
B
2mm
C

3.7 The Fate of Neural Fold Cells from Zone "3"

Neural fold cells originating from zone "3" of the stage 20 axolotl embryo had migrated primarily towards the branchial arches of the cranial skeleton. However, some neural crest cells, albeit a very small number, were also found in the hyoid arch and in the posterior end of the Meckel's cartilage (refer to Table 2 for general results).

The labelled cells populating the branchial arches were concentrated in the first, second and third branchial arch (see Figs. 21A and 21B). The labelled neural crest-derived cells formed the chondrocytic core of the branchial arches. Interestingly, hardly any labelled chondrocytes were seen in the more posteriorly located fourth branchial arch. Figure 21B shows the typical labelling pattern of the chondrocytes in the branchial arches of the stage 45 axolotl. In this figure, no fluorescence was detected in the chondrocytes of the fourth branchial arch. This suggests that the neural crest cells of zone 3 migrate ventrally towards the first three branchial arches and do not migrate posteriorly enough to target the fourth gill arch.

Zone 3 cells also made a minor contribution to other cranial cartilaginous elements (see Fig. 21C-F). As seen in Figure 21D and 21F, fluorescently labelled chondrocytes were seen in the ceratohyal, the first hypobranchial, and in the posterior Meckel's cartilage. These results suggest that each element of the cranial skeleton is not specified by only one small area along the neural fold. We have shown that the Meckel's cartilage comprised of cells from both zone 2 and zone 3. Zone 2 cells contributed to the more anterior portion of the element, while zone 3 contributed to the posterior portions of the element. These results suggest that the location of the derivatives along the antero-posterior axis of the embryo also plays a hand in establishing which zone contributes to which portion of a particular element.

Figure 21. Frontal sections of stage 44 axolotl embryos through the cranial skeleton after zone 3 labelling (ventral views shown); (a and p) in all the images, refer to the antero-posterior axis of the embryo. (A) Phase contrast image showing the left branchial arches; (ba1), first branchial arch; (ba2), second branchial arch; (ba3), third branchial arch; (ba4), fourth branchial arch. (B) Fluorescent image of the same section as in (A), through the branchial arches. Note the labelling in the chondrocytic core of the first three branchial arches (ba1, ba2, ba3, respectively). Some labelling is also seen around the epithelia of the first three branchial arches. No labelling is observed in the fourth branchial arch (ba4). This embryo was originally labelled in the left neural fold in zone 3. (C) Phase contrast image through the hyoid arch; (mc), Meckel's cartilage; (ch), ceratohyal; (hb), hypobranchial 1; (bb), basibranchial 1. (D) Fluorescent image of the same section as in (C). Note the presence of labelled cells in the posterior end of Meckel's cartilage (mc), the ceratohyal (ch), and hypobranchial 1 (hb). Few labelled cells were found in these regions compared to the branchial arches. Although the labelling shown is in the right-side elements, this embryo was originally labelled along the left neural fold in zone 3. (E) Phase contrast image through the left-side ceratohyal (ch) and posterior end of Meckel's cartilage (mc). (F) Fluorescent image of the same section as in (E). Labelling is shown in the posterior end of Meckel's cartilage and the ceratohyal cartilage (ch). This embryo was originally labelled in the left side neural fold in zone 3. Scale bars (A-F), 100 μm.

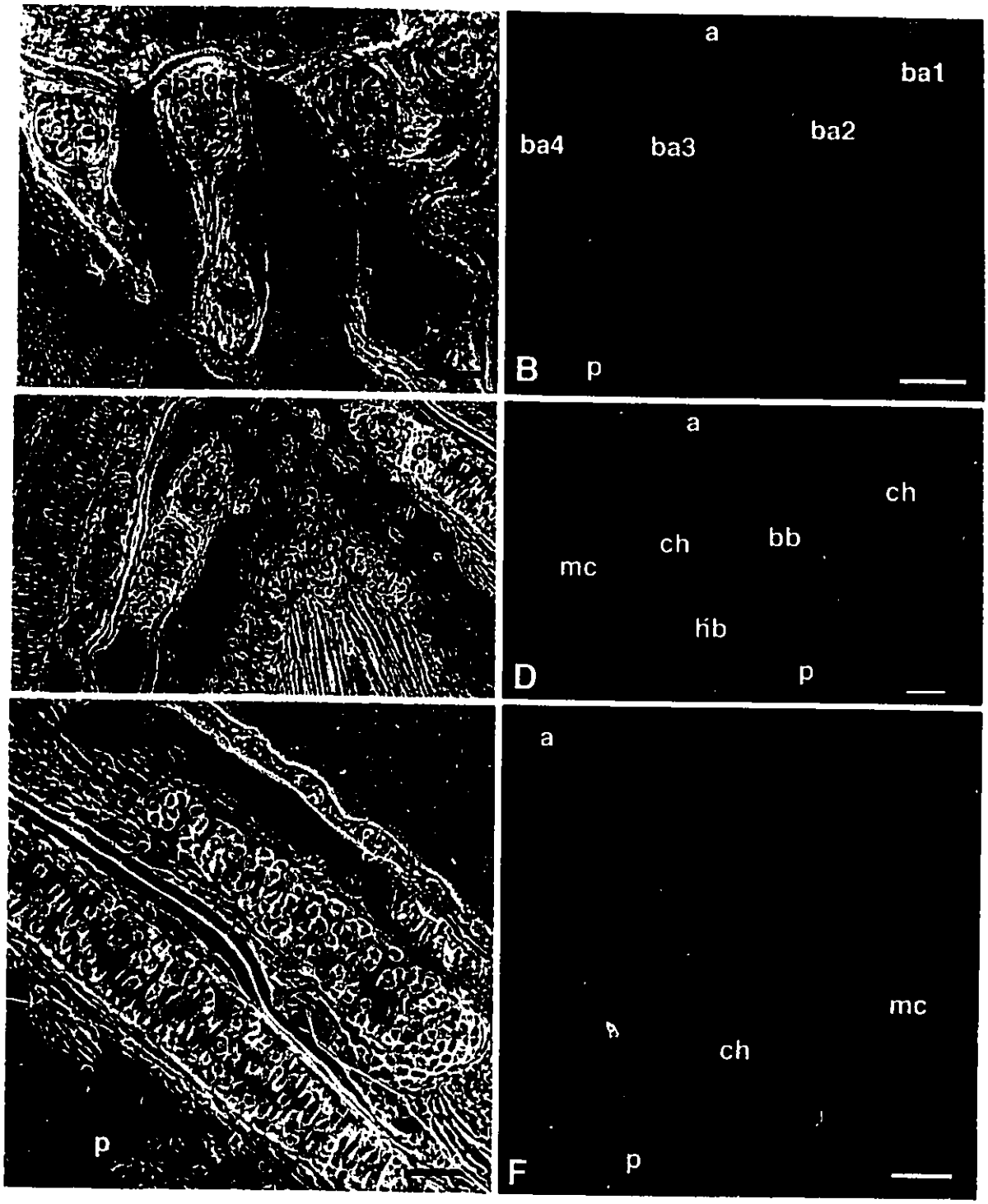
a
ba1
ba2
ba4
ba3
B
p
a
ch
ch
bb
mc
hb
D
p
a
mc
ch
F
p

The brain region that zone 3 cells corresponded to was the midbrain region (see Fig. 22). The intense fluorescence observed in Figure 22B, indicated that the mesencephalon is highly populated with neuronal cells from zone 3. Our observations indicate that zone 3 cells contribute more to the midbrain region than the cranial skeleton. As expected, cranial pigment cells were also of neural crest origin (see Fig. 22).

Figure 22. Labelled cells from zone 3 are located in the mesencephalon. (A) Frontal section through the midbrain of a stage 44 axolotl embryo (phase contrast image; ventral view shown). The mesencephalon, (me) located posterior to the prosencephalon is shown. A dark cranial pigment cell is also shown (arrow). (B) Fluorescent image of the same section as in (A). Note the intense labelling of neuronal cells in the right half of the mesencephalon, (me). This particular embryo was labelled along the right neural fold in zone 3. Also note the labelling of cranial pigment cells (arrow). Scale bars (A and B), 100 μm. (C) Schematic drawing of a stage 44 axolotl head indicating the plane of section shown for (A and B). Arrow indicates the region along the antero-posterior axis of the section in (A and B). In (A) and (B), the anterior end of the embryo is at the top of the plate.

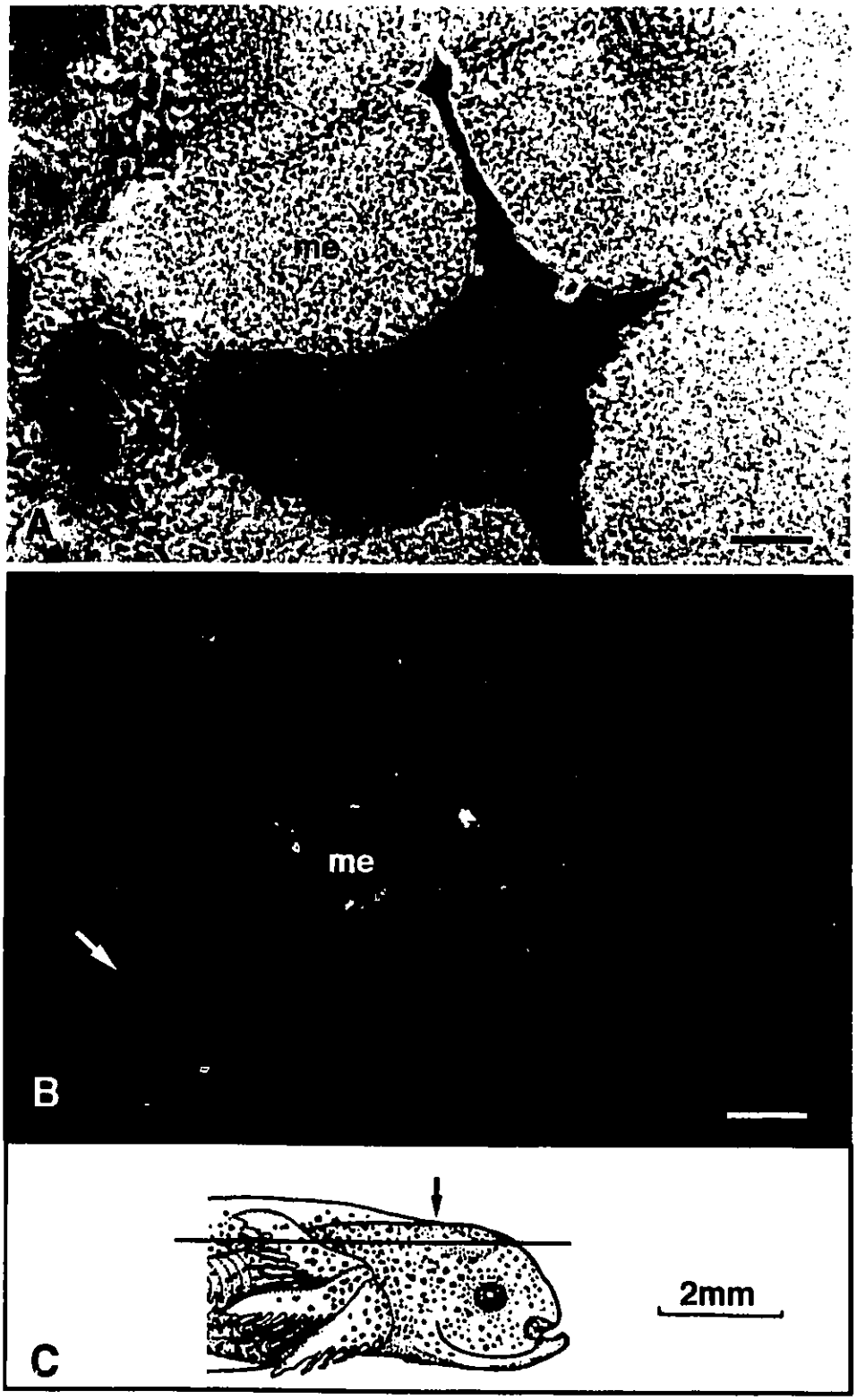
me
A
me
B
2mm
C

3.8 The Fate of Neural Crest Cells from Zone 4: The Isolation of the Cardiac Crest

The prime objective of the fate mapping experiments performed in this chapter was to identify the location and role of the cardiac neural crest in the axolotl. This was accomplished through DiI labelling of the neural fold and detecting the presence of fluorescently labelled cells in the cardiac cavity later in development. Fluorescent cells were detected in the developing pericardial cavity only after cells from zone 4 (refer to Figure 11) had been labelled. Zone 4 includes the neural fold cells located at the boundary between the cranial and trunk neural folds. This section of the fold is dorsally located on the stage 20 axolotl embryo and was arbitrarily demarcated as two somites in length.

Neural crest cells from this region migrated ventrally to contribute to the formation of the anterior outflow tract and lining of the heart (see Fig. 23). At stage 45 of development, the truncus arteriosis (anterior to the conus) is responsible for arterial blood flow. The large aortic arches branching off from the truncus arteriosis were lined with labelled ectomesenchymal cells of neural crest origin (see Fig. 24). These cells provided structural support to the hollow aortic tubes. Labelled cells were found in the aortic arches in both sides of the heart regardless of the neural fold side that was labelled. The walls of the truncus arteriosis itself were also populated with labelled crest cells (see Fig. 23 and Fig. 25B). These cells were scattered throughout the walls of the truncus and appeared to provide structural support. In 3/15 embryos, the walls of the conus arteriosis also contained labelled cells (see Fig. 25B). However, the more posteriorly located ventricle and atrium walls were not labelled (see Fig. 25E).

Neural crest cell derivatives from zone 4 were also detected as labelled chondrocytes in the third and fourth branchial arches of the stage 44-45 embryo (see Fig. 25B and 25E). Very few labelled chondrocytes were found in the second branchial arch (see Table 2). A "stream" of labelled cells connected the truncus arteriosis outflow tubes to the fourth and third branchial arches (see Fig. 25B). These labelled cells represented the

ectomesenchymal component of the aortic arches, as opposed to the mesodermal component.

In the brain, cells from zone 4 of the neural fold were found in the rhombencephalon (hindbrain) of the stage 45 axolotl embryo (see Fig. 26). Craniofacial mesenchyme surrounding the otic vesicle, as well as cranial pigment cells were also derived from the zone 4 neural fold.

No labelling was found in any region other than what we have mentioned above. As opposed to other vertebrates, no labelling was detected in the thymus or the parathyroids. It is possible however, that these elements had not become sufficiently distinguishable by stage 44.

The presence of fluorescently labelled cells in the anterior portion of the heart after the labelling of zone 4 of the neural fold, strongly suggests that zone 4 is the location of the cardiac neural crest in the axolotl embryo. Zone 4 was defined as a two-somite long region along the dorsal neural fold. To narrow down the exact boundary of the cardiac neural crest, zone 4 was further divided into two sections (area 4a and area 4b), each one somite in length (refer to Fig. 11). Stage 20 embryos were labelled with DiI in either area 4a or 4b of the neural fold. Three embryos were labelled in zone 4a and four embryos were labelled in zone 4b. (The data from these embryos were pooled with the rest of the data from zone 4 in Tables 2, 3 and 4.) The location of the labelled cells with respect to the developing heart was examined. No difference was detected between the labelling patterns of cells originally labelled in area 4a as opposed to 4b. Both areas contributed to the same elements of the cardiac outflow tract and to the posterior branchial arches. Therefore, we can assume that the cardiac neural crest extends throughout the whole length of zone 4, which passes over two somites along the neural fold.

In our experiments we did notice, however, that the embryos labelled on the right side of the zone 4 neural fold consistently displayed a larger number of labelled cells in the truncus arteriosis and the aortic arches than the left-side fold (4 embryos were labelled on

the right fold and 4 were labelled on the left). However, both sides of the fold contributed to the same elements (ie. the walls of the aortic arches on either side of the embryo) regardless of the side the element was located. This suggests that the right-side neural fold contributes more to the cardiac crest than the left neural fold.

Figure 23. The location of zone "4" cells in the heart region. (A) Frontal section through the anterior portion of a stage 44 axolotl heart (phase contrast image, ventral view is shown). The truncus arteriosis, (ta), is the most anterior region of the heart from which the major arteries branch off. Blood flows towards the gill arches (arrows indicate the direction of blood flow); (rta), right-side aortic arch; (lta), left-side aortic arch. (B) Confocal laser scanning image of the section shown in (A). Note the brightly fluorescing cells (arrowheads) in the outflow arteries and in the lining of the truncus arteriosis. These cells represent the cardiac neural crest in the axolotl. Scale bars (A and B), 100 μm. In (A) and (B), the anterior end of the embryo is at the top of the plate.

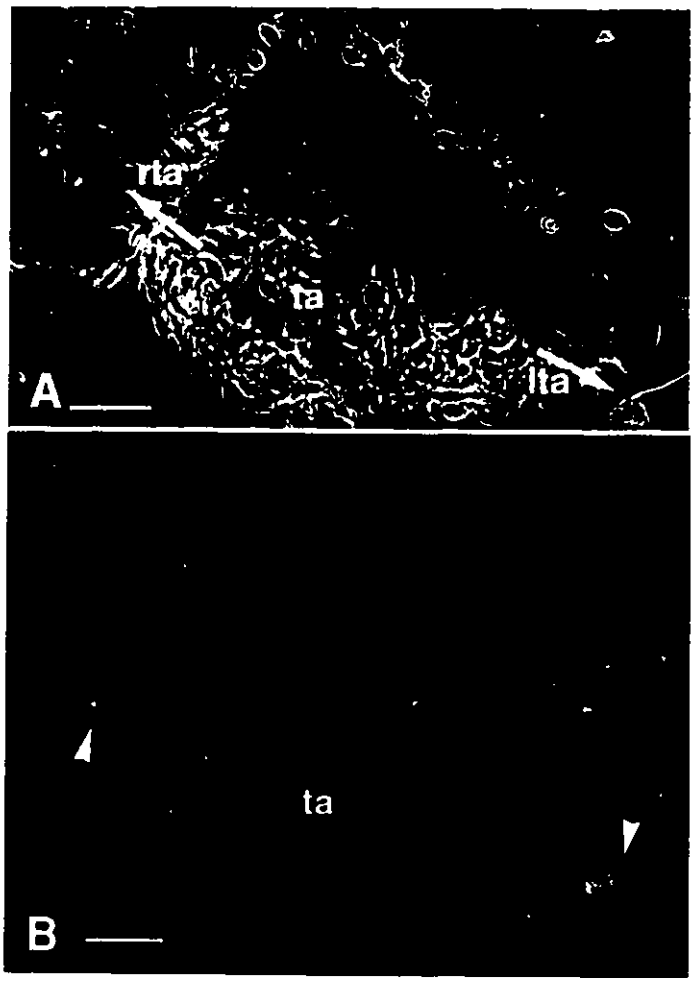
rta
ta
lta
A
ta
B

Figure 24. Cells lining the arterial walls are of neural crest origin. (A) Confocal laser scanning image (higher magnification than Fig. 23) of the aortic arch emerging from the right side of the truncus arteriosis seen in Figure 23. DiI-labelled cells (fluorescing red around the periphery of the cell), are seen to provide support for the walls surrounding the hollow arterial tubes. Arrow indicates a typical ectomesenchymal cell of neural crest origin. (B) Phase contrast image of the same frontal section as seen in (A). Arrow refers to the same labelled cell as in (A). (C) Confocal image (higher magnification) of the left aortic arch seen in Figure 23. The fluorescently labelled cells are shown to provide support for the aortic arches on both sides of the embryo. This embryo was initially labelled along the right neural fold in zone 4. Arrow indicates an intensely labelled cell lining the arterial tube. (D) Phase contrast image of the same section as in (C). Arrow refers to the same ectomesenchymal cell labelled in (C). Scale bars (A-D), 10 μm.

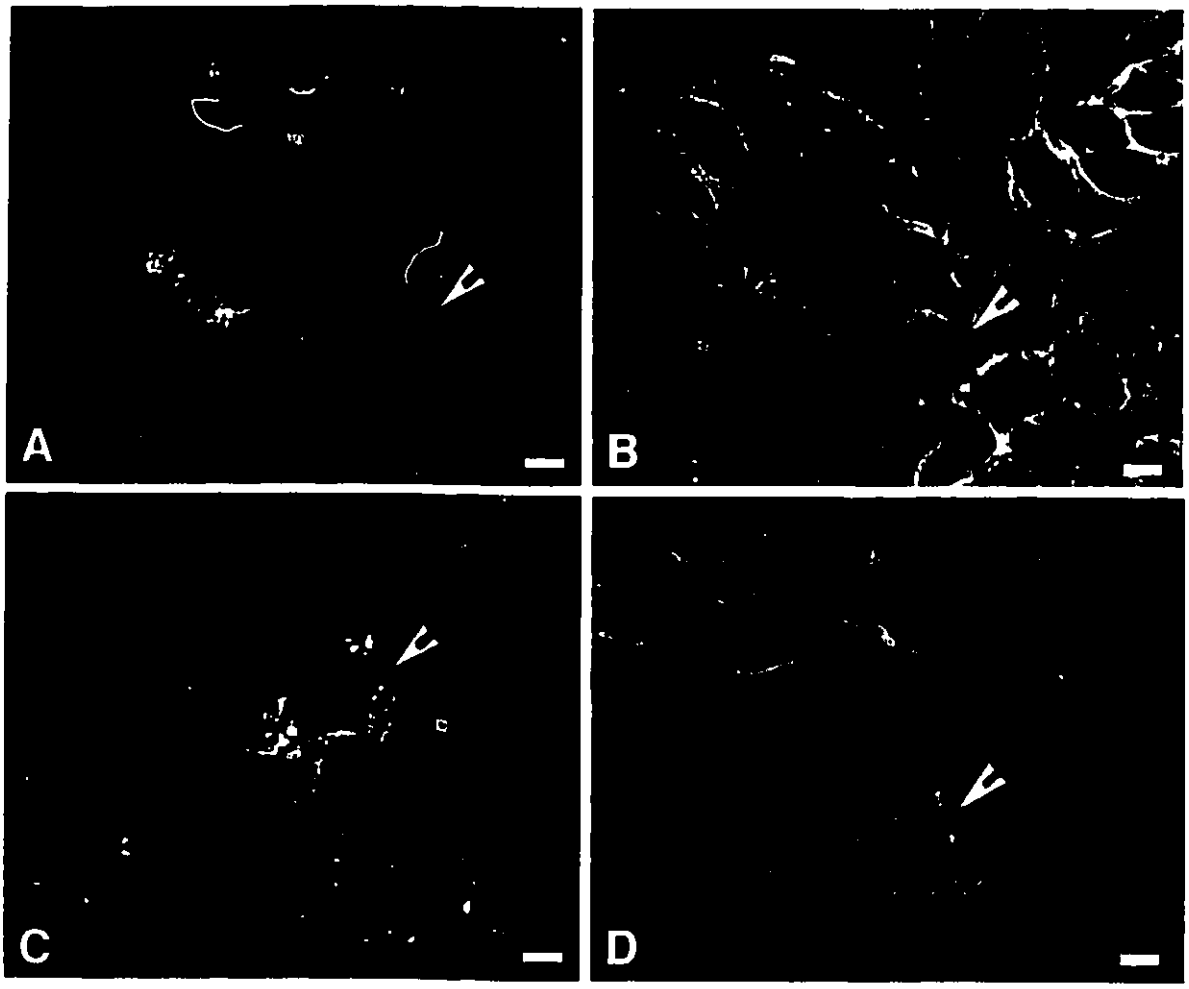
A
B
C
D

Figure 25. Zone 4 cells in the branchial arches and the anterior heart.
(A) Frontal section through the anterior portion of the stage 44-45 axolotl heart and gill filaments. In this phase contrast image, (ventral view), the location of the gill filaments in relation to the truncus arteriosis (ta) of the heart is shown. The location of the plane of section for this embryo is indicated in (F); (b4), gill arch 4; (b3), gill arch 3; (b2), gill arch 2; (ca), conus arteriosis. (B) Fluorescent image of the same section as in (A) indicating the labelled areas of the cardiac region. Labelled cells from zone 4 are shown to line the walls of the aortic arches (small arrows). Labelled cells (indicated with double-headed arrow) are also scattered throughout the walls of the truncus arteriosis (ta) and the conus arteriosis (ca). Chondrocytes of the posterior gill arches are also derived from zone 4 cells. Note the labelling of cells in the third (b3) and fourth (b4) gill arches. This embryo displayed the typical labelling pattern in the cardiac and gill region after DiI injection of zone 4. This particular embryo had been labelled along the right neural fold in zone 4. (C) and (D) Frontal section through the truncus arteriosis and gills of a stage 45 embryo; (phase contrast and fluorescent image, respectively). This embryo was used as a control for background fluorescence. The embryo was only injected with the DiI solvent solution (no DiI). The embryo was fixed and processed in the same manner as labelled embryos. Note the lack of any type of fluorescence in the anterior heart or gill arches. Therefore, no background fluorescence was detected.
(E) Fluorescent image of a cross section through the posterior heart region in a stage 44 embryo originally labelled in zone 4. Note the lack of fluorescent label in the walls of the atrium (a), the sinus venosus (sv), and the ventricle (v). Cardiac neural crest was not present in the posterior heart. Labelled cells are seen in the fourth gill arch (g4). (F) Schematic drawing of a stage 44-45 axolotl embryo indicating the plane of section for (A) and (B). Arrow indicates the location along the body axis of the anterior heart. Scale bars (A-E), 100 μm. In all panels, the anterior of the embryo is at the top of the plate.

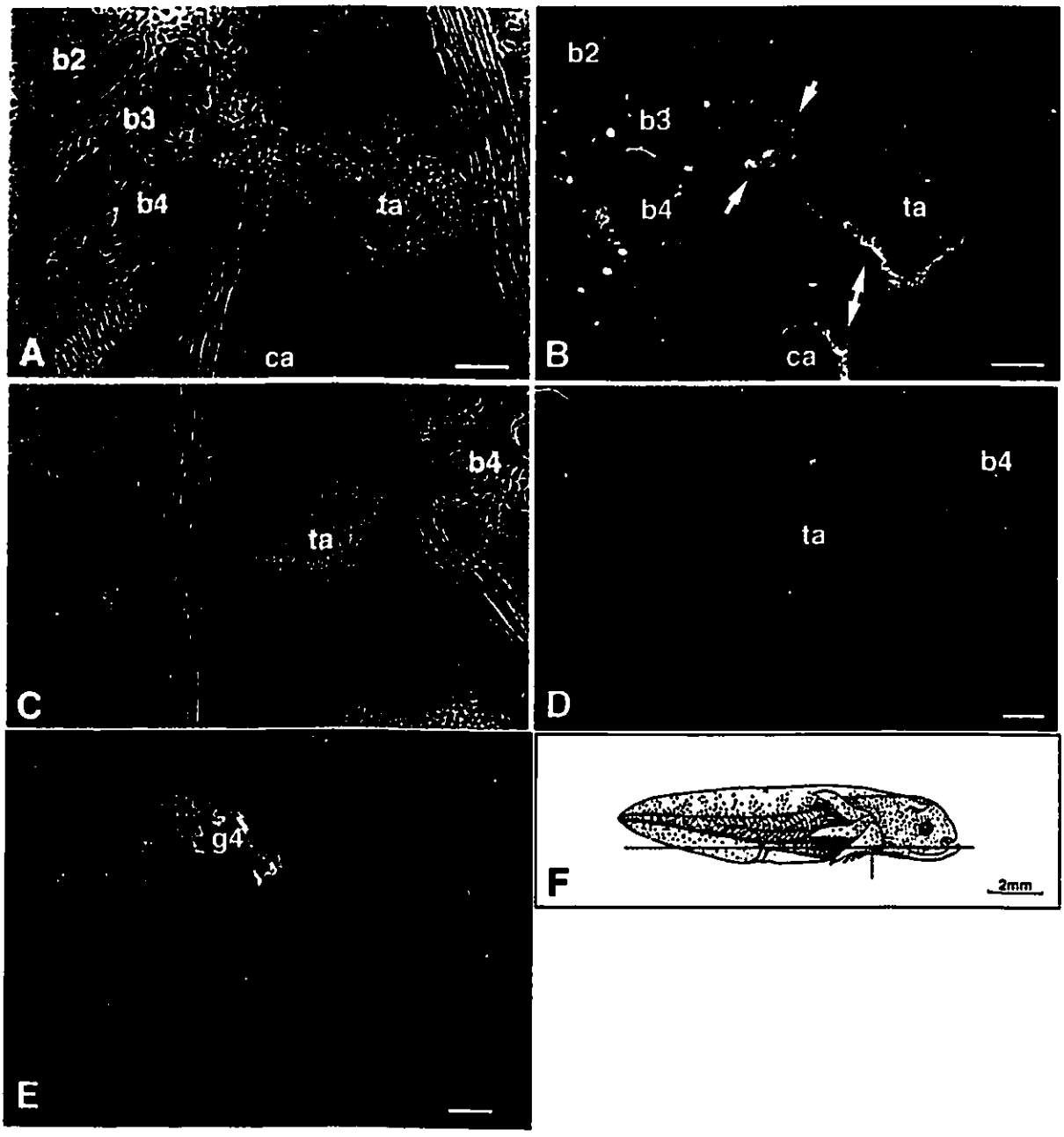
b2
b3
b4
ta
ca
A
b2
b3
b4
ta
ca
B
b4
ta
C
b4
ta
D
g4
E
F
2mm

Figure 26. The rhombencephalon contains cells from zone 4. (A) Frontal section through the hindbrain (rh) of a stage 44 axolotl embryo (phase contrast image; ventral view). The location of the otic vesicle (ot) in the relation to the rhombencephalon (rh) is shown. Arrow indicates cranial pigment cell.
(B) Fluorescent image of the same section as in (A). Note the presence of label in the rhombencephalon (rh) and in the mesenchyme (me) surrounding the otic vesicle (ot). Cranial pigment cells are also labelled (arrow). Scale bars (A and B), 100 µm. (C) Schematic drawing of a stage 44 axolotl embryo indicating the plane of section for (A) and (B). Arrow indicates the location along the body axis of the section in (A) and (B). In (A) and (B), the anterior end of the embryo is at the top of the plate.

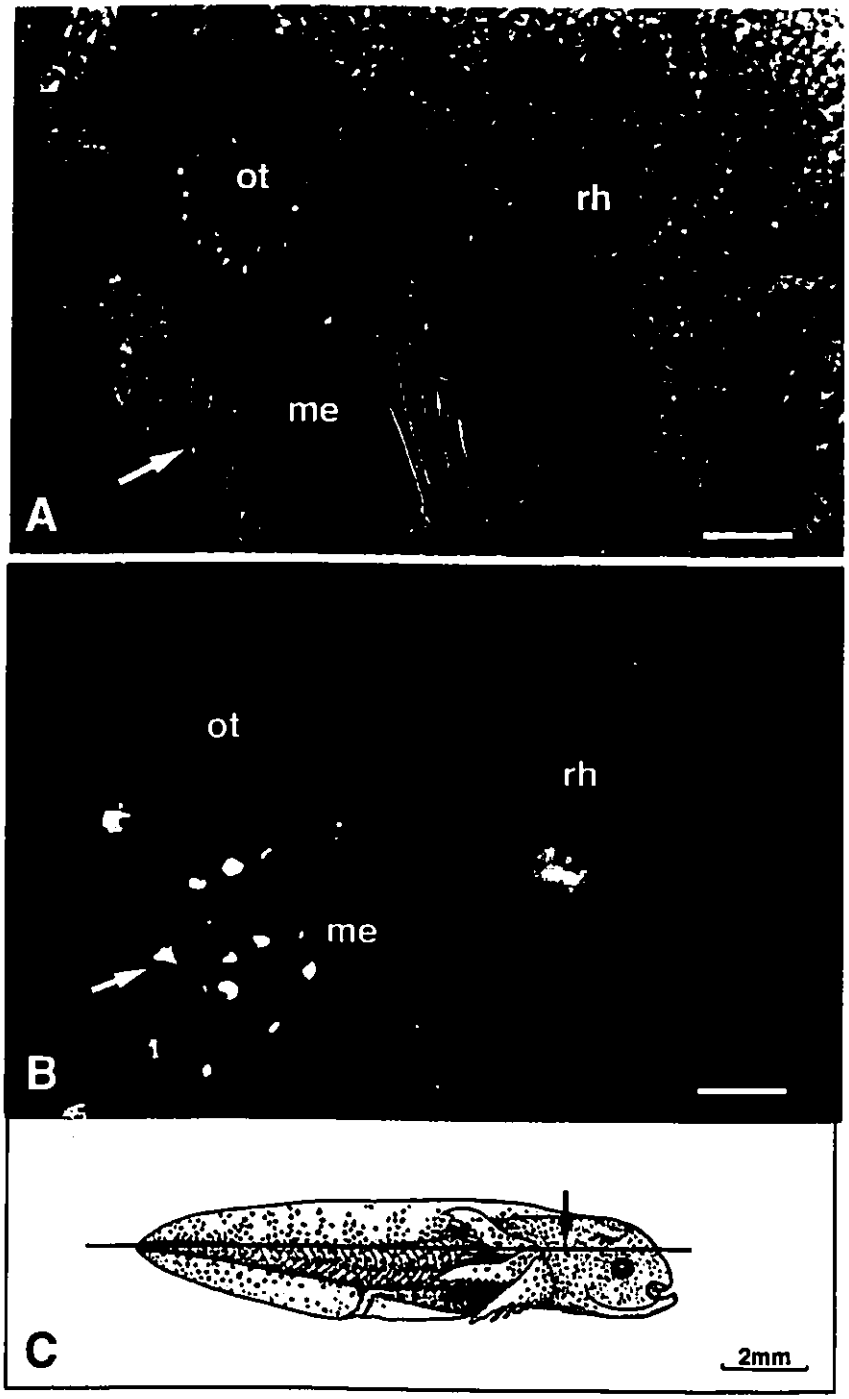
ot
rh
me
A
ot
rh
me
B
C
2mm

3.9 The Fate of Cells from Zone "5"

To ensure that the boundaries established for the cardiac neural crest did not exceed zone 4, we labelled the area behind zone 4 along the neural fold. This area, defined as zone 5, extends over two somites and marks the beginning of the trunk neural crest.

At stage 44-45, labelled zone 5 cells were found in the pronephric tubules, the spinal cord, and were found as pigment cells in the trunk region (see Fig. 27). Expectedly, pigment cells were the most obvious derivative of zone 5 cells (see Fig. 27 and 28). Interestingly, the walls of the pronephric tubules were labelled. This labelling would most likely represent the neural crest origin of the adrenal medulla (Le Douarin, 1982). Zone 5 cells also contributed to the neuronal network of the developing spinal cord midway along the body axis of the embryo.

No labelled cells were found in the cardiac region of the embryos after zone 5 labelling. This suggests that the boundary of the cardiac crest is restricted to zone 4 of the neural fold.

Figure 27. Zone 5 neural fold cells form pigment cells and contribute to the pronephric tubules. (A) Frontal section through the somites (s) just posterior to the gill filaments of a stage 44 axolotl embryo. Arrow indicates pigment cell. (B) Fluorescent image of the same section as in (A). Zone 5 neural crest forms pigment cells as indicated by the bright labelling in the pigment cells (arrow). (C) Frontal section through the pronephric tubules (pn) of a stage 44 axolotl embryo. Fluorescent image showing the bright labelling of pigment cells (arrowhead) surrounding the pronephric tubules. The walls of the pronephric tubules are also labelled. Labelling in the epithelium of this region is indicated by the long arrow. (D) Phase contrast image of the same section as in (C) showing the darkly pigmented cells (arrow) around the pronephric tubules (pn). Scale bars (A-D), 100 μm. (E) Schematic drawing of a stage 44 axolotl embryo indicating the plane of section for sections shown in (A-D). The arrow indicates the general location along the body axis for the sections shown in (A-D). In (A-D), the anterior end of the embryo is at the top of the plate.

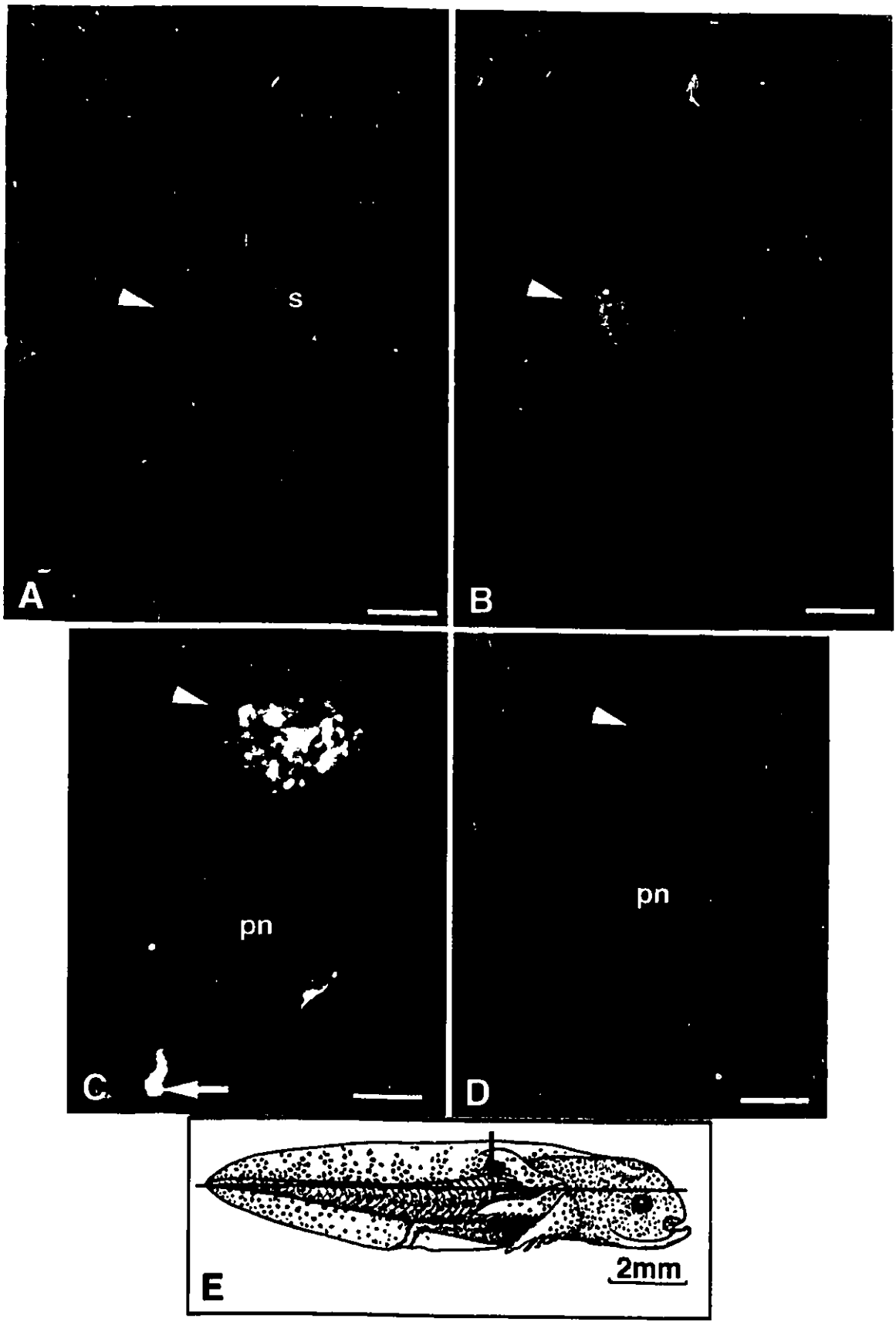
s
A
B
pn
C
pn
D
2mm
E

Figure 28. Zone 5 neural fold cells contribute to the spinal cord. (A) Frontal section (phase contrast image shown; ventral view; anterior end is up) through the spinal cord (*) of a stage 44 axolotl embryo. The arrow refers to a pigment cell in this region. The location of this section along the body axis is indicated in (C). (B) Fluorescent image of the same section as in (A). Zone 5 cells are found in the spinal cord (*), posterior to the hindbrain and as pigment cells (arrow). Scale bars (A and B), 100 μm. (C) Schematic drawing of a stage 44 axolotl embryo indicating the plane of section shown in (A) and (B). The arrow indicates the location of the sections along the body axis.

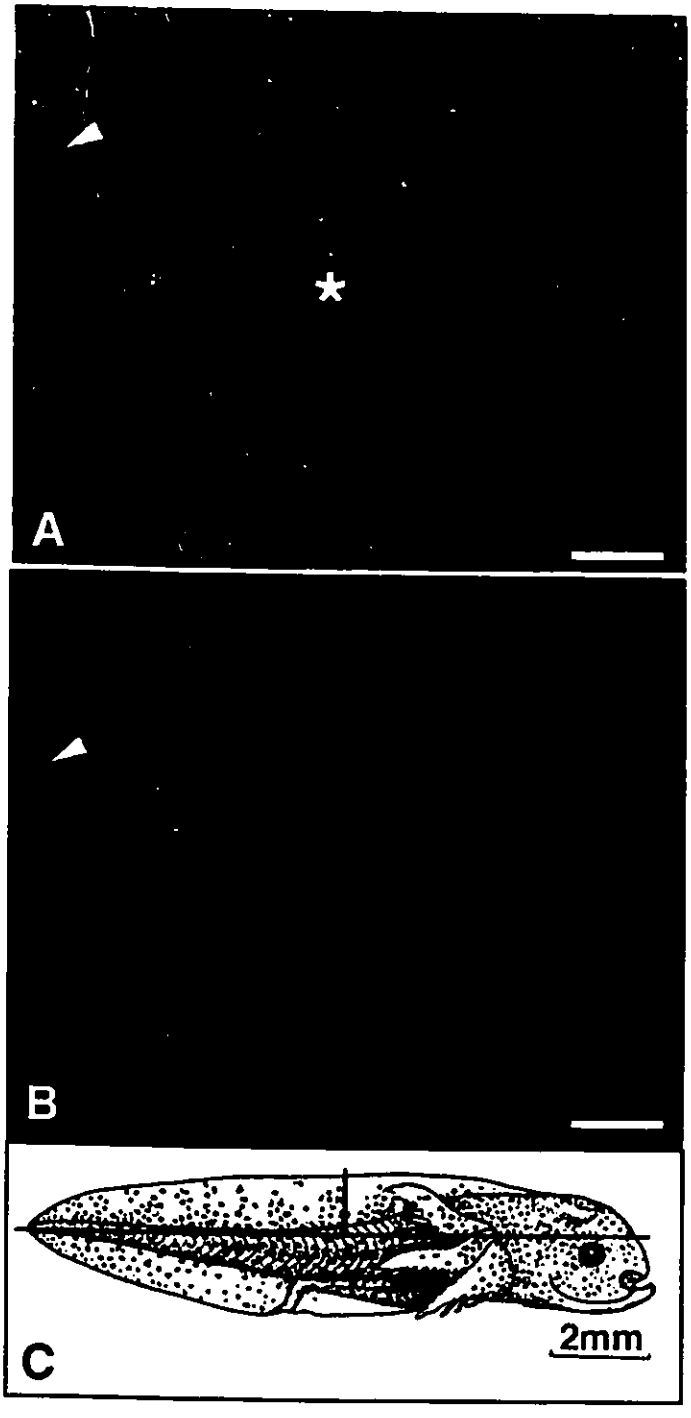
A
B
C
2mm

3.10 The Fate Map of the Cranial Neural Folds in the Late Neurula-Stage Axolotl Embryo

From the data pooled from our labelling studies, we have constructed a generalized fate map of the cranial folds of the stage 19-20 axolotl embryo. We have examined the contributions of different zones (defined in Fig. 11) along the anterior neural fold to the stage 44 cranial skeleton, brain and heart. Our data has shown that neural crest cells originally from an anterior position along the neural fold, migrate ventrally to form anterior elements of the cranial skeleton. There is a direct correlation between the position of the neural fold cells along the antero-posterior axis of the neural fold and the position along the antero-posterior axis of their derivatives later in development. The fate map is shown in Figure 29.

Figure 29. The Fate Map of the Stage 20 Axolotl Neural Fold. (A) Drawing of the lateral view of a stage 20 axolotl at the late neurula stage. The drawing indicates the zones (1-5) that we demarcated along the neural fold. The zones were labelled with DiI at stage 20, and their lineage was examined at stage 45. The derivatives of the "coloured" zones are seen in (B), (C), and (D) with the corresponding colours. (B) Drawing of the dorsal view of the stage 45 cranial skeleton. The colours indicate the origin along the neural folds for the different cartilaginous elements. The Meckel's cartilage, hyoid arch, palatoquadrates, and trabeculae are derivatives of zone 2 (in green). Zone 3 (blue) contributes to the anterior branchial arches and the posterior hyoid arch. Zone 4 (pink) derivatives are in the posterior branchial arches. Mc=Meckel's cartilage; Hy=hyoid arch; Ba=Branchial arches (1,2,3,4); A Trab=anterior trabeculae of the neurocranium; Pq=palatoquadrates; Bp=basal plate. (C) Drawing of the ventral view of a stage 45 axolotl heart. The pink colour indicates the scattering of cardiac neural crest from zone 4 in the truncus arteriosis (TA) and the aortic arches. B=bulbus cordis; C=conus arteriosis; V=ventricle; A=atrium; S=sinus venosus. (D) Drawing of the dorsal view of the stage 45 axolotl brain. The colours indicate the zone of origin along the neural fold for the different regions of the brain. Zone 1 (yellow) neural cells contribute to the anterior prosencephalon. Zone 2 (green) neural cells contribute to the posterior prosencephalon. Zone 3 (blue) neural derivatives are found in the mesencephalon at stage 45. Zone 4 (pink) cells are found in the rhombencephalon and zone 5 neural cells (purple) are found in the spinal cord. Pro=prosencephalon; Me=mesencephalon; Rhom=rhombencephalon; Sp C=spinal cord.

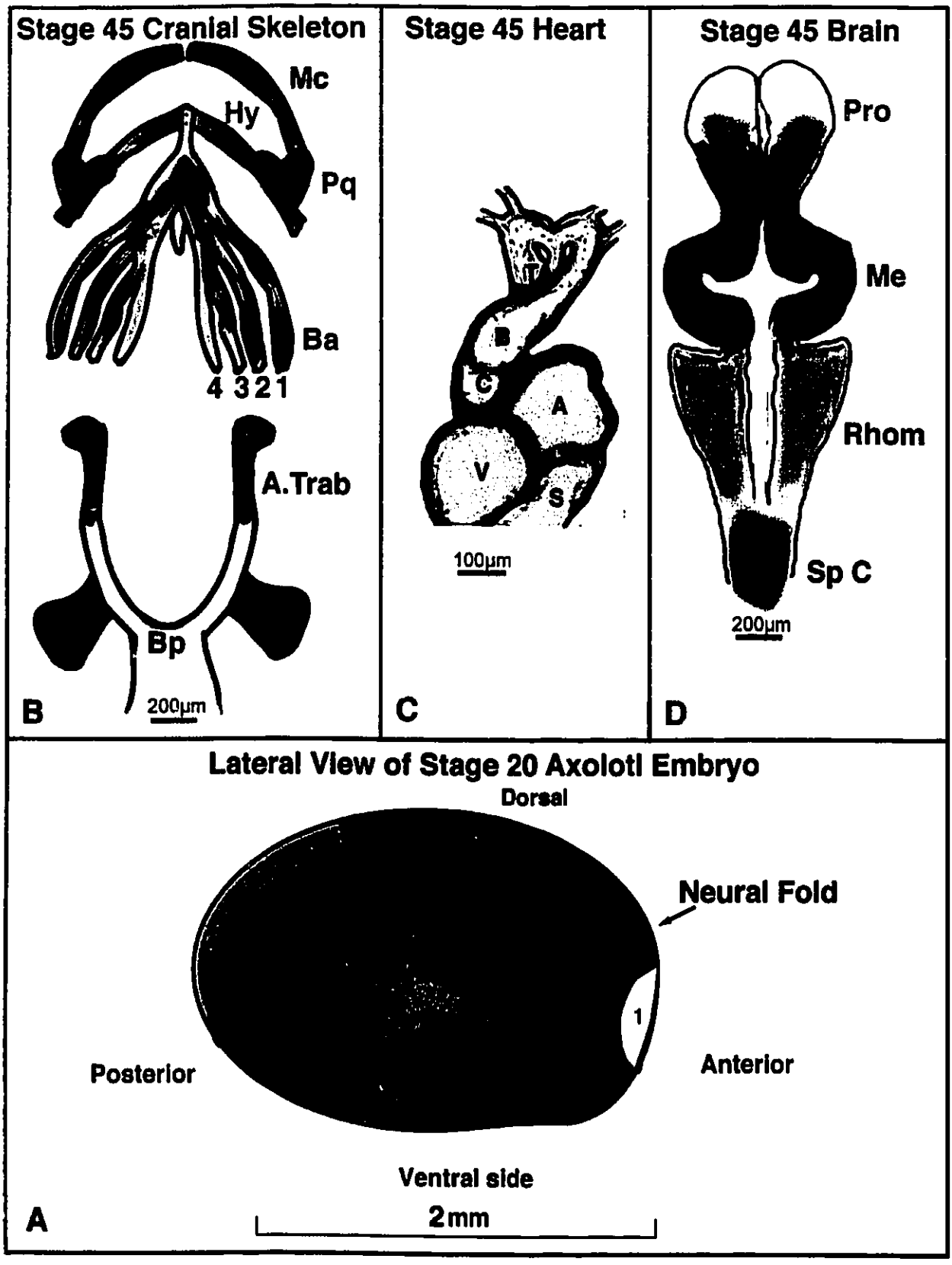
Stage 45 Cranial Skeleton
Mc
Hy
Pq
Ba
4 3 2 1
A.Trab
Bp
200µm
B
Stage 45 Heart
B
C
A
V
S
100µm
C
Stage 45 Brain
Pro
Me
Rhom
Sp C
200µm
D
Lateral View of Stage 20 Axolotl Embryo
Dorsal
Neural Fold
1
Posterior
Anterior
Ventral side
2mm
A

Discussion

Using the DiI fluorescent labelling technique, we have been successful in identifying the region along the neural fold which forms the cardiac neural crest in the axolotl. We have also confirmed that DiI can be used as a successful lineage label in the axolotl. Prior to our study, only one other case of DiI being used as lineage label in the developing embryonic axolotl has been documented. Barlow and Northcutt (1995) demonstrated, by using DiI, that the axolotl taste buds arise from the cephalic endoderm.

4.1 The Amphibian Cardiac Neural Crest

We have defined the region of the cardiac neural crest as being located from the anterior of somite 1 to the posterior end of somite 2 along the cranial neural fold in a stage 20 embryo. This area corresponds to zone 4 outlined in Figure 11. The neural crest cells migrate ventrally towards the posterior branchial arches (branchial arch 3 and 4) and the anterior portion of the heart. By stage 37 of development, the neural crest cells have reached their ventral position anterior to the developing heart tube. By stage 44 the cardiac neural crest cells have taken on their role of lining the truncus arteriosis of the heart and the walls of the aortic outflow tract. Our results demonstrate that the cardiac neural crest cells line the artery walls leading to the posterior branchial arches. The function of the cardiac neural crest and its position along the neural fold in the axolotl embryo correspond well with the location and role of the cardiac neural crest in the chick (Kirby, 1991) and in the rat (Fukiishi and Morris-Kay, 1992).

In the chick the cardiac neural crest is defined by the region between the otic placode and somite 3 (Kirby, 1991). In rat embryos neural crest cells from the first 3 occipital somites migrate to the cardiac outflow tract (Fukiishi and Morris-Kay, 1992). This area can be considered analogous to the hindbrain region within the first two somites

in the axolotl. This suggests that the components and development of the cardiac outflow tract in amphibians is similar to that of other vertebrates. Therefore the axolotl heart can be used as a suitable model for vertebrate cardiac development. Sadaghiani and Thiébaud (1987) had noted that in *Xenopus* some cells from the branchial arch segment (at the posterior part of the rhombencephalon) penetrated the wall of the truncus arteriosis. Our results indicate that in amphibians, it is these posterior rhombencephalic cells, and also cells located further posteriorly from the crest over the first two somites which encompass the full extent of the cardiac neural crest. Since Sadaghiani and Thiébaud did not investigate the cardiac derivatives of any region posterior to the branchial arch segment, these results do not contradict their observations, but simply add on to their findings.

Our results indicate that, in the axolotl, the region of the posterior cranial neural fold (zone 4) also gives rise to chondrocytic cells in the posterior branchial arches (branchial arch: 3 and 4). These results are also concomitant with those in mammals (Fukiishi and Morris-Kay, 1992; Trainor and Tam, 1995) and birds (Kirby, 1991).

The region defined as cardiac neural crest in avians also has been shown to contribute to the formation of the thymus and the parathyroid and thyroid glands (Le Lièvre and Le Douarin, 1975). However, we did not observe any distinct label in these glands. At stage 45 only the anterior heart, the posterior branchial arches and the caudal hindbrain region displayed any signs of the fluorescent label. Two reasons may account for this. It is possible that the cardiac neural crest does not contribute to these components in the axolotl, or the labelled glandular tissue was not distinct enough from other labelled areas. The latter situation does not seem likely because, by stage 44, the thyroid should be easily distinguishable.

Our results establish, for the first time, the involvement of cardiac neural crest in axolotl heart development. This finding has several implications in the study of cardiac specification. The heart is primarily of mesodermal origin and is induced by the pharyngeal endoderm (Smith and Armstrong,1990). Lateral plate mesoderm moves towards the ventral

mid-line of the embryo slowly coming into contact with the inductive endoderm. Induction begins during the neurula stage before the mesoderm reaches its final location at the ventral midline (Smith and Armstrong, 1990). However, the time when cardiac neural crest is specified and induced to migrate is unknown, and was not examined in our experiments. Experiments would have to be performed to determine if induction of the neural crest and mesodermal component of the heart coincide or whether one is induced after the other. The most plausible inducer of the cardiac neural crest would be the pharyngeal endoderm. The pharyngeal endoderm not only induces lateral plate mesoderm to form heart but also induces cranial neural crest to form cartilage (Graveson and Armstrong, 1987).

The role of the cardiac neural crest in the axolotl heart appears to be a minor one. Our results have shown that the cardiac neural crest provides ectomesenchymal support for the anterior walls of the heart and the aortic arches. This implies that it is involved in circulation. In avians, cardiac neural crest ablation causes "persistent truncus arteriosis" which results in severe disruptions in circulation (Nishibatake et al., 1987). This result has two significant implications. One being that the cardiac neural crest (at least in birds) is required for proper circulation, and secondly, that the cardiac neural crest is determined early on in development and not subject to regulation by other neural crest cells.

In amphibians, cardiac neural crest ablation studies have not been specifically performed to determine the extent of the cardiac crest's role in circulation. Graveson and Armstrong (1994) showed that the ablation of cranial neural crest cells (which happened to include the region of cardiac neural crest) caused circulation to be hindered initially but was eventually restored. This suggests that cardiac neural crest is not vital to the establishment of circulation (in amphibians), and regulation by other cells can take over the function of the cardiac crest. Further studies specifically aimed at examining the role of cardiac crest in the axolotl could verify this notion. In vitro clonal analysis in avians has demonstrated that the early migratory cardiac neural crest is a heterogenous population of pluripotent cells, some of which have a partially restricted developmental potential, while others are

committed to a particular cell lineage (Ito and Sieber-Blum, 1991). The developmental potential of the cardiac neural crest was not examined in our experiments. However, we did establish that the neural crest cells originating from the same region along the neural fold as cardiac neural crest have the ability to form chondrocytes of the posterior branchial arches. From our results we cannot exclude the possibility that the neural crest cells from zone 4 are composed of two distinct populations of cells: the cardiac neural crest and the cells that have the ability to form chondrocytes.

In our observations, we noticed that the right side neural folds contribute more cells to the cardiac region that the left side neural folds. This difference between adjacent lateral folds may be accounted for by the asymmetry of the heart itself. This asymmetric phenomenon regarding the cardiac neural crest and the heart is also seen in chicks (Rosenquist et al., 1989; Takamura, et al., 1990).

We also noticed that after labelling only one side of the fold, fluorescence can be found in both sides of the heart. Crossing over of migrating crest over the dorsal midline has been documented previously for cranial neural migration (Hall and Horstadius, 1988) in amphibians. However, in the rat, after unilateral labelling, no crossing over of cardiac crest cells was detected (Fukiishi and Morriss-Kay, 1992). Our results are probably due to the inadvertent diffusion of the dye into the contralateral side of the fold of the same zone. Even if both sides of adjacent folds did get labelled, the derivatives of the adjacent folds are the same and thus would not greatly affect the outcome of our experiments.

We have shown that by stage 44-45 of axolotl development, the cardiac neural crest has migrated ventrally and has formed the ectomesenchymal support structure of the aortic arches and the anterior heart. We did not examine the development or further differentiation of cardiac ectomesenchyme beyond stage 45. Stage 45 represents the stage at which the cardiac neural crest has just begun to serve its function in the heart. Prior to this stage the cardiac neural crest has just managed to complete its ventral migration towards the cardiac cavity (see next chapter).

In other vertebrates, it has been observed that later in development, cardiac ectomesenchyme forms the smooth muscle of the *tunica media* of the large arteries (Le Douarin and Teillet, 1984), and expresses α-smooth muscle actin (Rosenquist et al., 1990). We have yet to examine the further differentiation of the cardiac ectomesenchyme in the axolotl. Studies at older stages of development, such as immunoassays for smooth muscle proteins would help in establishing the final fate of the cardiac neural crest in the heart of the axolotl.

The work presented in this thesis represents the beginning stages of examining the role and differentiation of cardiac neural crest in amphibians. Although we have only identified the presence and location of cardiac neural crest in early cardiovascular development, our work provides a good foundation for further studies of cardiac neural crest in amphibians. The study of cardiac neural crest in avians and mammals has provided some insight into the pathogenesis of certain congenital abnormalities (Van Mierop, and Kutsche, 1986; Wells et al., 1986; Siebert, et al., 1985; Bellah, et al., 1989). The examination of the cardiac neural crest in axolotls may provide similar insight into the mechanisms involved in axolotl mutations such as the *cardiac* (*c*) and *premature death* (*p*) mutation, and hopefully in mutations of other vertebrates as well.

4.2 The Fate of the Cranial Neural Fold from the Stage 20 Axolotl Embryo

The secondary objective of these experiments was to create a fate map of the cranial neural crest in the stage 20 (late neurula) axolotl embryo (see Results section p.65). Previous fate maps have been created in early neurula stage embryos (Horstadius and Sellman, 1946; Chibon, 1966). We have focussed primarily on the formation of the visceral skeleton of the head and the developing brain. We have not examined smaller neuronal components such as cranial ganglia. It is important to note that as seen in Figure 13, we have not only labelled the premigratory neural crest, but the converging neural folds, which form the neural tube. Therefore, our results are not restricted to the fate of

neural crest cells alone, but of neural tube cells as well. Neural derivatives that have migrated away from the dorsal neural folds, such as chondrocytes, represent neural crest derivatives while elements such as the brain, originate from the neural tube (Le Douarin, 1982).

We have found that the anterior most region of the cranial neural fold (zone 1) contributes to the anterior prosencephalon of the brain, once the embryos have reached the larval stage. No cartilaginous elements originated from this region. As expected, these results correspond exactly with those of Chibon (1966) and Horstadius and Sellman (1946).

Further posterior along the cranial neural fold, our results differ slightly from those obtained by Chibon and Horstadius. The main reason for this was the fact that both previous fate maps divided the neural fold into at least 6 regions, while we have only divided this region into 3. We have used the landmarks outlining the presumptive brain regions as guides for defining our boundaries.

In our experiments we found that zone 2 cells (refer to Fig. 11) formed the Meckel's cartilage, the anterior portion of the trabeculae, part of the hyoid arch and the palatoquadrates. This region would correspond to regions 3, 4 and part of 5 in Horstadius' drawing (refer to Fig. 8). According to Horstadius and Sellman, these regions form the trabecular material, the mandibular arch and the hyoid arch. Similarly in Chibon's map, our "zone 2" would correspond to the area defined as 30^0-90^0, which forms the anterior and posterior trabeculae, the basal plate, the palatoquadrates, Meckel's cartilage and the hyoid arches. Our results show that the posterior trabeculae and the basal plate were not from zone 2 cells. Our results agree with Horstadius and Sellman's, but not with Chibon's. Horstadius and Sellman (1946) mentioned that the posterior trabeculae and the basal plate were not of neural crest, but of endodermal origin. The lack of labelled cells in the posterior trabeculae and the basal plate after labelling from any zone agrees with this suggestion.

Our results also show that zone 2 cells form the posterior prosencephalon. This agrees with the brain regions outlined in Baker and Graves (1939) for *Ambystoma punctatum*. The fact that zone 2, the posterior prosencephalic region of the fold, also forms the trabeculae corresponds to results obtained by Langille and Hall (1988), in the lamprey. When the presumptive posterior prosencephalic region was ablated, the trabeculae had not formed (Langille and Hall, 1988).

Our results showed that zone 3 cells contributed to the anterior three branchial arches, the hypobranchials, and even some posterior portions of the hyoid and Meckel's cartilage. These last two elements do not correspond with Chibon's and Horstadius' results. According to our results zone 2 and zone 3 form the great majority of the visceral skeletal components. We also noted a slight overlap between the origin of certain components. Our results show that if an element has a large domain in the rostral-caudal direction (such as the Meckel's cartilage and the hyoid arch), then the anterior portions of the element are derived from anterior regions of the neural fold, while posterior portions of the element are formed from more caudal regions of the neural fold. This suggests that the regional specificity between zone 2 and 3 is not extremely strict once the neural folds fuse. Cells corresponding to these regions do migrate into similar regions of the head, according to Landacre (1921). However, it is possible that this result was achieved because of discrepancies in experimental technique. It is possible that when labelling zone 3, some cells at the caudal end of zone 2 may have also been labelled with the dye. In any case, the correlation between the anterior-posterior location of the element and the anterior-posterior location along the neural fold, still remains.

We have also shown that zone 3 cells also contribute to the anterior branchial arches. This result corresponds to Chibon's (1966) for the stage 17 embryo and to Horstadius and Sellman's (1946). Our results for zone 2 and 3 suggest that these two regions contribute to the majority of the components of the cranial skeleton. We have also shown that zone 3 cells of the neural tube form the mesencephalon. The fact that this

region also houses the anterior branchial arch crest corresponds with ablation studies performed by Langille and Hall (1988).

We have shown that the posterior branchial arches and the hindbrain contain neural crest cells from zone 4, the region also specifying cardiac neural crest. This corresponds to similar observations in birds and mammals (Kirby,1991; Fukiishi and Morris-Kay, 1992).

As expected, pigment cells were found to be derived from every zone examined. Anteriorly located pigment cells were derived from the anterior neural fold, and likewise, posteriorly located pigment cells had their origin in a more posterior region of the fold. This was a general trend with respect to neural fold derivatives. Thus, substantiating that neural crest migration occurs mainly in a ventral direction.

Fluorescence was detected in the liver and gut of most embryos. This could have been attributed to ganglionic derivatives of the neural crest in these regions (Le Douarin, 1982). However it was difficult to distinguish this type of fluorescence from background fluorescence since it was very dim, so consequently, we disregarded these results.

Our results concerning the fate of the cranial neural crest mirrors the work of other studies. The fate map that we created allowed us to establish the definitive boundaries along the neural fold of various neural derivatives at the late neurula stage. Previously, if one wanted to define the boundaries of the derivatives of the stage 20 neural fold, one would have to extrapolate the data from fate maps created for early-mid neurula stages.

Our lineage labelling experiments concerning zone 1, 2, 3, and 5 did not contradict any of the previous work published on the amphibian neural crest, but it did reconfirm what has already been known. With respect to these zones we did not attempt to gain any new insight into the mechanisms of neural induction. We simply wanted to ensure that the fate maps for early to late neurulation stages of development correlated with each other. And, as seen by our results, they did correlate. The isolation of the amphibian cardiac neural crest however, did provide new insight into amphibian cardiovascular development.

Chapter II

Introduction

1.1 The Premature Death Mutation of the Mexican Axolotl

The *premature death* mutation (*p*) of *A. mexicanum* is a recessive lethal mutation and causes a variety of abnormalities in the homozygous (*p/p*) state. The mutant embryos develop up to stage 37 after which the superficial tissue begins to disintegrate (Trottier and Armstrong, 1977). The embryos are incapable of normal swimming and righting movements. Primary gill filaments form, but secondary gill filaments never develop and bulb-like structures form at the distal ends of the primary filaments (see Fig. 30) (Mes-Hartree and Armstrong, 1980). However, pigment cell appearance and migration is not affected in the homozygotes. The eyes are often underdeveloped. Internally, the morphology of the pharyngeal pouches and the midgut is abnormal. The liver and myotomes appear underdeveloped, and undergo rapid degeneration after stage 37. A plug of undifferentiated cells replaces the endocardium in the anterior regions of the heart (ventricle and conus arteriosis) (Trottier and Armstrong, 1977). Though the heart begins to beat weakly, circulation is never established.

Because most of the affected tissues were either endodermally derived or induced, Trottier and Armstrong (1977) hypothesized that the *p* mutation caused a defect in the endoderm. However, more recently Graveson and Armstrong (1990) discovered that a subpopulation of cranial neural crest cells is affected by the mutation. The mutant neural crest cells were incapable of chondrogenesis and could not form mature cartilage *in vitro* (Graveson and Armstrong, 1990). However, other neural crest derivatives such as pigment cells, Rohon-Beard cells and the mesenchymal portion of the dorsal fin appeared to differentiate normally (Graveson and Armstrong, 1990). Graveson and Armstrong

(1994) have shown that the spatial and temporal migration patterns of mutant (*p/p*) neural crest is normal when transplanted onto a normal host. However, when wild-type neural crest is transplanted into a mutant host, the mutant environment supports cartilage development and there is also a slight improvement in the extent of gill development. However, the life span and other mutant characteristics of these embryos stay the same. This suggests that the mutation affects not only chondrogenic neural crest precursors, but also other subpopulations of neural crest.

Neural crest ablation in wild-type embryos results in similar gill structure to that of *p/p* mutants (Graveson and Armstrong, 1994). Blood pooling and a delay in the establishment of circulation are also seen in neural crest deficient wild-type embryos (Graveson and Armstrong, 1994). However, the phenotypes observed in neural crest deficient embryos are transient and they soon regulate themselves to normalcy (Graveson and Armstrong, 1994).

S.C. Smith et al. (1994) established that the *p/p* mutation also affects the development of the lateral-line system, a derivative of placodal ectoderm, in the axolotl. They observed that the migration of lateral-line primordia and differentiation of mechanoreceptive neuromast organs are disrupted in *p/p* embryos and arrest at stage 37. They also showed that mutant placodes develop abnormally in wild-type hosts, suggesting that it is not the mutant environment that causes the arrest in lateral line development. Their results suggest that certain neural crest cells are not the only targets of the *p/p* mutation, but that at least one type of ectodermal placode, the precursor to the lateral-line primordia is also affected. Clearly, the mutation selectively affects certain ectodermal derivatives, such as chondrogenic neural crest and lateral line primordia, but not others.

The complete extent of the mutation's effect on the neural crest is presently unknown. Since mutant and the neural crest deficient embryos exhibit circulatory problems and other abnormalities associated with heart development, the cardiac neural crest, a non-chondrogenic population of the cranial neural crest, may also be affected by the premature death mutation. Neural crest cells normally contribute to proper heart development in chicks and in *Xenopus* (Sadaghiani and Thiébaud, 1987; Kirby and Waldo, 1990). We have established that the neural crest is also involved in heart development in the axolotl, and we have also established the location of this cardiac crest in the axolotl embryo (see chap.I of this thesis). In the following pages, we examine the effect of the premature death mutation on mutant cardiac neural crest *in vivo*. We unilaterally labelled the region of cardiac neural crest in the stage 20 neural fold of the mutant embryo with DiI, and observed its progression prior to disintegration of the embryo (stage 37). We have characterized the distribution and morphology of mutant neural crest cells in the axolotl heart, and have shown that the plug of undifferentiated cells in the endocardium of mutant heart is not of cardiac neural crest origin.

Since cardiac neural crest plays a minor role in heart development and only appears in the heart region much after the embryo has already begun to disintegrate, we conclude that mutant cardiac neural crest does not appear to be a major contributor to the circulatory problems observed in the mutant.

Figure 30. (A) Lateral view of a phenotypically wild-type axolotl embryo. (B) Dorsal view of a *p/p* axolotl embryo. The embryos shown are of the same chronological age (stage 37). Note the simple, unbranched nature of the mutant's gills, with the characteristic bulb-like structures at the distal ends of the primary filaments (thick arrows). Note also the curved nature of the body axis in the mutant. The wild-type embryo has, by this stage, long primary gill filaments (thin arrows) and an elongated body axis. Bars, 1.7 mm; (photos courtesy of Tom Trottier).

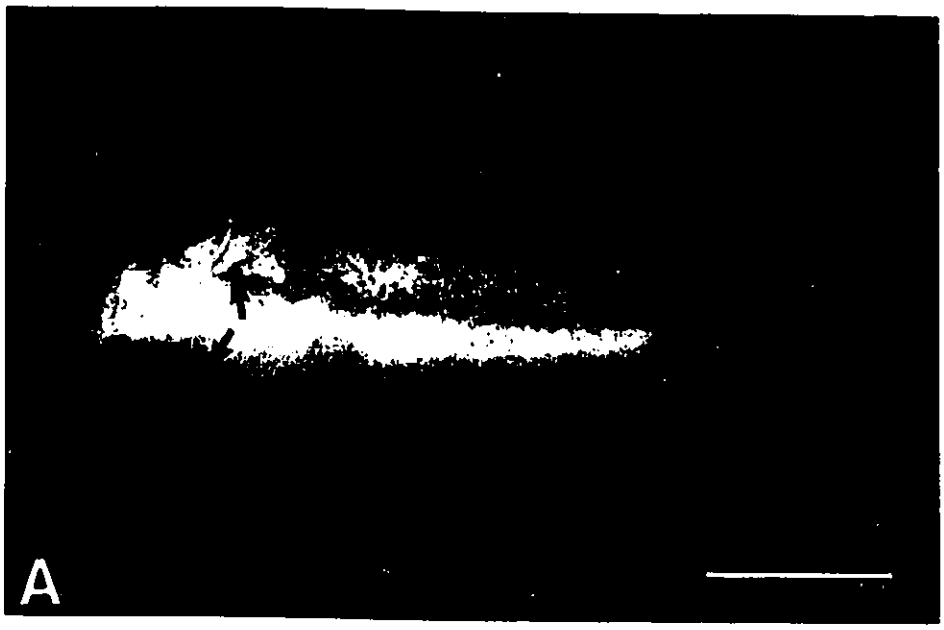
A

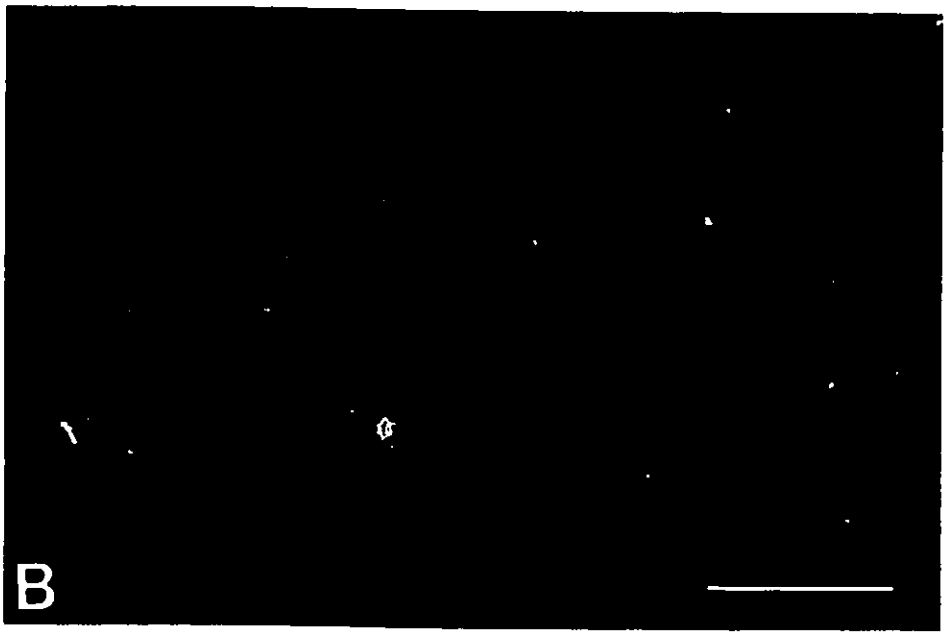
B

Materials and Methods

2.1 Embryos

A *p/* + x *p/* + *A. mexicanum* spawning was performed to obtain +/+, *p/*+, and *p/p* embryos. These embryos were injected with DiI at stage 19-20 using the technique described in Chapter I. All embryos were injected on the right side neural fold in the area designated as "zone 4" (see Figure 11). At stage 20, the premature death (*p/p*) mutant is not distinguishable from the wild-type, so several embryos had to be injected to obtain some labelled mutants. The embryos were otherwise treated in the same manner as outlined in Chapter I (see Materials and Methods section).

Once the embryos reached stage 37-38, the *p/p* mutants could be distinguished due to their characteristic phenotype and their failure to progress further in development. All embryos were allowed to develop until the normal embryos from the spawning reached stage 39. At this point, the *p/p* mutants had already begun deteriorating, and the embryos with a normal phenotype looked healthy. The normal-looking injected embryos from the same spawning served as controls. The injected normal and *p/p* mutants were fixed, processed and sectioned using the technique outlined in the Materials and Methods section of Chapter I.

Results

3.1 The Internal Gill Morphology of the *p/p* Mutant

A *p/+* x *p/+* spawning was performed. From this spawning, 28 eggs were injected with the DiI solution at stage 20 in zone 4 (the location of the cardiac neural crest and posterior branchial arch crest) of the right-side neural fold. The embryos were allowed to develop for six days. At that point it was determined which embryos displayed the characteristic *p/p* phenotype and which embryos exhibited the normal stage 39 wild-type phenotype. Six of the 28 injected embryos had "stubby", unbranched primary gill filaments and seemed to have arrested in development, indicating that they were homozygous for the *p/p* mutation. The other embryos appeared to have a normal stage 39 wild-type appearance with well developing primary gill filaments. The 6 *p/p* embryos and the other +/+ or *p/+* embryos were then fixed, sectioned and examined. The distribution pattern of the DiI-labelled neural crest cells in the embryos was compared between the *p/p* mutants and the wild-type embryos.

All six of the mutants exhibited very similar internal morphology. The most obvious difference between the *p/p* mutants and their wild-type counterparts was the organizational pattern of the labelled neural crest cells. In the wild-type stage 37-39 embryos, the neural crest cells which formed the gill arches, migrated as three defined "streams" of cells and populated the gill buds (see Fig. 31). The labelled neural crest cells in the mutant did not follow this pattern of migration. The mutant labelled neural crest cells were found in the vicinity of the gill arches but exhibited a haphazard "clumping" pattern (see Fig. 32). The mutant primary gill filaments were surrounded by an epithelial layer of labelled cells, (similar to that of wild-type gill filaments), but were internally very sparse of neural crest tissue (see Fig. 31B, 32B). It appeared that the cell population in the budding gill filaments of the mutant was lacking because of the clustering of cells proximal to them. The migration of the labelled cells appeared to have been altered by the mutation both

temporally and spatially because the labelled cells had not migrated into the gill filaments by the appropriate developmental stage. Any of the labelled cells could not be classified as being in ectopic locations because they had initially migrated along their proper pathways but had just fallen short of reaching their proper destination corresponding to their developmental stage. The zone 4 cells initially migrated towards their intended position in the branchial arches (established in Chap I), indicating that the mutation did not completely obliterate the regional specification of these cells.

Figure 31. The pattern of neural crest migration toward the gills in the *p/p* mutant and wild-type embryo. (A) Frontal section (phase-contrast image; ventral view shown) through the developing primary gill filaments of a typical stage 37 *p/p* embryo. (B) Fluorescent image of the same section as in (A). The fluorescent label shows an unorganized migration pattern of the neural crest cells towards the gill filaments. In (A) (B),(C), and (D): g1=first primary gill filament; g2=second primary gill filament; g3=third primary gill filament.
(C) Frontal section through the primary gill filaments of a stage 37 wild-type embryo. (D) Fluorescent image of the same section as in (C). The arrows indicate the direction of flow of the "streams" of fluorescently labelled neural crest cells towards the developing gill filaments. Note the differences in the migrational "flow" between the mutant (B) and the wild-type embryo (D). The number of labelled cells in the mutant gill filaments appears to be much less than in the wild-type embryo. In the mutant, the labelled cells are not organized into three streams flowing into the primary gill filaments as in the wild-type embryo. Scale bars for (A-D), 100 µm. In (A-D) the anterior of the embryo is towards the top of the plate.

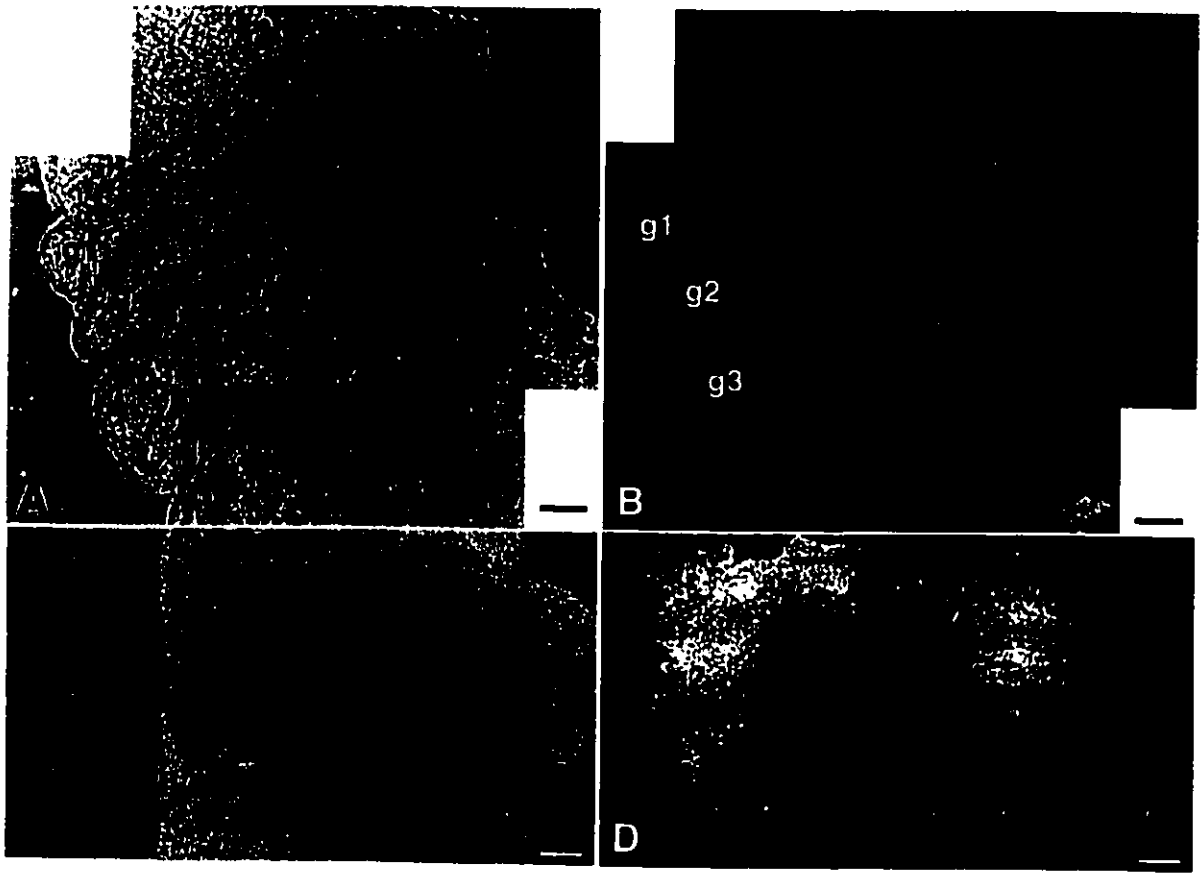
g1
g2
g3
B
D

Figure 32. The typical primary gill filaments of the *p/p* mutant.. (A) Frontal section through the left second and third primary gill filaments of the stage 37 p/p embryo. For (A) and (B), g2=second primary gill filament; g3=third primary gill filament. (B) Fluorescent image of the same section as in (A). There is a lack of neural crest cells in the actual gill filaments. There is also an abnormal clustering of labelled cells (arrow) proximal to the third gill filament. It appears as if these labelled cells have failed to assume their proper position (according to their developmental stage) in the developing gill filaments. Scale bars (A and B), 100 μm. In (A) and (B) the anterior of the embryo is at the top right of the of the plate.

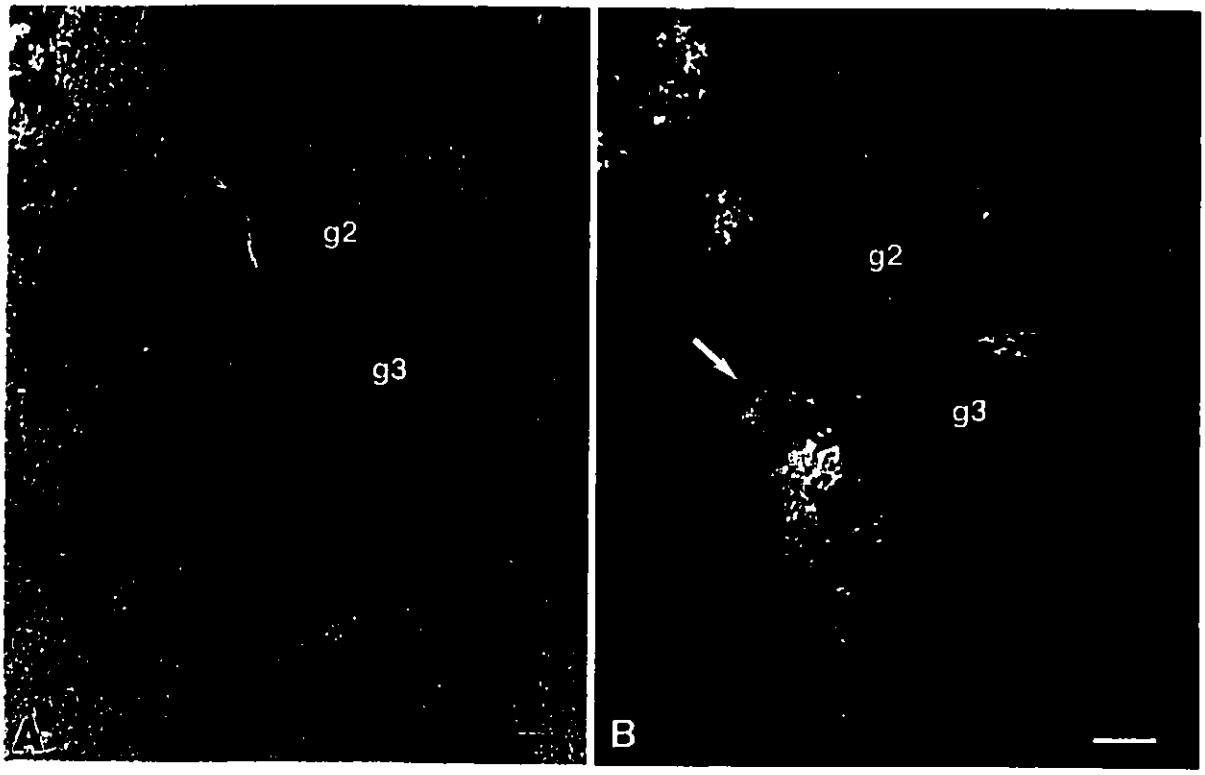
g2
g3
A
g2
g3
B

3.2 The Effect of the Premature Death Mutation on the Cardiac Neural Crest

The cardiac neural crest does not seem to be affected by the (*p*) mutation. In the mutant embryo, the cardiac neural crest (from zone 4 of the neural fold) migrated ventrally towards the heart region as initially specified (see Fig. 33B). Zone 4 neural fold cells normally migrate ventrally towards the anterior heart in wild-type embryos (see Fig. 33D and Chap I). By stage 39, they have migrated to the branchial arches and are about to enter the cardiac cavity (see Fig. 33C and 33D). At this point the aortic arches and the truncus arteriosis have not completely developed, so fluorescent labelling of cardiac crest was not detected in these elements. Our results show that the characteristic plug of undifferentiated cells in the conus of the mutants was not of cardiac neural crest origin (as seen by the absence of label in the cells of the plug, see Fig. 33A and 33B). From these figures, we can see that the cardiac neural crest has migrated toward the developing heart but has not reached the conus arteriosis in the mutant (Fig. 33B) or in the wild-type embryo (Fig. 33D). The characteristic "plug" of cells (in Fig. 33A) is ventral to the position of the labelled cardiac neural crest. It is also important to note that cardiac neural crest is found in the anterior outflow tract of the truncus arteriosis, and not in the other more posterior regions of the heart such as the ventricle or the atrium. The gross migrational pattern of the cardiac neural crest appeared normal (Fig. 33B). There were no signs of abnormal "clumping" in the labelled cardiac crest cells near the heart (see Fig. 33B), such as seen in the rudimentary gills. It is interesting to note that in Figure 33B, we see that the cardiac neural crest has migrated ventrally towards the heart region but the adjacent primary gill filament does not contain any labelled cells, contrary to a normal embryo of this stage (see Fig. 33D). This suggests that the neural crest cells from zone 4 which are fated for the posterior gill arches are affected by the mutation but cardiac neural crest cells, originating from the same area, are not affected.

Figure 33. The plug of undifferentiated cells in the conus arteriosis is not of cardiac neural crest origin. (A) Cross section of the stage 38 *p/p* mutant embryo (phase-contrast image) indicating the dark plug of undifferentiated cells (arrow) in the conus arteriosis (c) of the heart. The location of the otic vesicle (ot), rhombencephalon (rh), pharynx (p) and ventricle (v) are also shown. (B) Fluorescent image of the same section as in (A). Labelled zone 4 neural fold cells are seen in the rhombencephalon (rh) and are shown to migrate ventrally towards the heart. The conus (c) does not contain any labelled cells. Therefore the "plug" of undifferentiated cells is not of neural crest origin. The neural crest cells in the mutant do appear to be migrating normally. No abnormal clumping of cells is seen as the cardiac crest is migrating ventrally. (C) Frontal section through the stage 38 anterior heart of a wild-type embryo. The fourth branchial arch leading to the gill filament (gf) is indicated. The location of the developing truncus arteriosis (ta) and conus arteriosis (c) are shown. (D) Fluorescent image of the same section as in (C). Note that at this stage of development, the migrating cardiac crest has not yet reached its final destination in the truncus arteriosis. Labelled cells are seen in the developing gill filament. Note also in the mutant (B), that there is an absence of labelled cells in the gill filament (gf). (E) Diagram of the stage 37 axolotl indicating the plane of section along the body axis for the section in (A) and (B). Scale bars (A-D), 100 μm.

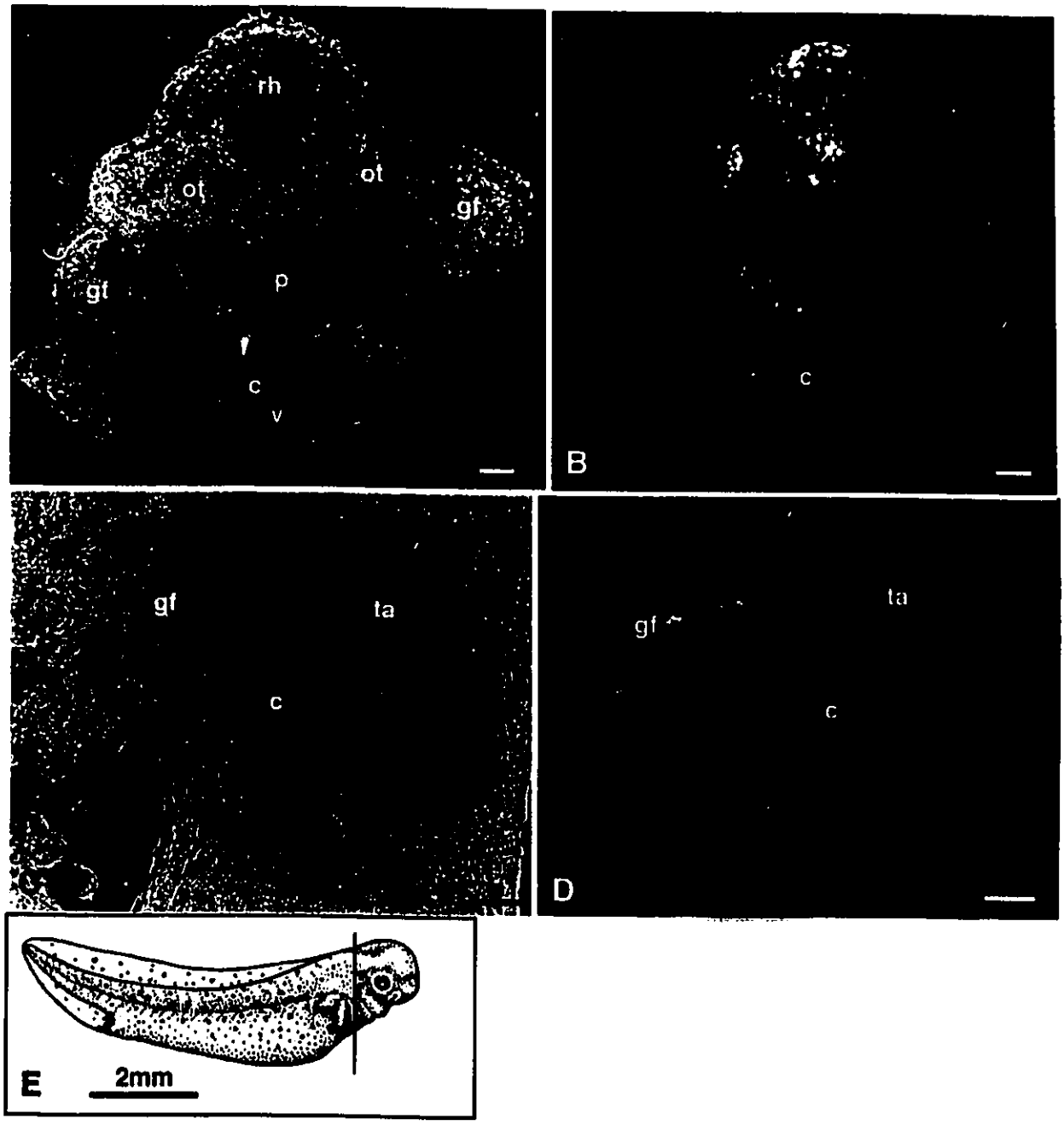
rh
ot
ot
gf
gf
p
c
v
B
c
gf
ta
c
gf
ta
c
D
E
2mm

3.3 The Mutant Hindbrain

As stated in the previous chapter, zone 4 cells of the neural fold are involved in the development of the hindbrain. Therefore, the resultant labelling of zone 4 cells in the stage 39 hindbrain of the mutants and the wild-type embryos was also compared. The hindbrain region, adjacent to the otic vesicle, did not appear grossly abnormal in the mutant embryos. However, this area did appear thinner than in the wild-type embryos (see Fig. 34), but there was not any obvious aggregation of labelled cells in the rhombencephalic region. In the mutants the spinal cord also appeared slightly crooked.

Figure 34. Labelling in the hindbrain of the mutant and wild-type embryos. (A) Angled frontal section (phase contrast image) through the rhombencephalon (rh) in a typical *p/p* embryo at stage 37. The location of the otic vesicle (ot) is also shown. Note that in (A), (B), (C), and (D), a line drawn between "a" and "p" would indicate the anterior-posterior axis of the embryo. (B) Fluorescent image of the same section as in (A). The labelled cells are from zone 4 of the neural fold. Note that the labelling pattern in the rhombencephalon (rh) appears normal. The cells from zone 4 are not ectopically located but, as in the wild type embyo, are located in the rhombencephalon in close proximity to the otic vesicle (ot). No abnormal clustering of cells is visible. However, it does appear that the cells in this region are not as uniformly labelled as in the hindbrain of the wild-type embryo, [(C) and (D)]. (C) Angled section through the stage 37 embryo originally labelled in zone 4 of the neural fold. The region of the rhombencephalon (rh) is shown at the level of the otic vesicle (ot). (D) Fluorescent image of the same section as in (C). Note the uniform labelling pattern of neural tube cells from zone 4. (E) Diagram of a stage 37 axolotl embryo indicating the plane of section for the sections in A-D. Scale bars (A-D), 100 μm.

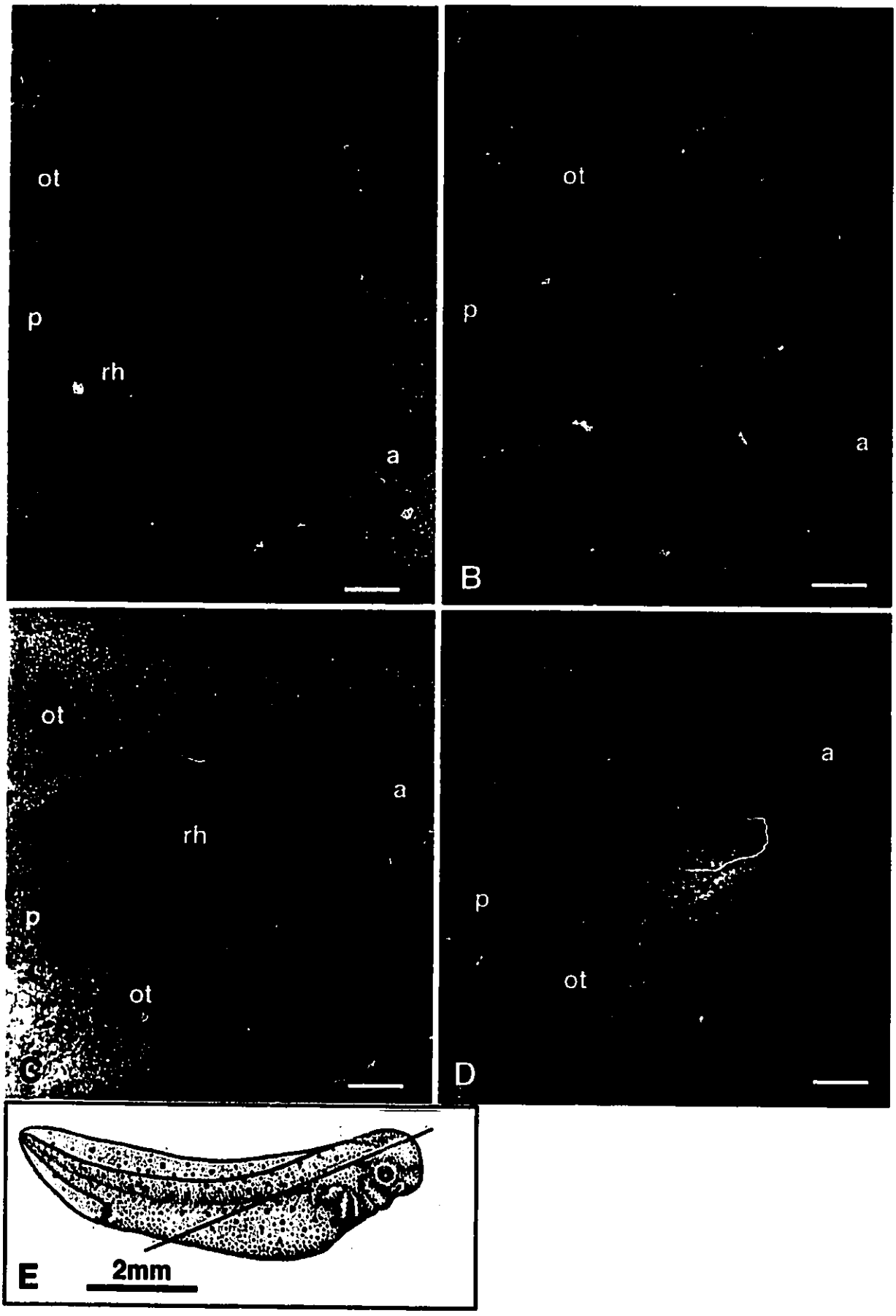
ot
p
rh
a
B
ot
p
a
ot
a
rh
p
ot
C
a
p
ot
D
E
2mm

3.4 Summary of Results

By using the DiI labelling technique, we focussed on one particular area of the neural fold and examined the *p* mutation's effect on those specific neural crest cells, namely cardiac neural crest cells. The labelling allowed us to determine that cells abnormally clustered together, such as those among the gill filaments, were of neural crest origin. The technique also allowed us to distinguish between abnormally clustered cells of neural crest origin and those of either mesodermal or endodermal origin. For example, the DiI labelling indicated that the aggregated cells around the gill filaments of the mutant were neural crest cells, but the plug of undifferentiated cells in the conus arteriosis was not derived from the cardiac neural crest.

The cardiac neural crest cells which go on to become part of the walls of the outflow tract do not seem to be affected by the mutation. However, the cells from the same, initial "zone 4" region which are involved in gill development are affected by the mutation. Therefore, it is safe to assume that, so far, only the prechondrocytic subpopulation of the cranial neural crest is a target of the mutation, while the cardiac neural crest is not.

Discussion

We have attempted to further characterize the targets of the premature death mutation. Previously, it has been established that the mutation affects the chondrogenic differentiation of cranial neural crest cells (Graveson and Armstrong, 1994; 1996), the migration of the lateral-line primordia, and the differentiation of the mechanoreceptive neuromast organs (which are derivatives of placodal ectoderm) (S.C. Smith et al., 1994).

Because gill development is abnormal in the *p/p* mutants and because mutant embryos contain a plug of undifferentiated cells in the conus arteriosis, we hypothesized that the cardiac neural crest may also be a target of the *p/p* mutation. After establishing the premigratory location of the cardiac neural crest along the neural fold of the axolotl (see chapter I of thesis), we tagged the area with a fluorescent dye and compared its development in mutants and wild-type embryos. Our results indicate that the cardiac neural crest does not appear to be a target of the *p* mutation. However, cranial neural crest cells involved in gill formation, from the same original location along the neural fold, are affected.

The main reason for assuming that cardiac neural crest is not affected by the mutation is the fact that the cardiac crest did not exhibit any migrational problems in reaching the cardiac cavity, and did not exhibit the same characteristic "aggregation" or clumping of migratory cells. However, from our results we cannot determine whether the cardiac crest is affected by the mutation after it has reached the cardiac area, because by this time, degeneration of the embryo has already taken place. Even if the cardiac crest is affected by the mutation after stage 37, we can rule out the possibility that the cardiac crest is the major cause of death of the embryo. Two reasons account for this. First, if we assume that the lack of circulation in the mutants could be attributed to the plugs of undifferentiated tissue in the heart, then the fact that these plugs are not derived from cardiac neural crest, "absolves" the cardiac crest from being a factor in the prevention of

circulation. Secondly, we have established (see chapter I of this thesis) that the amphibian cardiac neural crest contributes little to the whole cardiovascular system at stage 37 and only plays a minor role in circulation. Our results show that the role of the cardiac neural crest is to aid in lining the walls of the truncus arteriosis and the walls of the branchial aortic arches, and that this role is established much after stage 37. We have shown that by stage 44, after further heart development, and the development of the aortic arches, that the function of the cardiac crest is fully established. Thus, at stage 37, the time at which the mutants begin to disintegrate, heart development has not progressed to the point where the cardiac crest is even a minor player in the cardiovascular system in the axolotl. At stage 37, the cardiac crest only makes its way to the heart region, which, as we observed, was not hindered in the mutant. Furthermore, Graveson and Armstrong (1994) showed that the ablation of the posterior cranial neural crest in wild-type embryos can still result in the eventual establishment of circulation. Thus, indicating that even without the presence of cardiac neural crest, (which also happened to get ablated), blood can still circulate.

So, the question still remains. What causes these embryos to die? Our results indicate that the migration of neural crest may be more affected that originally anticipated. The migration of neural crest in the mutants has been studied before. Graveson and Armstrong (1994) showed that the migration of cranial neural crest cells in the mutant followed the same pathway as wild-type cranial crest. These observations were made by the transplantation of mutant cranial neural folds onto albino host embryos. The migration of the pigmented mutant crest was then followed along the surface of the albino embryo until the embryo had reached stage 32 and the pigmented branchial neural crest had migrated too deeply to be clearly visible through the unpigmented ectoderm. These experiments examine mutant cranial neural crest migration only up to stage 32 and only superficially through the ectoderm. Our work has taken these experiments one step further and looked at internal mutant crest migration up to stage 38. Our results correspond with those of Graveson and Armstrong (1994) in that we also observed that initially during

migration, mutant cranial crest cells follow the same pathways as wild type cranial crest. However, our results also show that migration in the mutant does not follow the same organizational pattern of flow as that of the wild-type embryos. When the mutant cells have reached the general area of their final destination, they appear to have stopped migrating and become clustered together in a haphazard arrangement. Also, their migration has not progressed as far as their wild-type counterparts of the same age. Our results imply that cranial neural crest migration is affected in the *p* mutants but only at a later stage of development. Since Graveson and Armstrong showed that cranial neural migration appears normal up to stage 32, then we can infer that migration is perturbed sometime between stage 32 and stage 37.

This late-onset cessation of migration has also been observed in the lateral-line system of the *p/p* axolotl mutants. S.C. Smith et al, (1994) observed that early migration and development of the lateral-line primordia appeared normal in mutant embryos, but at stage 37, migration of the middle-body lateral-line primordia arrested, and neuromast differentiation did not occur. Upon close scrutiny, we can notice the parallels between the effects on the lateral-line system and the gill arch primordia in the mutants. In both systems, we see a cessation of migration late in development and a subsequent inability to undergo further differentiation. In the lateral-line system, the middle body lateral-line primordia arrests in migration at stage 37 and further neuromast differentiation does not occur (S.C. Smith et al., 1994). In the gill arches, branchial arch crest migration halts (see results section) and subsequent chondrogenic differentiation is inhibited (Graveson and Armstrong, 1990). Clearly from these two examples, something in the mutant renders the cells incapable of completing migration beyond a certain point and undergoing further differentiation. From previous studies it has been established that it is not the mutant environment which causes the phenotypic effects because certain mutant primordia transplanted into normal hosts are not rescued (Mes-Hartree and Armstrong, 1980; S.C. Smith et al., 1994). Therefore, it is certain populations of cells which are directly affected

by the mutation. It still remains unclear as to what exactly causes these cells to arrest in development. From our labelling experiments, we have shown that there are no ectopically located cells originating from the cranial neural folds. This reinforces the statement that axial specification of the mutant cells is normal (Graveson and Armstrong, 1994). However, other factors regarding neural crest specification may be involved.

It has been suggested that the *p* gene renders certain cell populations incapable of normally responding to inductive signals (Graveson and Armstrong, 1990; 1996; S.C. Smith et al., 1994). Our results, with respect to mutant cranial neural crest cells not being able to complete their migration into the gill arches, corresponds with this theory. The fact that these cells do not follow an organized stream-like pattern in their migration suggests that these cells are unable to maintain an organized path of migration. The reason that they do not migrate in an orderly manner may be because they have not been properly induced to do so. In the wild-type embryo, it appears that the gill-forming cranial crest has been instructed to migrate ventrally and assume a position in the gill arches. The mutant crest manages to migrate ventrally, but cannot complete the task in the gill arches. Either the crest has not been specified to participate in gill formation once it has completed its ventral migration, or the mutant crest cannot respond to the instructions that it has been given. Some evidence points to the latter possibility. Graveson and Armstrong (1996) showed that when wild-type dorsal lips were transplanted into *p/p* hosts, secondary neural structures were induced but these secondary neural structures could not form cartilage. The authors suggested that the ectoderm was unable to respond to the inductive signals provided by the mesoderm. Our results also point to an inability to respond to an inductive signal. However, it is unclear whether it is the ectoderm that is defective, or whether it is a more specialized cell lineage, like the chondrogenic cranial neural crest, that has the problem. Our results suggest that it may be only certain specialized cell lineages that are the target of the mutation since chondrogenic cranial crest appears to be affected, but cardiac crest is not. This also implies that the cardiac neural crest, the cranial chondrogenic neural

crest, and even lateral line primordia, may have different hierarchal positions in a cascading series of neural specification. This idea may be supported by the fact that cardiac neural crest ablation in the chick is not subject to regulation by other neural crest cells and may be determined at an even earlier stage than other cranial crest (Kirby, 1989). The early determination of cranial neural crest has also been suggested by Noden (1983).

Why the mutation affects certain populations of cells and not others is still unknown. Neuronal brain cells are not grossly affected and neither are pigment cells, but chondrogenic neural crest cells are affected (Trottier and Armstrong, 1977). We have shown that the mutation affects the cranial neural crest cells from zone 4 (refer to Fig.11), which go on to form parts of the gill filaments, but does not affect the cardiac neural crest from the same area along the neural fold. It is important to note however, that from our results, we cannot fully determine if the mutation completely bypasses the cardiac neural crest, or if it does, in fact, target the cardiac crest, but manifests its effects only beyond stage 39, the point at which the cardiac crest becomes involved in aortic arch development. It would be difficult to assess *in situ* whether aortic arch development is affected by the mutation since complete development of the cardiovascular system does not occur until the mutant embryos are in a severe state of disintegration. Transplantation of DiI labelled mutant cardiac neural folds into wild-type hosts may give us further insight into the pattern of development of mutant cardiac crest beyond stage 39.

Abnormal heart development, depicted by the appearance of plugs of cells in the endocardium is a main feature of the premature death mutation. Our results have shown that this plug of cells is not of neural crest origin. Since cardiac myocytes are mesodermal, it is highly likely that it is of mesodermal origin. This can be determined by similarly labelling, with DiI, the heart field mesoderm in *p/p* embryos. The results from this experiment would confirm that migration of mesodermal tissue is also affected by the mutation. Graveson and Armstrong (1990) showed that *p/p* mesoderm is capable of forming normal, beating heart tissue *in vitro*, but whether this tissue can develop further,

and form a functional heart capable of circulation remains to be seen.

In the *p/p* mutants there is strong evidence that there is an inability by the target cells to respond to an inductive signal (Graveson and Armstrong, 1996). If these cells are deficient in receiving inductive signals or lack the machinery to carry out their instructions once they have received them, then regardless of the time the cells are specified, the mutant would exhibit the same phenotype. Clearly, particular mutant cells fall short of reaching their final destination and are unable to undergo subsequent differentiation (our results and S.C. Smith et al., 1994). It may be possible that these cells lack the ability to undergo proper migration and subsequent differentation because of a deficiency in a cell surface receptor.

Several studies have been performed in which antibodies to cell surface receptors were injected into embryos and as a result, neural crest migration was severely disturbed. Bronner-Fraser (1985) noted that upon addition of JG22 (an antibody recognizing a 140-kD cell surface complex in neural crest adhesion that interacts with fibronectin and laminin), neural crest cells plated on a fibronectin or laminin substrate became detached from the culture dish and formed aggregates of rounded cells. These and other experiments involving the addition of antibodies have also shown that only certain cell populations display abnormal morphology (Bronner-Fraser, 1985; 1986; Poole and Thiery, 1986; Bronner-Fraser and Lallier, 1988; Kintner, 1988; Bronner-Fraser et al., 1992; Milos et al., 1993). For example, cranial crest cells are more affected by the addition of JG22 than trunk crest (Bronner-Fraser, 1985) and antibodies against galactoside-binding lectins specifically cause abnormal development in melanophore patterns, the cranial cartilages, the heart, and the gut (Frunchak and Milos, 1990; Milos et al., 1993). These experiments show that abnormal effects can be linked to particular cell populations, but that these cell populations may not arise from the same germ tissue. The experiments also suggest that a deficiency in a cell surface receptor common to certain migrating primordia may account for

the abnormalities observed. It may be this same phenomenon which is occurring in the premature death mutant of the axolotl.

Bronner-Fraser's observation (1985; 1986) that addition of antibodies results in the aggregation of cranial neural crest cells may be analogous to the "clumping" of cranial crest cells that we have observed in the developing gill filaments. It is possible that the clustering of cells that we observed is due to a lack, or block of a cell surface receptor involved in cell migration which expresses itself at a late stage in development, and that this deficiency may also prevent subsequent differentiation. The varying temporal expression of cell adhesion molecules involved in cell migration has been previously established (Thiery et al., 1982; Hatta et al., 1986). The resultant death of the embryos may also be attributed to the lack of proper migration and differentiation of certain tissue. It is possible that the "clumping" of cells, that we observed near the gill, prevents circulation from being established. The correlation between gill development and circulation has been alluded to previously by Graveson and Armstrong, (1994). They found that a return to normal gill morphology corresponds to a return in circulation in neural-crest deficient embryos after a period of regulation (Graveson and Armstrong, 1994).

From our observations and those of other experimenters, we have tried to suggest possible explanations for the phenotype exhibited by the *premature death mutation* in the axolotl. We believe that the mutation affects the ability of certain cell populations to respond to an inductive signal. The reason these cells cannot carry out their instructions may be because the signal can't get through due to a lack of a cell surface receptor. At present, none of these hypotheses have been tested. Experiments using antibodies to perturb cell migration might answer some questions regarding the premature death mutation. Such experiments may also result in a *p* mutant phenocopy.

The many pleiotropic effects, on several cell types in the premature death mutation, make the mutation a useful model for studying the commonalities between cell types and their responses to inductive signals for migration and differentiation. The pleiotropic

effects of the mutation also liken it to several human congenital abnormalities such as DiGeorge syndrome (Van Mierop et al., 1986), Down's Syndrome (Kirby, 1991), CHARGE association (Siebert et al., 1985), neurofibromatosis (Riccardi and Eichner, 1986) etc. Each of these congenital defects results in patients with a multitude of abnormalities in organs originating from various cell types, but which are somehow linked. By further studying the premature death mutation and elucidating its very elusive "modus operandi," we may shed further light on the mechanisms involved in congenital abnormalities found in other organisms, and the general mechanisms involved in tissue differentiation.

Appendix I

Tables of Culture Media

Table 1. Holtfreter's Medium :

NaCl	3.46 g
KCl	0.05 g
$CaCl_2$	0.10 g
$MgSO_4.7H_2O$	0.20 g
$NaHCO_3$	0.20 g

per litre of dechlorinated tap water
pH 7.4

This medium was diluted to a working concentration of 25% and 0.10 g of penicillin and 0.10 g of streptomycin was added to the solution.

Table 2. Steinberg's Medium :

NaCl	3.40 g
KCl	0.05 g
$CaCl_2$	0.05 g
$MgSO_4.7H_2O$	0.21 g
Tris	0.56 g

per litre of distilled water
pH 7.7

This medium was used at full concentration with 0.1% gentamicin added.

Appendix II

Table I. The stages of embryonic development in *Ambystoma mexicanum* (see following pages)

Measurements: L=length; H=height; B=breadth; D=diameter

Table I

Stages of normal development of Ambystoma mexicanum

(incubation at 20°C)

N of Stages	Time from the cleavage furrow I: In hours and minutes	Time from the cleavage furrow I: In number of τ_o	Features, size, in mm
1	2	3	4
1			Freshly laid fertilized egg in membranes Egg diameter without membranes - 1.85 - 2.00 mm
1½			Activated egg, a broad perivitellin space formed. D = 2.0
2-	0	0	First appearance of the I cleavage furrow on animal pole. Beginning of time reckoning (picture fails). D = 2.0
2	65	0.72	2 cells. D = 2.0
3	2.40	1.7	4 cells. D = 2.0

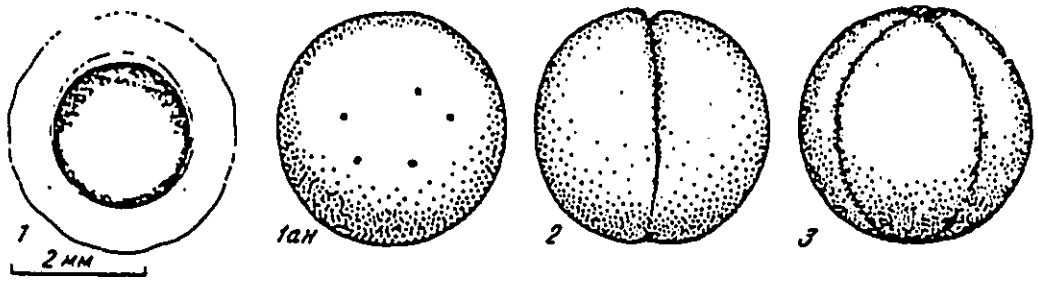

4	4.12	2.7	8 cells. D = 2.0
5	5.22	3.5	16 cells. D = 2.0
6	6.45	4.5	32 cells. D = 2.0

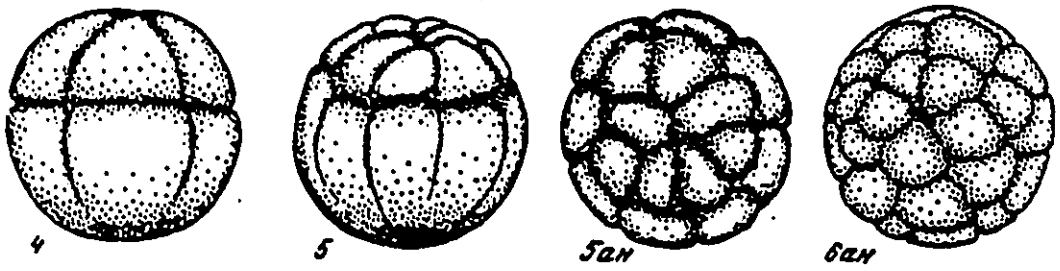

1	2	3	4
7	8.26	5.5	64 cells. D = 2.0
8	16.06	10.5	Early blastula (Fall of mitotic index in animal blastomeres (Rott a. Beritashwili, 1974). D = 2.0
9	21.28	14	Late (epithelial) blastula. The surface is smooth.
9½	24.32	16	Beginning of morphogenetic function of nuclei (Ignat'eva, 1972). D = 2.0
10	26.00	17	Early gastrula I. First signs of dorsal blastopore lip formation. D = 2.0

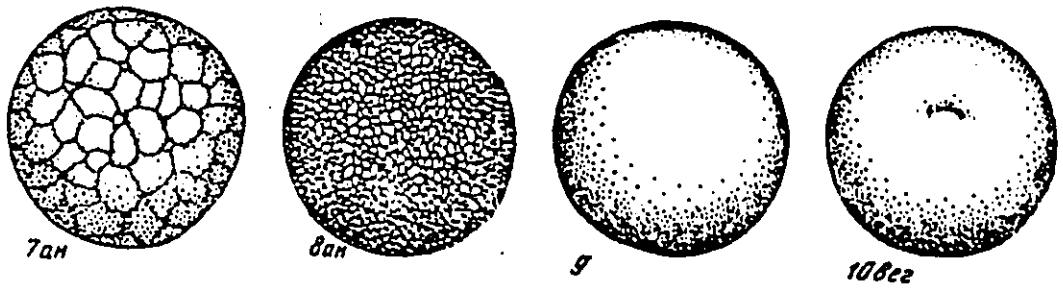

10½	32.10	21	Early gastrula II. Invagination continues. Blastopore is a slit going almost horizontally (one quadrant). D = 2.0
10 3/4	37.00	24	Middle gastrula I. Dorsal lip of blastopore forms a semicircle. D = 2.0
11	38.30	25-26	Middle gastrula II. Blastopore is three quadrants of circle. Lateral lips of blastopore formed, ventral lip only marked by pigment accumulation. Yolk plug reaches maximum diameter, d = 1.2 mm; D = 2.0
11½	40-42	27-28	Late gastrula I. Blastopore forms a circle. Invagination continues, yolk plug decreases, d = 0.6 mm; D = 2.0

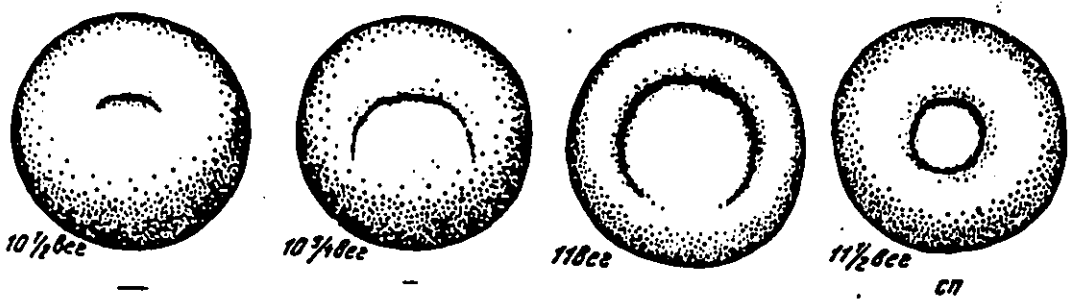

1	2	3	4
12	47.30	31	Late gastrula II. Blastopore has an oval or circular form. Size of yolk plug: 0.40 x 0.45; D = 2.0
12½	49-51	32-34	Late gastrula III. Closing oval blastopore. Size of yolk plug: 0.15 x 0.20 mm; D = 2.1
13-	50.30-54	33-35	Stage of slitlike blastopore. Boundaries of neural plate are still not distinct
13	55-56.30	36-37	Early neurula I. Blastopore is a narrow vertical slit. Groove in the midline of the neural plate. Boundaries of neural plate are outlined but neural folds are not yet elevated above the surface of the embryo. The dorsal side is slightly flattened. D = 2.1

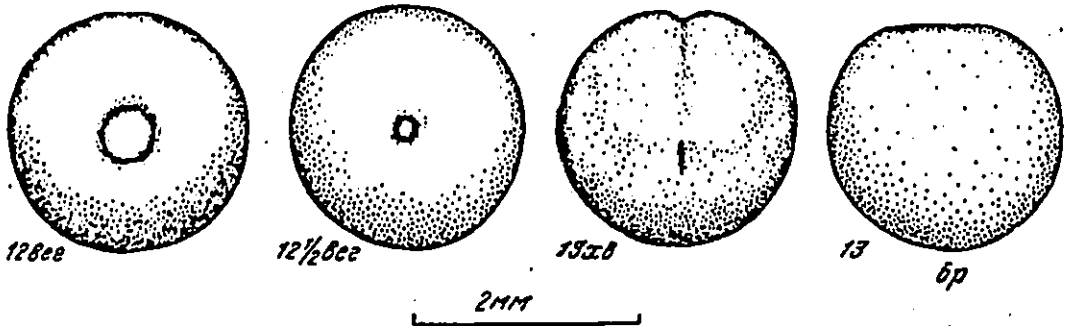

14	58.15	38	Early neurula II. Neural plate is broad. Neural folds are outlined and begin to raise above the surface in the head region. Embryo becomes slightly elongated. Length = 2.2; Breadth = 2.0
15	59.50	39	Early neurula III. Neural plate has the shape of a shield. Neural folds are raised and bind all the regions of the neural plate. L = 2.25; B = 2.1
16	63	41	Middle neurula II. Neural folds become higher, the spinal region of neural plate narrows, the neural plate becomes sunken. L = 2.25; B = 2.1

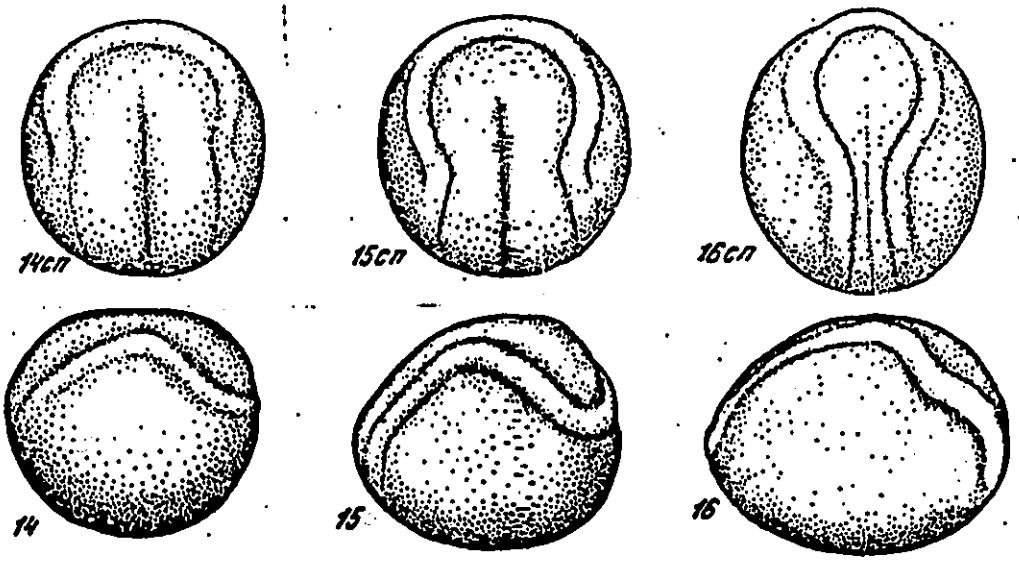

17 64.30 42

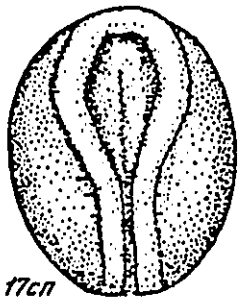

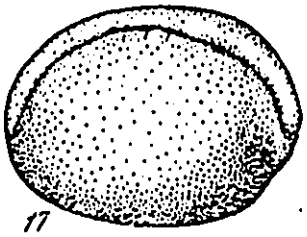

Late neurula I. Neural folds higher especially in the head region. Further narrowing and deepening of the neural plate both in the head and in the spinal regions. Hyomandibular furrow limiting the mandibular arch is outlined (yet very slightly). The segmentation of mesodermal material begins. 2 pairs of somites formed. L = 2.35; B = 2.0

---

18 66 43-44

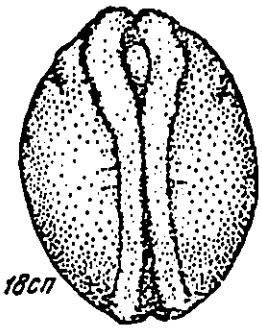

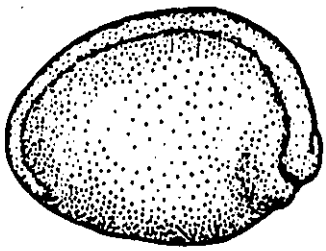

Late neurula II. The neural plate is deeply sunken. Neural folds are developing and are especially high in the head region where three expansions (still yet very slight) corresponding to fore, middle and hind brain vesicles are outlined. The neural folds of spinal region are about to come into contact. Hyomandibular furrow becomes more marked. 2 pairs of somites. L = 2.4; B = 1.9

---

19 69.00 45

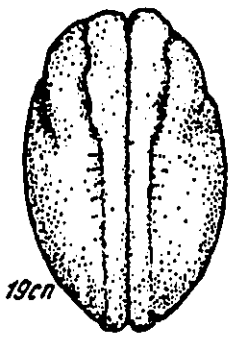

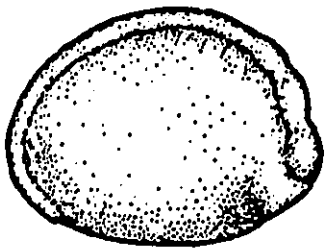

Late neurula III. Neural folds are coming in contact throughout but yet do not fuse. Brain curvature is quite distinct in profile; fore, middle and hind brain vesicles are also distinct. The swelling of optic vesicles are outlined. Hyomandibular furrow becomes deeper. 3 pairs of somites. L = 2.7; B = 1.7; Height = 2.1

20 70.30 46

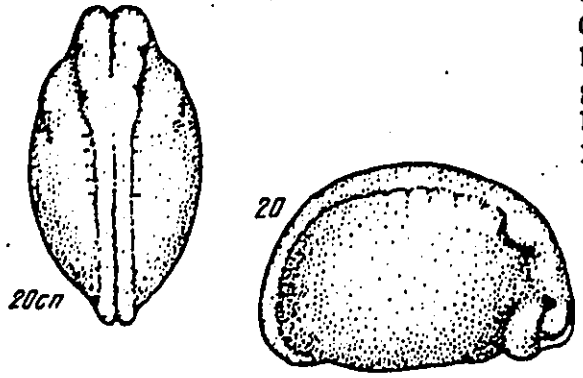

Late neurula IV. Neural folds fused in spinal region. In brain region they are only in contact. Optic vesicles are distinct and increasing. Grooves in ectoderm appear at the level of the hindbrain. Very slight swelling of the future gill region is faintly marked. Mandilbular arch becomes prominent. 4 pairs of somites. L = 2.7; B = 1.5; H = 1.7

---

21 72 47

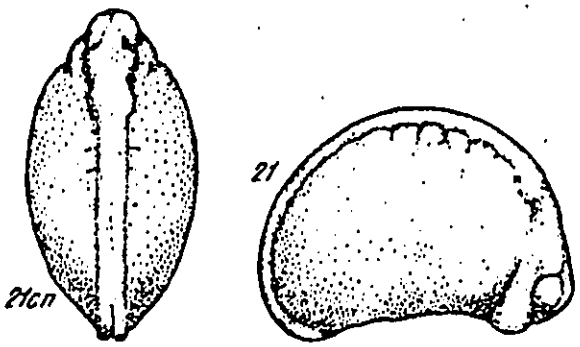

Neural folds are completely fused. The hind boundary of gill region becomes more distinct. Pronephros begin to outline (very slight swelling 4 pairs of somites. The ventral side of embryo is a lightly concave line; the head region (from the level of mandibular arch) is somewhat downwardly curved. The dorsal side is a semicircle; occipital and parietal brain curvatures become apparent.

---

22 73 48

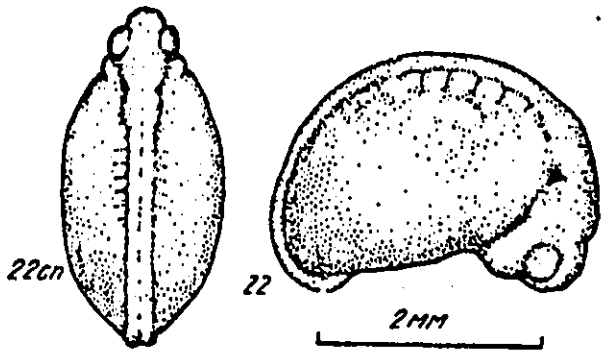

The gill region and the pronephros are now more distinct. The tail bud is outlined (but still very slightly). 5-6 pairs of somites. The ventral side of the embryo becomes more concave in relation with a greater curving downward of the head. L = 2.8; B = 1.4; H = 2.3

---

23 74.00 48.5

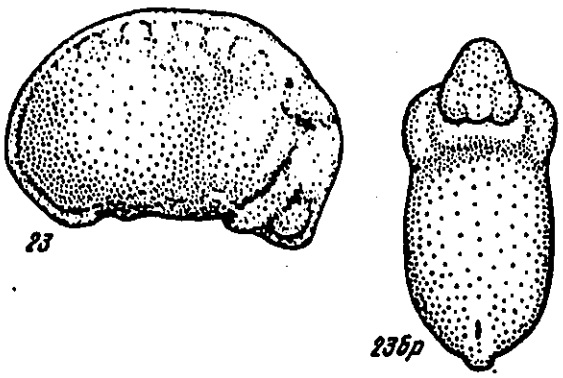

The primordium of the ear outlined as a shallow depression in ectoderm in the region above the future hyoid arch. In the dorsal region of the gill swelling the hyobranchial furrow appears outlining the boundary between the hyoid arch and the branchial arch I.

24 80 52

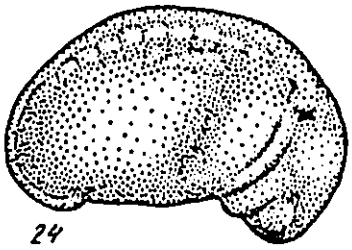

24

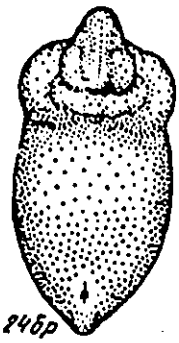

24б

Ear pit becomes more distinct. The hyobranchial furrow continues to lengthen running to the ventral side. The pronephric swelling is clearly outlined and not only the pronephros itself are well seen but the beginning of the pronephric duct also: 8-9 pairs of somites. L = 3.0; B = 1.3; H = 1.85

---

25 83 54

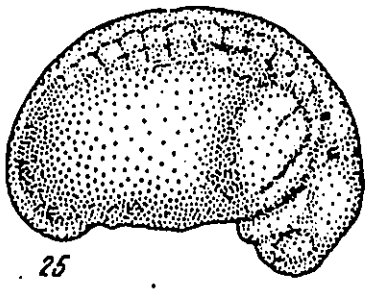

25

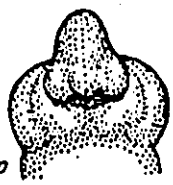

25б

The gill swelling continues to increase, the hyobranchial furrow lengthens further. The branchial furrow I appears (still faintly outlined) in the dorsal region of the gill swelling. The tail bud continues to be small. 9 pairs of somites. The body of the embryo continues to lengthen, the ventral side becomes more concave, the head protudes more downwardly. L = 3.25; B = 1.45; H = 2.0

---

26 84.30 55

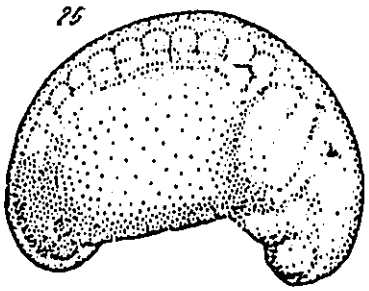

25

26б

Ear pit is quite distinct. The branchial furrow I becomes more marked and longer. The whole gill region is a considerable, distinctly outlined swelling, the height of which is accentuated by a deep groove formed between the developing pronephr and the gill region. Pronephric duct is seen along 6 somites. The primordium of the olfactory organ appears as a tubercle in the anterior part of the head. The tail bud gradually increases. The body of the embryo is stretched, the head is curved down. 10-11 pairs of somites. L = 3.25; B = 1.45; H = 2.0

---

27 86 56 (54-59)

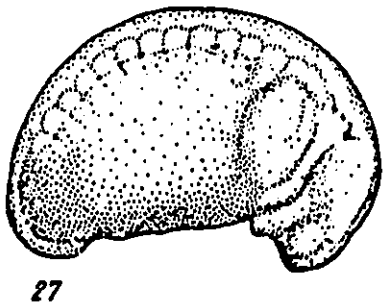

27

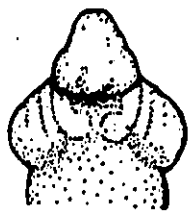

27б

The branchial furrow II appears in the dorsal part of the gill swelling (still very faintly marked). 12 pairs of somites. L = 3.35; B = 1.6; H = 1.85.

28	92.30	60 (57-63)	Further stretching of the body of embryo. Maximu downward curvature of the head is shown. The olfactory pit is distinctly outlined in front of the eye. 14 pairs of somites. L = 3.55; B = 1.6, H = 1.75

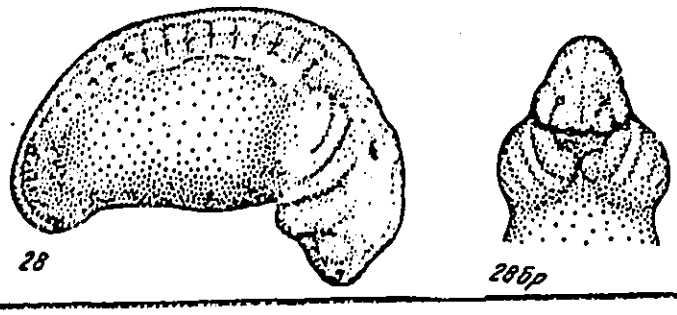

29	97	63.5-64	The straightening of the body of embryo begins but that can be seen only by somewhat less curvatı of the head. The tail bud increases. 16 pairs of somites. L = 4.2; H = 1.75

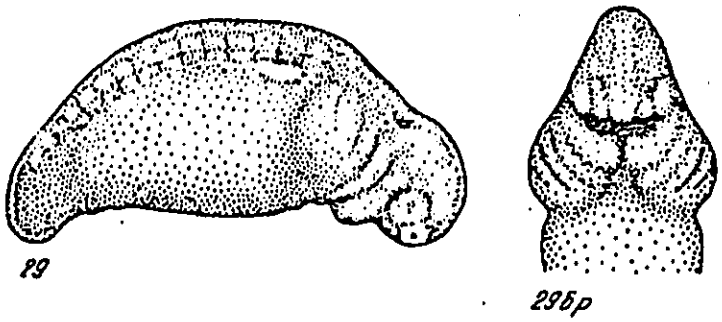

30	102	67 (65-68)	The straightening of the head curvature continues and the dorsal curvature of the body reduces. The body elongates and the tail bud becomes greate The fin fold appears for the first time. The dors fin fold begins on the level of the 14th somite. L = 4.5; H = 1.65

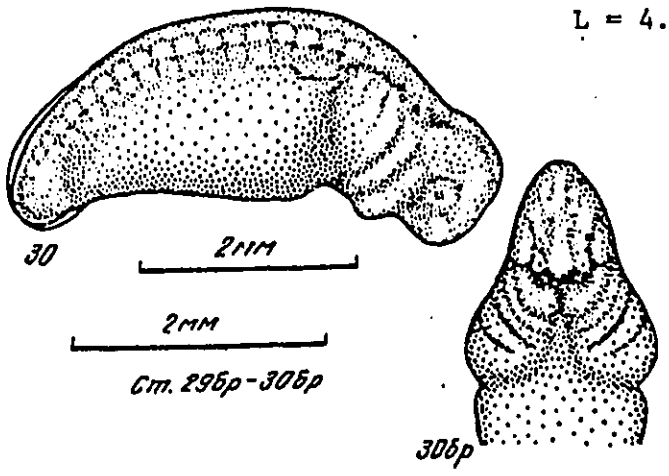

1	2	3	4
31*	109	71 (69-74)	19 pairs of somites. In the region of the lens primordium a groove appears. The branchial fur III becomes apparent in the dorsal part of the gill region. The dorsal fin fold begins on the level of the 12th somite. L = 4.7; H = 1.7

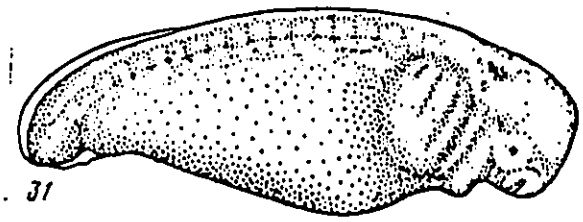

31

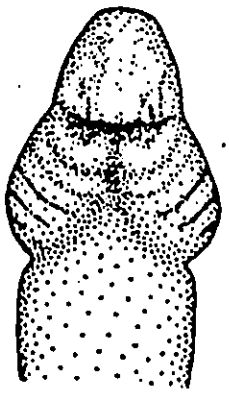

32	113	74	20 pairs of somites. The dorsal fin begins on the level of 10th somite. L = 5.0; H = 1.7

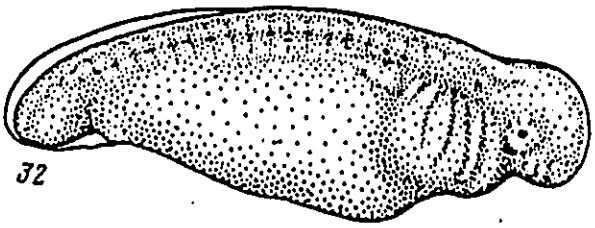

32

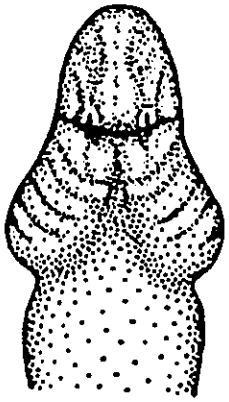

33*	113	71	21-22 pairs of somites. The dorsal fin begins on the level of the 8th somite. L = 5.25; H = 1

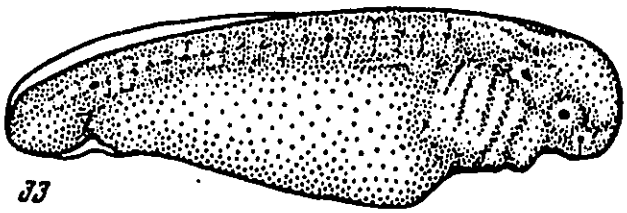

33

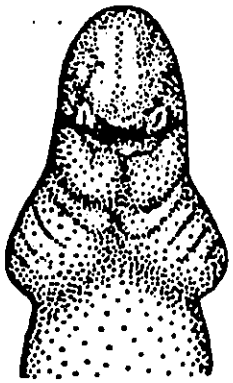

34	115	75	24-25 pairs of somites. The dorsal fin begins on the level of the 7th somite. L = 5.5; H = 1

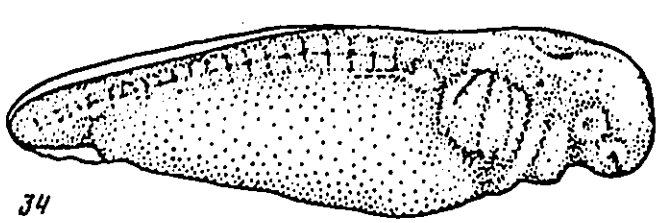

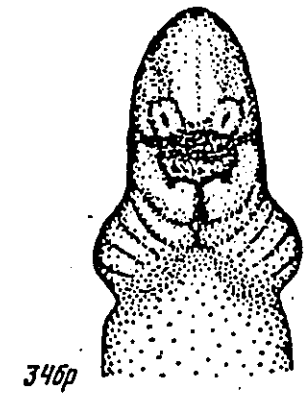

35	122	80	From this stage on the body axis from the hind-brain to the tail base is quite straight. Thre external gills show as nodules on the surface c gill swelling. The lateral line reaches to the 6th somite. The dorsal fin begins on the level of the 5th somite. The first chromatophores appear and also heart pulsation begins. The somites are now difficult to count. L = 6.25; H = 1.6

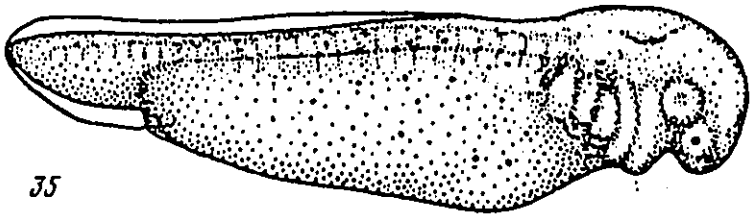

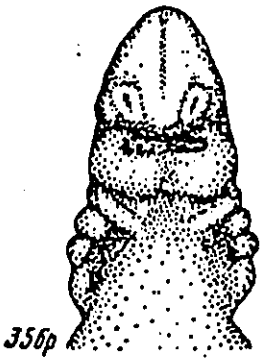

36	130	85-98	External gills have the form of short sprouts directed to the side from the gill swelling. L = 7.1; H = 1.7

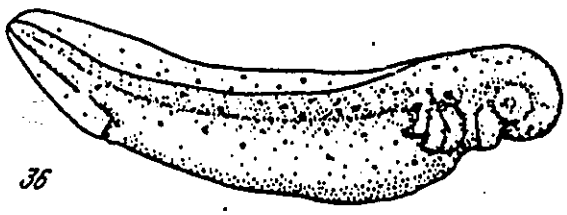

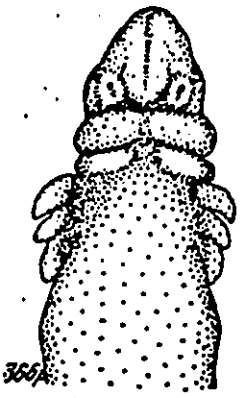

37* 177 115

Gills elongate and push ventroposteriorly. Tl
limb buds fail. L = 7.5; H = 1.7

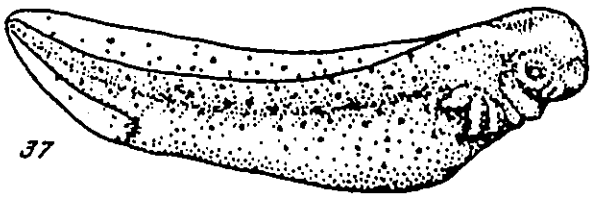

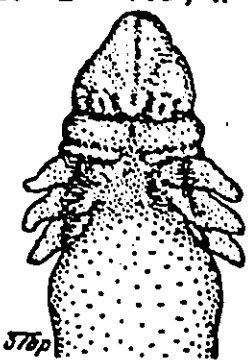

38* 178 114-132

In the gills the filament sprouts appear as nodules, two in each gill. The primordium of operculum becomes visible as a fold upon the hyoid arch. At this stage both rudiments of operculum do not yet reach the mid-line. The limb buds are still slightly outlin
L = 7.9; H = 1.8

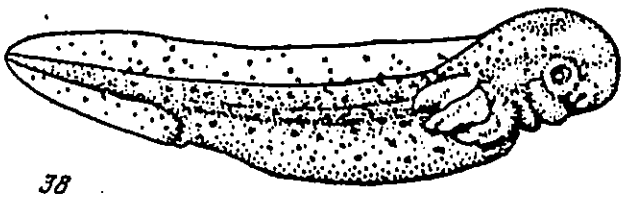

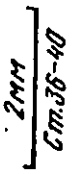

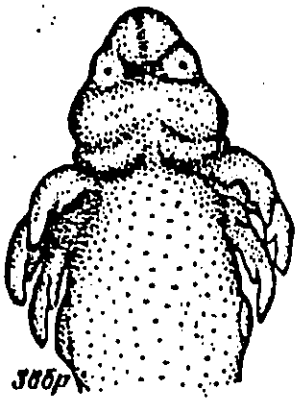

---

39 220 144

The gill I has 2 pairs of filament sprouts, t
gills II and III - 3 pairs. The gills cover
limb buds. Both rudiments of operculum almos
approach the midline. The angles of the mout
begin to show. L = 9.0; H = 1.9

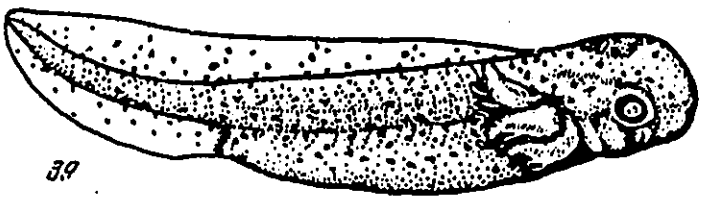

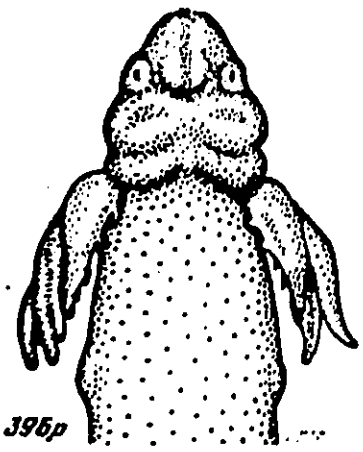

40	240	137	The gills become longer and the number of filame. increases: on the gill I are 4 pairs of filament on the gills II and III – 6-7 pairs of filaments. Both rudiments of operculum join at the midline. The angles of the mouth are marked more distinctl The limb buds form small tubercles. L = 9.3; H = 2.1

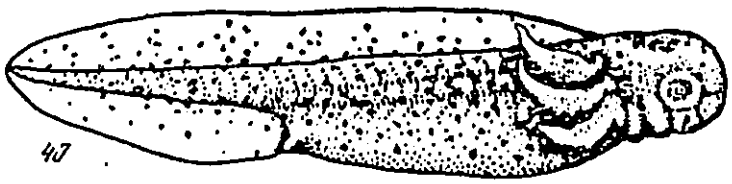

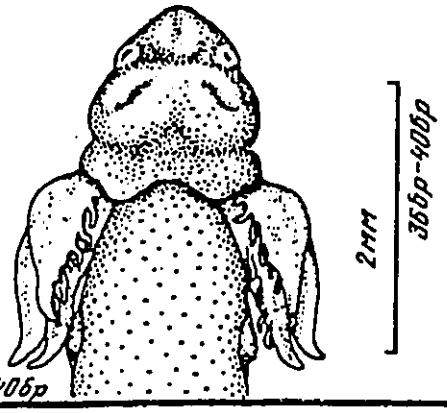

41	265	173-177	The gills continue to elongate. The number of filaments increases; filaments also become longer. The mouth is distinctly outlined. Th lateral line 2 runs on the flank toward the lir bud and passes around it on the ventral side. The forelimb buds are still small tubercles. this stage hatching begins. L = 10.0; H = 2.2

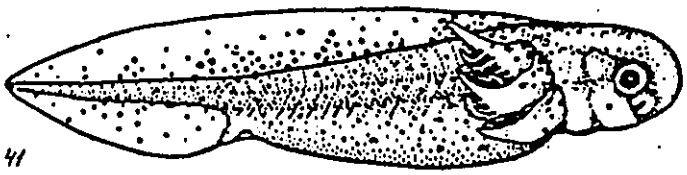

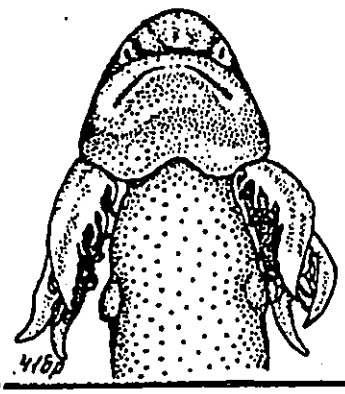

42	296	193	The gills reach far from the level of the fore-limb buds. The mouth is completely outlined bu is not broken through. L = 10.5; H = 2.1

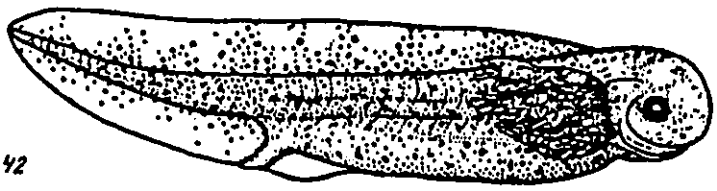

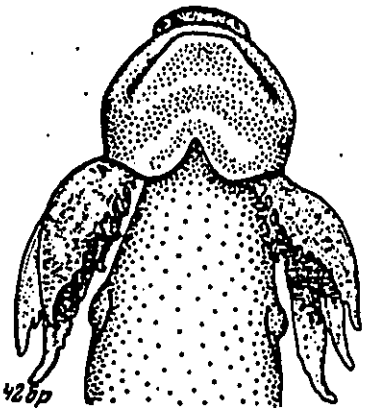

43 342 223 The breaking through of the mouth or the mout is already open. L = 11.3; H = 2.3

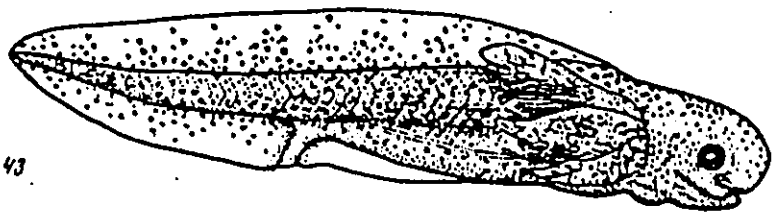

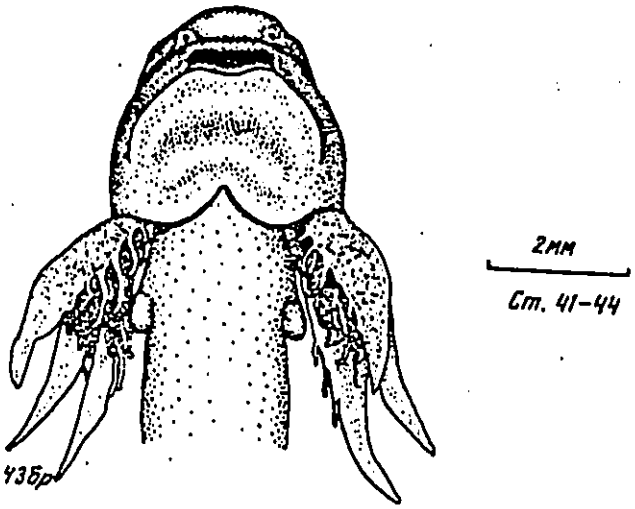

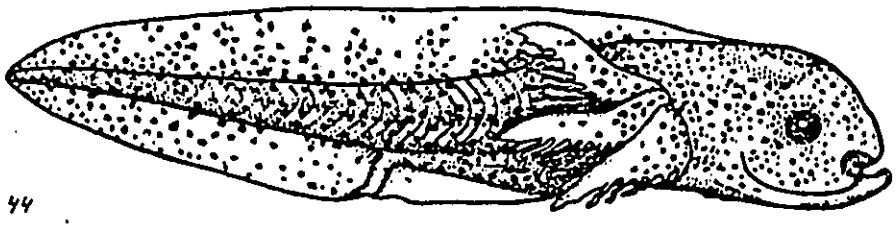

References

Abo, T., and Balch, C.M. (1981). A differentiation antigen of human NK and K cells identified by a monoclonal antibody (HNK-1). *J. Immunol.* **127**: 1024-1029.

Armstrong, J.B. (1985). The axolotl mutants. *Dev. Genetics.* **6**: 1-25.

Armstrong, J.B., and Muneoka, K. (1989). "Genetic markers and their use in chimeras" in Developmental Biology of the Axolotl, Armstrong, J.B. and Malacinski, G.M. eds., Oxford University Press, New York, pp. 236-244.

Armstrong, J.B., Duhon, S.T., and Malacinski, G.M. (1989). "Raising the axolotl in captivity" in Developmental Biology of the Axolotl, Armstrong, J.B. and Malacinski, G.M. eds., Oxford University Press, New York, pp. 220-235.

Baker, R. C., and Graves, G. O. (1939). The behavior of the neural crest in the forebrain region of Amblystoma. *J. Comp. Neurol.* **71**: 389-415.

Barlow, L.A., and Northcutt, R.G. (1995). Embryonic origin of amphibian taste buds. *Dev. Biol.* **169**: 273-285.

Bellah, R., Darillis, A., and Fellows K.E. (1989). The association of congenital neuroblastoma and congenital heart disease. Is there a common embryological basis? *Pediatr. Radiol.* **19**: 119-121.

Bockman, D.E., Redmond, M. E., and Kirby, M.L. (1989). Alteration of early vascular development after ablation of cranial neural crest. *Anat. Rec.* **225**: 209-217.

Bordzilovskaya, N.P., and Dettlaff, T.A. (1979). Table of stages of the normal development of axolotl embryos and the prognostication of timing of successive developmental stages at various temperatures. *Axolotl Newslett.* **7**: 2-22.

Bordzilovskaya, N.P., and Dettlaff, T.A., Duhon, S.T., and Malacinski, G.M. (1989). Developmental stage series of axolotl embryos. In "Developmental Biology of the Axolotl", J.B. Armstrong and G.M. Malacinski eds., Oxford University Press, New York.

Bronner-Fraser M. (1985). Alterations in neural crest migration by an antibody that affects cell adhesion. *J. Cell Biol.* **101**: 610-617.

Bronner-Fraser M. (1986). An antibody to a receptor for fibronectin and laminin perturbs cranial neural crest development *in vivo*. *Dev. Biol.* **117**: 528-536.

Bronner-Fraser M., and Lallier, T. (1988). A monoclonal antibody against a laminin-heparan sulfate proteoglycan complex perturbs cranial neural crest migration *in vivo*. *J. Cell Biol.* **106**: 1321-1330.

Bronner-Fraser, M., Wolf, J. J., and Murray, B.A. (1992). Effects of antibodies against N-cadherin and N-CAM on the cranial neural crest and neural tube. *Dev. Biol.* **153**: 291-301.

Bronner-Fraser, M. (1993). Mechanisms of neural crest cell migration. *BioEssays* **15**: 221-230.

Chan, W. Y., and Tam, P.P.L. (1988). A morphological and experimental study of the mesencephalic neural crest cells in the mouse embryo using wheat germ agglutinin-gold conjugate as the cell marker. *Development* **102**: 427-442.

Chibon, P. (1964). Analyse par la méthode de marquage nucléaire à la thymidine tritiée des derivés de la crête neurale céphalique chez l'Urodèle *Pleurodeles waltlii C.r. Acad. Sci.* **259**: 3624-3627.

Chibon, P. (1966). Analyse expérimentale de la régionalisation et des capacités morphogénètiques de la crête neurale chez l'amphibien urodèle *Pleurodeles waltlii Michah. Mem. Soc. zool. Fr.* **36**: 1-107.

Collazo, A., Bronner-Fraser, M., and Fraser, S.E. (1993). Vital dye labelling of Xenopus laevis trunk neural crest reveals multipotency and novel pathways of migration. *Development* **118**: 363-376.

Copenhaver, W.M. (1926). Experiments on the development of the heart of *Amblystoma punctatum. J. Exp. Zool.* **43**: 103-126.

Detweiler, S.R. (1937). Observations upon the migration of neural crest cells and upon the development of the spinal ganglia and vertebral arches in *Amblystoma* . *Amer. J. Anat.* **61**: 63-94.

Detweiler, S.R., and Kehoe, K. (1939). Further observations on the origin of the sheath cells of Schwann. *J. Exp. Zool.* **81**: 415-433.

Duband, J.L., and Thiery, J.P. (1987). Distribution of laminin and collagens during avian neural crest development. *Development* **101**: 461-478.

Elberger, A.J. (1993). Distribution of transitory corpus callosum axons projecting to developing cat visual cortex revealed by DiI. *J. Comp. Neurol.* **333**: 326-342.

Fraser, S. E., and O'Rourke, N.A. (1990). *In situ* analysis of neuronal dynamics and positional cues in the patterning of nerve connections. *J. exp. Biol.* **153**: 61-70.

Frost, S. K., Neff, A., and Malacinski, G. M. (1989). Primary and long-term culture of axolotl cells. In "Developmental Biology of the Axolotl", J.B. Armstrong and G.M. Malacinski eds., Oxford University Press, New York. pp. 244-254.

Frunchak, Y.N., and Milos, N.C. (1990). Studies on cellular adhesion of *Xenopus laevis* melanophores: pigment pattern formation and its alteration in vivo by endogenous galactoside-binding lectin or its sugar inhibitor. *Pigment Cell. Res.* **3**: 101-114.

Fukiishi, Y., and Morriss-Kay, G.M. (1992). Migration of cranial neural crest cells to the pharyngeal arches and heart in rat embryos. *Cell Tissue Res.* **268**: 1-8.

Gansmuller, A., Kruger, F., Gumpel, M., and Baron-Van Evercooren, A. (1992). Photoconverted carbocyanine DiI allows direct visualization of transplanted glial cells at the ultrastructural level. *Neurosci. Lett.* **147**: 151-154.

Gont, L., Steinbeisser, H., Blumberg, B., and De Robertis, E.M. (1993). Tail formation as a continuation of gastrulation: the multiple cell populations of the Xenopus tailbud derive from the late blastopore lip. *Development* **119**: 991-1004.

Graveson, A.C. (1990). Studies on the differentiation of cranio-visceral cartilage in normal and premature death mutant embryos of *Ambystoma mexicanum*. PhD. Thesis, University of Ottawa, Ottawa, Canada.

Graveson, A.C. (1993). Neural crest: contributions to the development of the vertebrate head. *Amer. Zool.* **33**: 424-433.

Graveson, A.C., and Armstrong, J.B. (1987).Differentiation of cartilage from cranial neural crest in the axolotl (*Ambystoma mexicanum*). *Differentiation* **35**: 16-20.

Graveson, A.C., and Armstrong, J.B. (1990). The premature death (p) mutation of Ambystoma mexicanum affects a subpopulation of neural crest cells. *Differentiation* **45**: 71-75.

Graveson, A.C., and Armstrong, J.B. (1994). In vivo evidence that the premature death (p) mutation of Ambystoma mexicanum affects an early segregating subpopulation of neural crest cells. *J. Exp. Zool.* **269**: 327-335.

Graveson, A.C., and Armstrong, J.B. (1996). Premature Death (*p*) mutation of *Ambystoma mexicanum* affects the ability of ectoderm to respond to neural induction. *J. Exp. Zool.* **274**: 248-254.

Graveson , A.C., Hall, B.K., and Armstrong, J.B. (1995). The relationship between migration and chondrogenic potential of trunk neural crest cells in *Ambystoma mexicanum* . *Roux's Arch. Dev. Biol.* **204**: 477-483.

Griffith, C. M., and Hay, E. D. (1992). Epithelial-mesenchymal transformation during palatat fusion: carboxyfluorescein traces cells at light and electron microscopic levels. *Development* **116**: 1087-1099.

Hall, B. K., and Hörstadius, S. (1988). The Neural Crest. Oxford University Press, Oxford.

Hall, C. V., Jancob, P.E., Ringold, G.M., and Lee, F. (1983). Expression and regulation of Escherichia coli lacZ gene fusions in mammalian cells. *J. Mol. Appl. Genet.* **2**: 101-109.

Holley, J., and Yu, R.K. (1987). Localization of glucoconjugates recognized by the HNK-1 antibody in mouse and chick embryo during early neural development. *Dev. Neurosci.* **9**: 105-119.

Holmqvist, B. I., Östholm, T., and Ekström, P. (1992). DiI tracing in combination with immunocytochemistry for analysis of connectivities ad chemoarchitectonics of specific neural systems in a teleost, the Atlantic salmon. *J. Neurosci. Methods* **42**: 45-63.

Honig, M. G., and Hume, R.I. (1986). Fluorescent carbocyanine dyes allow living neurons of identified origin to be studied in long-term culture. *J. Cell Biol* . **103**: 171-187.

Hörstadius, S., and Sellman, S. (1946). Experimentelle untersuchungen über die Determination des Knorpeligen Kopfskelettes bei Urodelen. *Nova Acta R. Soc. Scient. Upsal, ser IV.* **13**: 1-170.

Ito, K., and Sieber-Blum, M. (1991). In vitro clonal analysis of quail cardiac nerual crest development. *Dev. Biol.* **148**: 95-106.

Jacobson, A.G. (1960). Influences of ectoderm and endoderm on heart differentiation in the newt. *Dev. Biol.* **2**: 138-154.

Jacobson, A.G. (1961). Heart determination in the newt. *J. Exp. Zool.* **146**: 139-151.

Jacobson, A.G., and Duncan, J.T. (1968). Heart induction in salamanders. *J. Exp. Zool.* **167**: 79-103.

Jacobson, M., and Hirose, G. (1978). Origin of the retina from both sides of the embryonic brain: a contribution to the problem of crossing at the optic chiasma. *Science* **202**: 637-639.

Jacobson, M., and Hirose, G. (1981). Clonal organization of the central nervous system of the frog. II. Clones stemming from individual blastomeres of the 32- and 64-cell stages. *J. Neurosci.* **1**: 271-284.

Johnston, M.C., Noden, D.M., Hazelton, R.D., Coulombre, J.L., and Coulombre, A.J. (1979). Origins of avian ocular and periocular tissues. *Exp. Eye. Res.* **29**: 27-44.

Kaethner, R.J., and Stuermer, C.A.O. (1992). Dynamics of terminal arbor formation and target approach of retinotectal axons in living zebrafish embryos: a time-lapse study of single axons. *J. Neurosci.* **12**: 3257-3271.

Kintner, C. (1988). Effects of altered expression of the neural cell adhesion molecule, N-CAM, on early neural development in *Xenopus* embryos. *Neuron* **1**: 545-555.

Kirby, M.L. (1989). Plasticity and predetermination of mesencephalic and trunk neural crest transplanted into the region of the cardiac neural crest. *Dev. Biol.* **134**: 401-412.

Kirby, M.L. (1991). Neural crest and the morphogenesis of Down Syndrome with special emphasis on cardiovascular development in "The Morphogenesis of Down Syndrome: Progress in Clinical and Biological Research volume 373, Charles J. Epstein ed., Wiley Liss Inc., New York.

Kirby, M. L., and Bockman, D.E. (1984). Neural crest and normal development: a new perspective. *The Anatomical Record* **209**: 1-6.

Kirby, M.L., and Stewart, D.E. (1983). Neural crest origin of cardiac ganglion cells in the chick embryo: identification and extirpation. *Dev. Biol.* **97**: 433-443.

Kirby, M.L., and Waldo, K.L. (1990). Role of neural crest in congenital heart disease. *Circulation* **82**: 332-340.

Kirby, M.L., Gale, T.F., and Stewart, D.E. (1983). Neural crest cells contribute to normal aorticopulmonary septation. *Science* **220**: 1059-1061.

Kirby, M.L., Kumiski, D. H., Myers, T., Cerjan, C., and Mishima, N. (1993). Backtransplantation of chick cardiac neural crest cells cultured in LIF rescues heart development. *Dev. Dynamics* **198**: 296-311.

Krotoski, D., Domingo, C., and Bronner-Fraser, M. (1986). Distribution of a putative cell surface receptor for fibronectin and laminin in the avian embryo. *J. Cell Biol.* **103**: 1061-1072.

Krotoski, D.M., Fraser, S.E., and Bronner-Fraser, M. (1988). Mapping of neural crest pathways in *Xenopus laevis* using inter- and intra-specific cell markers. *Dev. Biol.* **127**: 119-132.

Krug, L., Wicht, H., and Northcutt, R. G. (1993). Afferent and efferent connections of the thalamic eminence in the axolotl, *Ambystoma mexicanum. Neuroscience Letters* **149**: 145-148.

Kruse, J., Mailhammer, R., Wernecke, H., Faissner, A., Sommer, I., Goridis, I., and Schachner, M. (1984). Neural cell adhesion molecules and myelin-associated glycoprotein share a common carbohydrate moiety recognized by monoclonal antibodies L2 and HNK-1. *Nature* **311**: 153-155.

Kuratani, S.C., and Kirby, M.L. (1992). Migration and distribution of circumpharyngeal crest cells in the chick embryo. *Anat Rec.* **234**: 263-280.

Kuratani, S.C., Miyagawa-Tomita, S., and Kirby, M.L. (1991). Development of cranial nerves in the chick embryo with special reference to the alterations of cardiac branches after ablation of the cardiac neural crest. *Anatomy and Embryol.* **183**: 510-514.

Landacre, F.L. (1921). The fate of neural crest in the head of the Urodeles. *J. Comp. Neurol.* **33**: 1-43.

Langille, R.M., and Hall, B.K. (1988). Role of the neural crest in development of the trabeculae and branchial arches in embryonic sea lamprey, *Petromyzon marinus* (L). *Development* **102**: 301-310.

Le Douarin, N. (1982). The Neural Crest. Cambridge University Press, Cambridge.

Le Douarin, N., and Teillet, M-A.M. (1984). Experimental analysis of the migration and differentiation of neurectodermal mesenchymal derivatives, using a biological cell marking technique. *Dev. Biol.* **41**: 162-184.

Le Lièvre, C.S. and Le Douarin, N.M. (1975). Mesenchymal derivatives of the neural crest: analysis of chimaeric quail and chick embryos. *J. Embryol. exp. Morph.* **34**: 125-154.

Lemanski, L.F. (1971). "Histological, histochemical, and ultrastructural study of myocardiogenesis in Mexican axolotls, *Ambystoma mexicanum*." Ph.D. Thesis, Arizona State University.

Lemanski, L.F. (1973). Heart development in the Mexican salamander, Ambystoma mexicanum.Gross anatomy, histology and histochemistry. *J. Morph.* **139**: 301-328.

Lübke, J. (1993). Photoconversion of diaminobenzidine with different fluorescent neuronal markers into a light and electron microscopic dense reaction product. *Microscopy Res. and Technique* **24**: 2-14.

Luider, T.M., Bravenboer, N., Meijers, C., van der Kamp, A.W.M., Tibboel, D., and Poelmann, R.E. (1993). The distribution and characterization of HNK-1 antigens in the developing avian heart. *Anat. Embryol.* **188**: 307-316.

Mes-Hartree, M., and Armstrong, J.B. (1980). Evidence that the premature death mutation (*p*) in the Mexican axolotl (*Ambystoma mexicanum*) is not an autonomous cell lethal. *J. Embryol. Exp. Morphol.* **60**: 295-302.

Metcalfe, W.K., Meyers, P. Z., Trevarrow, B., Bass, M.B., and Kimmel, C.B. (1990). Primary neurons that express the L2/HNK-1 carbohydrate during early development in the zebrafish. *Development* **110**: 491-504.

Meyer, G., and Gonzalez-Hernandez, T. (1993). Developmental changes in layer I of the human neocortex during prenatal life: a DiI-tracing and AChE and NADPH-d histochemistry study. *J. Comp. Neurol.* **338**: 317-336.

Milos, N.C., Frunchak, Y.N., and Mohamed, Z.(1993). Probing the functions of endogenous lectins: effects of a monoclonal antibody against the neural-crest stage lectin of *Xenopus laevis* on trunk development. *J. Exp. Zool.* **266**: 240-247.

Miyagawa, S.T., Waldo, K., Tomita, H., and Kirby, M.L. (1989). Migraton of cardiac neural crest cells: A temporospatial study in early quail-chick chimeras. *NY Acad Sci.* **588**: 427-429.

Nagai, T. (1993) Transcellular labeling of DiI demonstrates the glossopharyngeal innervation of taste buds in the lingual epithelium of the axolotl. *J. Comp. Neurol.* **331**:122-133.

Newgreen, D.F. and Thiery, J.P. (1980). Fibronectin in early avian embryos: synthesis and distribution along the migration pathways of neural crest cells. *Cell Tiss. Res.* **211**: 269-291.

Nishibatake, M., Kirby, M.L., and Van Mierop, L.H.S. (1989). Pathogenesis of persistent truncus arteriosis and dextroposed aorta in the chick embryo after neural crest ablation. *Circulation* **73**: 360-364.

Noden, D.M. (1983). The role of the neural crest in patterning of avian cranial skeletal, connective, and muscle tissues. *Dev. Biol.* **96**: 144-165.

Noden, D.M. (1984). The use of chimeras in analyses of craniofacial development. In "Chimeras in Developmental Biology", N.M. LeDouarin and A. McLaren eds. Academic Press, London.

Norlander, R.H. (1989). HNK-1 marks earliest axonal outgrowth in *Xenopus* . *Dev. Brain Res.* **50**: 147-153.

Norlander, R.H. (1993). Cellular and subcellular distribution of HNK-1 immunoreactivity in the neural tube of *Xenopus* . *J. Comp. Neurol.* **335**: 538-551.

Perris, R., Krotoski, D., and Bronner-Fraser, M. (1991). Collagens in avian neural crest cell development: distribution *in vivo* and migration-promoting ability *in vitro*. *Development* **113**: 969-984.

Perris, R., Krotoski, D., Domingo, C., Lallier, T., Sorrell, J.M., and Bronner-Fraser, M. (1991). Spatial and temporal changes in the distribution of proteoglycans during avian neural crest development. *Development* **111**: 583-599.

Phillips, M.T., Kirby, M.L., and Forbes, G. (1987) Analysis of cranial neural crest distribution in the developing heart using quail-chick chimeras. *Circulation Res.* **60**: 27-30.

Pires-Neto, M.A., and Lent, R. (1993). The prenatal development of the anterior commissure in hamsters: pioneer fibers lead the way. *Dev. Brain Res.* **72**: 59-66.

Pomeranz, H. D., Rothman, T.B., and Gershon, M.D. (1991). Colonization of the post-umbilical bowel by cells derived from the sacral neural crest: direct tracing of cell migration using an intercalating probe and a replication-deficient retrovirus. *Development* **111**: 647-655.

Poole, T., and Thiery, J.P. (1986). Antibodies and a synthetic peptide that block cell-fibronectin adhesion arrest neural crest cell migration in vivo. In "Progress in Developmental Biology," Part B. A. R. Liss, New York. pp. 235-238.

Ragnarson, B., Bengtsson, L., and Hægerstrand, A. (1992). Labeling with fluorescent carbocyanine dyes of cultured endothelial and smooth muscle cells by growth in dye-containing medium. *Histochemistry* **97**: 329-333.

Raible, D. W., and Eisen, J. (1994). Spatiotemporal restriction of neural crest cell fate in the trunk of the embryonic zebrafish. *Development* **120**: 495-503.

Raven, C. P. (1931). Die eigentümliche Bildungsweise des Neuralrohrs beim Axolotl und die Lage des Ganglienleistenmaterials. *Anat. Anz.* **71**: 161-6.

Riccardi, V.M., and Eichner, J.E. (1986). Neurofibromatosis: phenotype, natural history and pathogenesis. Johns Hopkins University Press, Baltimore.

Riuz i Altaba, A., Warga, R.M., and Stern, C. D. (1994). "Fate maps and cell lineage analysis" in Essential Developmental Biology: a practical approach. C. D. Stern and Holland P.W. eds. IRL Press at Oxford University Press, Oxford. pp. 81-95.

Rosenquist, T.H., Fray-Gavalas, C., Waldo, K, and Beall, A.C. (1990). Development of the musculoelastic septation complex in the avian truncus arteriosis. *Am. J. of Anatomy* **189**: 339-356.

Rosenquist, T.H., Kirby, M.L., and Van Mierop, L.H.S. (1989). Solitary aortic arch artery. A result of surgical ablation of cardiac neural crest and nodose placode in the avian embryo. *Circulation* **80**: 1469-1475.

Ruffins, S. W., and Ettensohn C. A. (1993). A clonal analysis of secondary mesenchyme cell fates in the sea urchin embryo. *Dev. Biol.* **160**: 285-288.

Sadaghiani, B., and Thiébaud, C.H. (1987). Neural crest development in the Xenopus laevis embryo, studied by interspecific transplantation and scanning electron microscopy. *Dev. Biol.* **124**: 91-110.

Sadaghiani, B., and Vielkind, J.R. (1990). Distribution and migration pathways of HNK-1 immunoreactive neural crest cells in teleost fish embryos. *Development* **110**: 197-209.

Sanes, J. R., Rubenstein, J. L. R., and Nicolas, J.F. (1986). Use of recombinant retrovirus to study post-implantation cell lineage in mouse embryos. *EMBO J.* **5**:3133-3142.

Sater, A.K., and Jacobsen, A.G. (1989). The specification of heart mesoderm occurs during gastrulation in *Xenopus* . *Development* **105**: 821-830.

Scherson, T., Serbedzija, G., Fraser, S., and Bronner-Fraser, M. (1993). Regulative capacity of the cranial neural tube to form neural crest. *Development* **118**: 1049-1061.

Schilling, T.F., and Kimmel, C.B. (1994). Segment and cell type lineage restrictions during pharyngeal arch development in the zebrafish embryo. *Development* **120**: 483-494.

Schwarting, G.A., Jungalwala, F.B., Chou, D.K.H., Boyer, A.M., and Yamamoto, M. (1987). Sulfated glucuronic acid-containing glycoconjugates are temporally and spatially regulated antigens in the developing mammalian nervous system. *Dev. Biol.* **120**: 65-76.

Selleck, M.A.J., and Stern, C.D. (1991). Fate mapping and cell lineage analysis of Hensen's node in the chick embryo. *Development* **112**: 615-626.

Serbedzija, G.N., Bronner-Fraser, M., and Fraser, S.E. (1989). A vital dye analysis of the timing and pathways of avian trunk neural crest cell migration. *Development* 106: 809-816.

Serbedzija, G., Burgan, S., Fraser, S., and Bronner-Fraser, M. (1991). Vital dye labelling demonstrates a sacral neural crest contribution to the enteric nervous system of chick and mouse embryos. *Development* . **111**:857-866.

Serbedzija, G., Bronner-Fraser, M., and Fraser, S. (1992). Vital dye analysis of cranial neural cell migration in the mouse embryo. *Development* . **116**: 297-307.

Siebert, J.R., Graham, J.M., and MacDonald, C. (1985). Pathological features of the CHARGE association: support for involvement of the neural crest. *Teratology*. **31**: 331-336.

Smith, J.C., and Slack, J. M.W. (1983). Dorsalization and neural induction: properties of the organizer in Xenopus laevis. *J. Embryol. Exp. Morphol.* **78**: 299-317.

Smith, J.L., Gesteland, K.M., and Schoewolf, G.C. (1994). Prospective fate map of the mouse primitive streak at 7.5 days of gestation. *Dev. Dynamics*. **201**: 279-289.

Smith, S.C., and Armstrong, J.B. (1990). Heart induction in wild-type and cardiac mutant axolotls (*Ambystoma mexicanum*) . *J. Exp. Zool.* **254**: 48-54.

Smith, S.C., Graveson, A.C., and Hall, B.K. (1994). Evidence for a developmental and evolutionary link between placodal ectoderm and neural crest. *J. Exp. Zool.* **270**: 292-301.

Smits-van Prooije, A.E., Poelmann, R. E., Dubbledam, J.A., Mentink, M.M.T., and Vermeij-Keers, C. (1986). Wheat germ agglutinin-gold as a novel marker for mesectoderm formation in mouse embryos cultured *in vitro* . *Stain Technol.* **61**: 97-106.

Soriano, H.E., Lewis, D., Legner, M., Brandt, M., Baley, P., Darlington, G., Finegold, M., and Ledley F.D. (1992). The use of DiI-marked hepatocytes to demonstrate orthotopic, intrahepatic engraftment following hepatocellular transplantation. *Transplantation* . **54**: 717-723.

Stephens, D. L., Miller, T.J., Silver, L., Zipser, D., and Mertz, J.E.(1981). Easy-to-use equipment for the accurate microinjection of nanoliter volumes into the nuclei of amphibian oocytes. *Analytical Biochem.* **114**:299-309.

Stewart, D.E., Kirby, M.L. and Sulik, K.(1986). Hemodynamic changes in chick embryos precede heart defects after cardiac neural crest ablation. *Circulation Res.* **59**: 545-550.

Stone, L.S. (1922). Experiments on the development of the cranial ganglia and the lateral line sense organs in *Amblystoma punctatum* . *J. Exp. Zool.* **35**: 421-496.

Stone, L.S. (1926). Further experiments on the extirpation and transplantation of mesectoderm in *Amblystoma punctatum.* . *J. Exp. Zool.* **44**: 95-131.

Stone, L.S. (1929). Experiments showing the role of migrating neural crest (mesectoderm) in the formation of head skeleton and loose connective tissue in *Rana palustris. Wilhelm Roux Arc. EntwMech. Org.* **118**: 40-77.

Takamura, K., Okishima, T., Ohdo, S., and Hayakawa, K. (1990). Association of cephalic neural crest cells with cardiovascular development, particularly that of the semilumar valves. *Anat and Embryol.* **182**: 263-272.

Tan, S.S., and Morriss-Kay, G.M. (1986). Analysis of cranial neural crest cell migration and early fates in postimplantation rat chimeras. *J. Embryol. exp. Morph.* **98**: 21-58.

Tan, S.S., Prieto, A.L. Newgreen, D.F., Crossin, K.L., and Edelman, G.M. (1991). Cytoactin expression in the somites after dorsal neural tube and neural crest ablation in chicken embryos. *Proc. Natl. Acad. Sci. USA.* **88**: 6398-6402.

Teillet, M.A., Kalcheim, C., and LeDouarin, N.M. (1987). Formation of the dorsal root ganglion in the avian embryo: segmental origin and migratory behaviour of neural crest progenitor cells. *Dev. Biol.* **120**: 329-347.

Thiébaud, C. H. (1983). A reliable new cell marker in *Xenopus*. *Dev. Biol.* **98**: 245-249.

Thiery, J. P., Duband, J.L. Rutishauser, U., and Edelman, G.M. (1982). Cell adhesion molecules in early chick embryogenesis. *Proc. Natl. Acad. Sci. USA* **79**: 6737-6741.

Trainor, P. A., and Tam, P.L., (1995). Cranial paraxial mesoderm and neural crest cells of the mouse embryo: co-distribution in the craniofacial mesenchyme but distinct segregation in branchial arches. *Development.* **121**: 2569-2582.

Trottier, T.M. and Armstrong, J.B. (1977). Experimental studies on a mutant gene (*p*) causing premature death of Ambystoma mexicanum embryos. *J. Embryol. exp. Morph.* **39**: 139-149.

Tucker, G.C., Aoyama, H., Lipinski, M., Tursz, T., and Thiery, J.P. (1984). Identical reactivity of monoclonal antibodies HNK-1 and NC-1: conservation in vertebrates on cells derived from the neural primordium and on some leukocytes. *Cell Differentiation.* **14**: 223-230.

Turner, D.L., and Cepko, C.L. (1987). A common progenitor for neurons and glia persists in rat retina late in development. *Nature.* **328**: 131-136.

Unthank, J.L., Lash, J.M., Nixon, J.C., Sidner, R.A., and Bohlen, H.G. (1993). Evaluation of carbocyanine-labeled erythrocytes for microvascular measurements. *Microvascular Res.* **45**: 193-210.

Van Mierop, L.H.S., and Kutsche, L.M. (1986). Cardiovascular anomalies in DiGeorge syndrome and importance of neural crest as a possible pathogenic factor. *Am. J. Cardiol.* **58**: 133-137.

Vincent, M., and Thiery, J.P. (1984). A cell surface marker for neural crest and placodal cells: further evolution in peripheral and central nervous system. *Dev. Biol.* **103**: 468-481.

Vincent, M., Duband, J.L., and Thiery, J.P. (1983). A cell surface determinant expressed early on migrating neural crest cells. *Dev. Brain Res.* **9**: 235-238.

Wadhwa, S., Jotwani, G., and Bijlani, V. (1993). Human retinal ganglion cell development in early prenatal period using carbocyanine dye DiI. *Neurosci. Lett.* **157**: 175-178.

Wells, T.R., Landing, B.H., Galliani, C.A., and Thomas, R.A. (1986). Abnormal growth of the thyroid cartilage in the DiGeorge Syndrome. *Pediatr. Pathol.* **6**: 209-225.

Weston, J. A. (1963). A radioautographic analysis of the migration and localization of trunk neural crest cells in the chick. *Dev. Biol.* **6**: 279-310.

Whiteley, M., and Armstrong, J.B.(1991). On the origin of the mesoderm in the Mexican axolotl, *Ambystoma mexicanum. Can. J. Zool.* **69**: 1221-1225.

Whiteley, M., Fletcher, W.S., and Armstrong, J.B. (1990). The use of *lacZ* fusion constructs as a cell marker in the axolotl. Axolotl Newsl. 19:22-27. (Available from the Indiana University Axolotl Colony, Dept. of Biology, Indiana University, Bloomington IN 47405).

Wilens, S. (1955). The migration of heart mesoderm and associated areas in *Amblystoma punctatum* . *J. Exp. Zool.* **129**: 579-606.